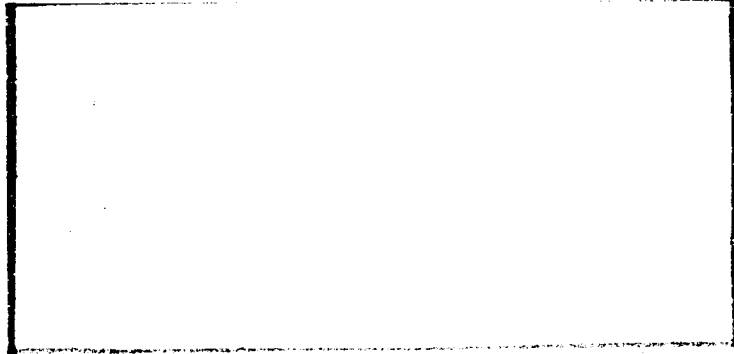


N O T I C E

THIS DOCUMENT HAS BEEN REPRODUCED FROM
MICROFICHE. ALTHOUGH IT IS RECOGNIZED THAT
CERTAIN PORTIONS ARE ILLEGIBLE, IT IS BEING RELEASED
IN THE INTEREST OF MAKING AVAILABLE AS MUCH
INFORMATION AS POSSIBLE

DRA



(KU-PRL-417-14) ACOUSTIC PLANE WAVES
INCIDENT ON AN OBLIQUE CLAMPED PANEL IN A
RECTANGULAR DUCT (Kansas Univ.) 137 p
HC A07/MF A01

N80-34215

CSCL 20A

G3/71

Unclass
16940



THE UNIVERSITY OF KANSAS CENTER FOR RESEARCH, INC.

2291 Irving Hill Drive—Campus West
Lawrence, Kansas 66045

Report for
A RESEARCH PROGRAM TO REDUCE INTERIOR
NOISE IN GENERAL AVIATION AIRPLANES
NASA Contract NCII-6

ACOUSTIC PLANE WAVES INCIDENT ON AN OBLIQUE
CLAMPED PANEL IN A RECTANGULAR DUCT

KU-FRL-417-14

by
Hillel Unz
Professor of Electrical Engineering

Principal Investigator: Jan Roskam
Professor of Aerospace Engineering

University of Kansas
Lawrence, Kansas 66045

August 1980

Technical Monitor: David Stephens
NASA Langley Research Center

ABSTRACT

The theory of acoustic plane waves incident on an oblique clamped panel in a rectangular duct is developed from basic theoretical concepts. The coupling theory between the elastic vibrations of the panel (plate) and the oblique incident acoustic plane wave in infinite space is considered in detail, and is used for the oblique clamped panel in the rectangular duct. The partial differential equation which governs the vibrations of the clamped panel (plate) is modified by adding to it stiffness (spring) forces and damping forces. The Transmission Loss coefficient and the Noise Reduction coefficient for oblique incidence are defined and derived in detail. The resonance frequencies excited by the free vibrations of the oblique finite clamped panel (plate) are derived and calculated in detail for the present case.

The detailed features and the oscillatory trends of the experimental Noise Reduction coefficient curves for oblique aluminum panels of angles $\theta = 15^\circ, 30^\circ, 40^\circ, 60^\circ$ in the square duct are explained in detail, based on the theory presented in this report. All the frequency positions of the downward and upward resonance spikes in the experimental data are identified theoretically as resulting from four major resonance phenomena: The cavity resonance, the acoustic resonance, the wooden back panel resonance and the plate resonance. Detailed tables are given for the values of these resonance frequencies in each case.

ACKNOWLEDGMENT

The author is grateful to Professor J. Roskam, Aerospace Department, University of Kansas, for his initiation of the author to this field of study, and for his encouragement, support and help throughout this project. Many thanks are due to Mr. F. Grosveld for supplying the extensive experimental data and for some discussions on certain aspects of this project. This is to thank Mr. R. Navaneethan for checking the numerical calculations in this report. Sincere thanks are due to Mrs. Charlotte Merrill for her experienced and accurate typing of the manuscript.

ACOUSTIC PLANE WAVES INCIDENT ON AN OBLIQUE
CLAMPED PANEL IN A RECTANGULAR DUCT

by

Hillel Unz

	<u>Page</u>
ABSTRACT	i
ACKNOWLEDGEMENT	ii
TABLE OF CONTENTS	iii
LIST OF TABLES	v
LIST OF FIGURES	vi
CHAPTER I: INTRODUCTION	1
II: OBLIQUE ACOUSTIC PLANE WAVES	4
III: OBLIQUE ACOUSTIC WAVE ON AN INFINITE PANEL	14
IV: NOISE REDUCTION FOR INFINITE PANEL	24
V: OBLIQUE ACOUSTIC WAVE ON FINITE PANEL	37
VI: NOISE REDUCTION FOR FINITE PANEL	49
VII: FREE VIBRATIONS OF THE FINITE PANEL	56
VIII: EXPERIMENTAL AND NUMERICAL RESULTS	65
A. THE AVERAGE NOISE REDUCTION COEFFICIENT	67
B. THE NOISE REDUCTION COEFFICIENT	71
C. THE CAVITY RESONANCE	73
D. THE ACOUSTIC RESONANCE	76
E. THE WOODEN BACK PANEL RESONANCE	79
F. THE PLATE RESONANCE	81

TABLE OF CONTENTS (CONTINUED)

	<u>Page</u>
CHAPTER IX: SUMMARY	99
BIBLIOGRAPHY	102
APPENDIX A - PLATE RESONANCE FREQUENCIES	103

LIST OF TABLES

	<u>Page</u>
TABLE A: Average Noise Reduction Coefficient	70
TABLE B: Cavity Resonance Frequencies	74
TABLE C: Acoustic Resonance Frequencies	77
TABLE D: Wood Resonance Frequencies	80
TABLE E-1: Plate Resonance Frequencies, $\theta=0^\circ$ (Downward Spikes) . .	85
TABLE E-2: Plate Resonance Frequencies, $\theta=0^\circ$ (Upward Spikes) . . .	86
TABLE F-1: Plate Resonance Frequencies, $\theta=15^\circ$ (Downward Spikes) .	87
TABLE F-2: Plate Resonance Frequencies, $\theta=15^\circ$ (Upward Spikes) . .	88
TABLE G-1: Plate Resonance Frequencies, $\theta=30^\circ$ (Downward Spikes) .	90
TABLE G-2: Plate Resonance Frequencies, $\theta=30^\circ$ (Upward Spikes) . .	91
TABLE H-1: Plate Resonance Frequencies, $\theta=40^\circ$ (Downward Spikes) .	92
TABLE H-2: Plate Resonance Frequencies, $\theta=40^\circ$ (Upward Spikes) . .	94
TABLE I-1: Plate Resonance Frequencies, $\theta=60^\circ$ (Downward Spikes) .	95
TABLE I-2: Plate Resonance Frequencies, $\theta=60^\circ$ (Upward Spikes) . .	97
TABLE J: Calculated Values for Equation (161)	104
TABLE K: Theoretical Plate Resonance Frequencies	106

LIST OF FIGURES

	<u>Page</u>
FIGURE 1: Geometrical Configuration for Oblique Incidence . .	121
FIGURE 2: KU-FRL Acoustic Panel Test Facility	122
FIGURE 3: Top Views of the Special Test Section	123
FIGURE 4: Noise Reduction Characteristics, $\theta=0^\circ$	124
FIGURE 5: Noise Reduction Characteristics, $\theta=15^\circ$	125
FIGURE 6: Noise Reduction Characteristics, $\theta=30^\circ$	126
FIGURE 7: Noise Reduction Characteristics, $\theta=40^\circ$	127
FIGURE 8: Noise Reduction Characteristics, $\theta=60^\circ$	128
FIGURE 9: The Acoustic Rays	129

CHAPTER I

INTRODUCTION

The acoustic research project started on April 15, 1976, when the Flight Research Laboratory of the University of Kansas began work under a grant from NASA, Langley Research Center, entitled, "A Research Program to Reduce Interior Noise in General Aviation Airplanes" (NASA Grant No. 1301). Over the past four years a research facility has been established, in the form of a Beranek tube and additional equipment, and a large volume of experimental data has been published.

In a previous report by the present author, listed in the Bibliography, a theory has been presented which explains reasonably well the detailed features of the experimental noise reduction curves for normal incidence of acoustic plane waves on a clamped panel in a rectangular duct (the Beranek tube). Such detailed features include the general behavior of the noise reduction curve in all its parts, as well as the frequencies of the numerous resonance spikes, which are superimposed on the curve both upward and downward.

This theory has been based on the interaction between two general fields of study: the theory of acoustic wave propagation in infinite space and in ducts, and the dynamic theory of plates and the theory of elasticity. Since the vibrations in the panel (plate) and the acoustic waves in the air are coupled strongly along the whole panel, and are affecting each other noticeably, the interaction between these two systems play a major role in this theory. When one sends an incident acoustic wave in the direction of the panel, this wave will be reflected from the panel. At the same time it will set the panel

into motion of vibrations, which will generate transmitted acoustic waves on the other side of the panel. The incident, reflected and transmitted acoustic waves will be coupled strongly together with the induced transverse displacement of the panel. Because of the experimental set up in the Beranek tube, the acoustic wave propagates in a duct with a square cross-section. Higher order acoustic wave modes of propagation in the square duct, as well as the fundamental mode of plane acoustic wave, have been taken into account, in order to explain the experimental results of resonance at certain particular frequencies.

The previous report has developed the theoretical derivations from the basic equations. The theory presented in the previous report has successfully explained the detailed features of the noise reduction curves for one particular aluminum panel, which has been taken as a typical example. One of the most challenging aspects of that theory, which has been met successfully, has been to avoid lengthy numerical analysis, in order not to mask the main features of the interaction between the different physical phenomena. All the calculations in that report have been done on a simple hand calculator.

The present report should be considered as a sequel to the previous report by the present author, but it is independent of the previous report in its presentation. The theory of oblique acoustic wave incident of an infinite panel (plate) and a clamped panel will be developed from the basic equations. Some of the general features of

the corresponding experimental noise reduction curves, given at the end of this report, will be discussed by using the present theory. As in the previous report, all the calculations in the present report have been done on a simple hand calculator.

The Meter, Kilogram, Second system of units is being used throughout this report, except at some places where the experimental data is given otherwise. The factor $e^{-i\omega t}$ is used for harmonic time variation.

In this report the following vector identities will be used, where $\bar{a}_x, \bar{a}_y, \bar{a}_z$ are the unit vectors in rectangular coordinates:

$$\nabla p = (\bar{a}_x \frac{\partial}{\partial x} + \bar{a}_y \frac{\partial}{\partial y} + \bar{a}_z \frac{\partial}{\partial z}) p = \bar{a}_x \frac{\partial p}{\partial x} + \bar{a}_y \frac{\partial p}{\partial y} + \bar{a}_z \frac{\partial p}{\partial z}$$

$$\nabla \cdot \bar{u} = (\bar{a}_x \frac{\partial}{\partial x} + \bar{a}_y \frac{\partial}{\partial y} + \bar{a}_z \frac{\partial}{\partial z}) \cdot \bar{u} = \frac{\partial u_x}{\partial x} + \frac{\partial u_y}{\partial y} + \frac{\partial u_z}{\partial z}$$

$$\nabla \times \bar{u} = \bar{a}_x \left(\frac{\partial u_z}{\partial y} - \frac{\partial u_y}{\partial z} \right) + \bar{a}_y \left(\frac{\partial u_x}{\partial z} - \frac{\partial u_z}{\partial x} \right) + \bar{a}_z \left(\frac{\partial u_y}{\partial x} - \frac{\partial u_x}{\partial y} \right)$$

$$\nabla^2 p = \nabla \cdot \nabla p = \frac{\partial^2 p}{\partial x^2} + \frac{\partial^2 p}{\partial y^2} + \frac{\partial^2 p}{\partial z^2}$$

$$\nabla \times \nabla p = 0 \quad \nabla \cdot \nabla \times \bar{u} = 0$$

$$\nabla \times (\nabla \times \bar{u}) = \nabla(\nabla \cdot \bar{u}) - \nabla^2 \bar{u}$$

CHAPTER II

OBLIQUE ACOUSTIC PLANE WAVES

The acoustic wave motion, when the wave amplitude is small, can be described by the following varying quantities:

$$p = p(x, y, z, t) = \text{acoustic or sound pressure (N/m}^2\text{)}$$

$$\bar{u} = \bar{u}(x, y, z, t) = \text{velocity vector of the air (m/sec)}$$

In order to relate these varying quantities for the acoustic wave motion, one requires one scalar equation and one vector equation.

From the equation of continuity one obtains:

$$\kappa \frac{\partial p}{\partial t} = -\nabla \cdot \bar{u} \quad (1)$$

which states that the velocity gradient produces a compression of the air, where the only forces involved are of compressive elasticity, measured by the compressibility κ . Since in the case of the acoustic wave motion there is zero heat conduction in the air, one should use the adiabatic compressibility given as follows for perfect diatomic gas, such as air:

$$\kappa = \frac{1}{\gamma P} = \frac{1}{1.4P} = \text{adiabatic compressibility (m}^2\text{/N) or (m}^3\text{/J)}$$

where P is the equilibrium pressure of the air.

From the equation of wave motion one obtains:

$$\rho \frac{\partial \bar{u}}{\partial t} = -\nabla p \quad (2)$$

which states that a pressure gradient produces an acceleration of the air, where ρ is the equilibrium density of the air.

Taking the divergence on both sides of (2) and substituting (1) one obtains:

$$\nabla^2 p - \frac{1}{c^2} \frac{\partial^2 p}{\partial t^2} = 0 \quad (3)$$

where

$$c = \frac{1}{\sqrt{\kappa\rho}} = \sqrt{\frac{\gamma P}{\rho}} = \text{acoustic velocity of wave (m/s)}$$

Taking the gradient on both sides of (1) and substituting (2), using $\nabla \times \bar{u} = 0$, one obtains:

$$\nabla^2 \bar{u} - \frac{1}{c^2} \frac{\partial^2 \bar{u}}{\partial t^2} = 0 \quad (4)$$

Assuming harmonic time variation $e^{-i\omega t}$, where ω is the circular wave frequency, one may write the basic quantities of the oblique acoustic plane wave by using the phasor convention as follows:

$$p(x,y,z,t) = \text{Re} \sqrt{2} P e^{i(\bar{k} \cdot \bar{r} - \omega t)} \quad (5a)$$

$$\bar{u}(x,y,z,t) = \text{Re} \sqrt{2} \bar{U} e^{i(\bar{k} \cdot \bar{r} - \omega t)} \quad (5b)$$

where P and \bar{u} are complex constant quantities, and one has:

$$\bar{k} = k_x \bar{a}_x + k_y \bar{a}_y + k_z \bar{a}_z = \text{propagation vector (constant)} \quad (6a)$$

$$\bar{r} = x \bar{a}_x + y \bar{a}_y + z \bar{a}_z = \text{position vector} \quad (6b)$$

$$\bar{k} \cdot \bar{r} = k_x x + k_y y + k_z z \quad (6c)$$

Omitting the convention $\text{Re}\sqrt{2}$ from (5), one may find from (5) and (6):

$$\frac{\partial P}{\partial t} = -i\omega P \quad \frac{\partial \bar{u}}{\partial t} = -i\omega \bar{u} \quad (7a)$$

$$\nabla P = (ik_x \bar{a}_x + ik_y \bar{a}_y + ik_z \bar{a}_z)P = i\bar{k}P \quad (7b)$$

$$\nabla \cdot \bar{u} = (ik_x u_x + ik_y u_y + ik_z u_z) = i\bar{k} \cdot \bar{u} \quad (7c)$$

where the operator $\nabla \equiv i\bar{k}$ when it operates on an oblique acoustic plane wave given in (5).

Substituting (7) in (1) and (2) one obtains:

$$-i\omega k P = -i\bar{k} \cdot \bar{u} \quad (8a)$$

$$-i\omega P \bar{u} = -i\bar{k}P \quad (8b)$$

Taking the dot product of both sides of (8b) with the propagation vector \bar{k} and substituting (8a) one obtains:

$$k^2 = \bar{k} \cdot \bar{k} = |\bar{k}|^2 = k_x^2 + k_y^2 + k_z^2 = \omega^2 \rho \kappa = \left(\frac{\omega}{c}\right)^2 = \left(\frac{2\pi}{\lambda}\right)^2 \quad (9)$$

where (9) gives the magnitude of the propagation vector \bar{k} . The direction of the propagation vector \bar{k} is given in (5) in the direction of the propagation of the oblique acoustic plane wave, and it is perpendicular to the planes of constant phase of the oblique acoustic plane wave. From (8b) one finds that the velocity vector \bar{u} of the oblique acoustic wave is in the direction of the propagation vector \bar{k} and the direction of propagation of the wave; this direction is usually called the longitudinal direction L, and the corresponding unit vector is denoted by \bar{a}_L :

$$\bar{k} = |\bar{k}| \bar{a}_L = k \bar{a}_L, \quad |\bar{a}_L| = 1 \quad (10)$$

where \bar{k} is the propagation vector and $k = |\bar{k}| = \frac{\omega}{c} = 2\pi/\lambda$ is the wave number, λ being the wavelength. Using (10) in (8b) one obtains:

$$\bar{u} = \frac{\bar{k}p}{\omega\rho} = \frac{k}{\omega\rho} p \bar{a}_L = u_L \bar{a}_L \quad (11)$$

From (9) and (11) one has:

$$\frac{p}{u_L} = \frac{\omega\rho}{k} = \frac{k}{\omega\kappa} = \sqrt{\frac{\rho}{\kappa}} = \frac{1}{\kappa c} = \rho c = Z \quad (12)$$

where Z is the characteristic acoustic wave impedance in infinite medium in (Nsec/m³) or (Kg/m²sec). An identical result is obtained

by substituting (10) and (11) in (8a). From the above discussion one may rewrite the oblique acoustic plane wave in (5) in the form:

$$p(x,y,z,t) = P e^{i(\bar{k} \cdot \bar{r} - \omega t)} \quad (13a)$$

$$\bar{u}(x,y,z,t) = \frac{P}{Z} \bar{a}_L e^{i(\bar{k} \cdot \bar{r} - \omega t)} = \frac{\bar{k}}{\rho c k} P e^{i(\bar{k} \cdot \bar{r} - \omega t)} \quad (13b)$$

where the convention terms $\text{Re}\sqrt{Z}$ have been omitted, and (13) represents a longitudinal wave.

Let the boundary between two acoustic media, medium 1 and medium 2, be given by $z = 0$, as in Figure 1. Let the incident oblique acoustic wave be propagating in medium 1 and be given from (13) by:

$$p_i(x,y,z,t) = P_I e^{i(\bar{k}_I \cdot \bar{r} - \omega t)} \quad (14a)$$

$$\bar{u}_i(x,y,z,t) = \frac{P_I}{Z_1} \bar{a}_{LI} e^{i(\bar{k}_I \cdot \bar{r} - \omega t)} \quad (14b)$$

The reflected wave from the boundary $z = 0$ into medium 1 will be given by:

$$p_r(x,y,z,t) = P_R e^{i(\bar{k}_R \cdot \bar{r} - \omega t)} \quad (15a)$$

$$\bar{u}_r(x,y,z,t) = \frac{P_R}{Z_1} \bar{a}_{LR} e^{i(\bar{k}_R \cdot \bar{r} - \omega t)} \quad (15b)$$

The transmitted wave into medium 2 will be given by:

$$p_t(x,y,z,t) = P_T e^{i(\bar{k}_T \cdot \bar{r} - \omega t)} \quad (16a)$$

$$\bar{u}_t(x,y,z,t) = \frac{P_T}{Z_2} \bar{a}_{LT} e^{i(\bar{k}_T \cdot \bar{r} - \omega t)} \quad (16b)$$

For a given oblique incident acoustic wave P_I and \bar{k}_I in (14), one would like to find the reflected wave P_R and \bar{k}_R in (15) and the transmitted wave P_T and \bar{k}_T in (16). The general configuration is given in Figure 1.

The first boundary condition will require that the pressure of the acoustic waves will be continuous across the boundary $z = 0$. Applying this boundary condition at $z = 0$ one obtains from (14a), (15a) and (16a):

$$P_I e^{i(k_{Ix}x + k_{Iy}y)} + P_R e^{i(k_{Rx}x + k_{Ry}y)} = P_T e^{i(k_{Tx}x + k_{Ty}y)} \quad (17)$$

The second boundary condition will require that the normal component to the boundary of the velocity vector of the acoustic waves will be continuous across the boundary $z = 0$. Applying this boundary condition at $z = 0$ one obtains from (14b), (15b) and (16b):

$$\begin{aligned} \frac{P_I}{Z_1} \bar{a}_{LI} \cdot \bar{a}_z e^{i(k_{Ix}x + k_{Iy}y)} + \frac{P_R}{Z_1} \bar{a}_{LR} \cdot \bar{a}_z e^{i(k_{Rx}x + k_{Ry}y)} = \\ = \frac{P_T}{Z_2} \bar{a}_{LT} \cdot \bar{a}_z e^{i(k_{Tx}x + k_{Ty}y)} \end{aligned} \quad (18)$$

Since (17) and (18) should apply to every point (x,y) on the boundary $z = 0$, one requires that all the exponential factors will have the same form, and one obtains:

$$k_x = k_{Ix} = k_{Rx} = k_{Tx} \quad (19a)$$

$$k_y = k_{Iy} = k_{Ry} = k_{Ty} \quad (19b)$$

Using (9) one obtains from (19):

$$\bar{k}_I = k_x \bar{a}_x + k_y \bar{a}_y + \sqrt{k_1^2 - k_x^2 - k_y^2} \bar{a}_z \quad (20a)$$

$$\bar{k}_R = k_x \bar{a}_x + k_y \bar{a}_y - \sqrt{k_1^2 - k_x^2 - k_y^2} \bar{a}_z \quad (20b)$$

$$\bar{k}_T = k_x \bar{a}_x + k_y \bar{a}_y + \sqrt{k_2^2 - k_x^2 - k_y^2} \bar{a}_z \quad (20c)$$

where $k_1 = \omega/c_1 = 2\pi/\lambda_1$ and $k_2 = \omega/c_2 = 2\pi/\lambda_2$. The angle of incidence θ_I will be designated as the angle between \bar{k}_I and the positive z axis direction \bar{a}_z . The angle of reflection θ_R will be designated as the angle between \bar{k}_R and the positive z direction \bar{a}_z . The angle of transmission θ_T will be designated as the angle between \bar{k}_T and the positive z direction \bar{a}_z . Taking the cross product of (20a), (20b) and (20c) with \bar{a}_z one obtains:

$$\bar{k}_I \times \bar{a}_z = \bar{k}_R \times \bar{a}_z = \bar{k}_T \times \bar{a}_z = -k_x \bar{a}_y + k_y \bar{a}_x \quad (21)$$

From (21) one finds that \bar{k}_I , \bar{k}_R and \bar{k}_T are all vectors in the same plane of incidence, defined by \bar{k}_I and \bar{a}_z . From the definition of the cross product of vectors one obtains from (21):

$$k_1 \sin \theta_I = k_1 \sin \theta_R = k_2 \sin \theta_T \quad (22a)$$

From (22a) one has, using (9):

$$\theta_R = \pi - \theta_I; \quad \frac{\sin\theta_I}{\sin\theta_T} = \frac{k_2}{k_1} = \frac{c_1}{c_2} = \frac{\lambda_1}{\lambda_2} \quad (22b)$$

where (22b) represents the Snell's law of reflection and refraction.

If $c_2 > c_1$ one has from (22b) $\theta_T > \theta_I$. For the case $\theta_T = 90^\circ$ the refractive wave will be grazing the boundary, and one has the corresponding critical angle of incidence θ_{Ic} given by:

$$\sin\theta_{Ic} = \frac{c_1}{c_2} \quad c_1 < c_2 \quad (23)$$

If the angle of incidence is equal or greater than the critical angle $\theta_I \geq \theta_{Ic}$, no acoustic wave energy is transmitted into the second medium.

Using (19) and the angles θ_I , θ_R and θ_T defined above, one obtains from (17) and (18):

$$P_I + P_R = P_T \quad (24a)$$

$$\frac{P_I}{Z_1} \cos\theta_I + \frac{P_R}{Z_1} \cos\theta_R = \frac{P_T}{Z_2} \cos\theta_T \quad (24b)$$

Substituting $\theta_R = \pi - \theta_I$ in (24b) one has:

$$P_T - P_R = P_I \quad (25a)$$

$$\frac{\cos\theta_T}{Z_2} P_T + \frac{\cos\theta_I}{Z_1} P_R = \frac{\cos\theta_I}{Z_1} P_I \quad (25b)$$

Equations (25a) and (25b) represent two equations of two unknowns

P_T and P_R in terms of P_I , and their solution gives:

$$R = \frac{P_R}{P_I} = \frac{Z_2 \cos \theta_I - Z_1 \cos \theta_T}{Z_2 \cos \theta_I + Z_1 \cos \theta_T} \quad (26a)$$

$$T = \frac{P_T}{P_I} = \frac{2Z_2 \cos \theta_I}{Z_2 \cos \theta_I + Z_1 \cos \theta_T} \quad (26b)$$

where $Z_1 = \rho_1 c_1$, $Z_2 = \rho_2 c_2$, R is the reflection coefficient and T is the transmission coefficient. For a given oblique incident acoustic wave (14a) on a plane boundary $z = 0$ between two media, one will obtain the reflected and transmitted oblique acoustic waves by substituting (20) and (26) in (15) and (16).

From (26a) one finds that there is no reflection under the following condition:

$$\rho_2 c_2 \cos \theta_I = \rho_1 c_1 \cos \theta_T \quad R = 0 \quad (27a)$$

Taking the square of both sides of (27a) and using (22b) one obtains:

$$\rho_2^2 c_2^2 \cos^2 \theta_I = \rho_1^2 c_1^2 (1 - \sin^2 \theta_T) = \rho_1^2 c_1^2 \left(1 - \frac{c_2^2}{c_1^2} \sin^2 \theta_I\right) \quad (27b)$$

which will give by using trigonometric identities:

$$\tan^2 \theta_I = \frac{\rho_2^2 c_2^2 - \rho_1^2 c_1^2}{\rho_1^2 c_1^2 - \rho_1^2 c_2^2} = \frac{(\rho_2/\rho_1)^2 - (c_1/c_2)^2}{(c_1/c_2)^2 - 1} \quad (27c)$$

where the angle of incidence θ_I in (27c) will give transmission only and no reflection $R = 0$. The incidence angle (27c) exists for this case if $\rho_2/\rho_1 > c_1/c_2 > 1$ or $\rho_2/\rho_1 < c_1/c_2 < 1$. This incidence angle is commonly referred to as the angle of intromission. In electromagnetic waves this angle of incidence, where there is no reflection, but only transmission, is known as the polarizing angle or Brewster angle.

For the case $c_1 > c_2$ if the angle of incidence $\theta_I \rightarrow 90^\circ$ one finds $\cos\theta_I \rightarrow 0$ and one has from (26b):

$$c_1 > c_2, \theta_I \rightarrow 90^\circ, T \rightarrow 0 \quad (28)$$

Consequently, as the angle of incidence approaches 90° there is complete reflection of the incidence acoustic wave energy, and no transmission, irrespective of the relative characteristics of the impedances of the two media.

CHAPTER III

OBLIQUE ACOUSTIC WAVE ON AN INFINITE PANEL

In the present chapter the case of an oblique acoustic plane wave in an infinite fluid (air), obliquely incident on an infinite panel (plate) will be discussed.

Assuming harmonic time variation $e^{-i\omega t}$, the inhomogeneous partial differential equation which governs the lateral displacement of the panel (plate) situated at $z = 0$ can be rewritten as follows:

$$\nabla^4 \eta - \frac{\rho_p h \omega^2}{D} \eta = \frac{P_z}{D} \quad (29a)$$

$$\text{where } \nabla^4 \eta = \left(\frac{\partial^2}{\partial x^2} + \frac{\partial^2}{\partial y^2} \right)^2 \eta = \frac{\partial^4 \eta}{\partial x^4} + 2 \frac{\partial^4 \eta}{\partial x^2 \partial y^2} + \frac{\partial^4 \eta}{\partial y^4}$$

where $\eta(x,y)$ = lateral displacement of the plate (m).

$P_z(x,y)$ = external net force per unit area in the positive z direction (N/m^2).

ρ_p = mass density of the plate (Kg/m^3).

h = thickness of the plate (m).

$\omega = 2\pi f$ = circular frequency of the wave (1/sec).

$D = \frac{Eh^3}{12(1-\nu^2)}$ = bending or flexural rigidity of the plate (Nm).

E = Young's modulus of elasticity (N/m^2).

ν = Poisson's ratio ($\nu = .03$ for steel and aluminum).

Equation (29a) may be rewritten in the form:

$$\nabla^4 \eta - \gamma^4 \eta = \frac{\gamma^4}{\rho_p h \omega^2} P_z \quad (29b)$$

where the plate wave number γ is defined by:

$$\gamma^4 = \frac{\rho_p h \omega^2}{D} = \frac{12(1 - \nu^2) \rho_p \omega^2}{Eh^2} \quad (1/m^4) \quad (29c)$$

Let an infinite panel (plate) be situated at $z = 0$ in the x - y plane as shown in Figure 1. Let an oblique acoustic plane wave propagating in the direction \bar{k}_I be incident on the infinite plate, and be given by (14) in the region $z \leq 0$ in the form:

$$p_I(x, y, z, t) = P_I e^{i(\bar{k}_I \cdot \bar{r} - \omega t)} \quad (z \leq 0) \quad (30a)$$

$$\bar{u}_I(x, y, z, t) = \frac{P_I}{\rho c k} \bar{k}_I e^{i(\bar{k}_I \cdot \bar{r} - \omega t)} \quad (z \leq 0) \quad (30b)$$

where $\bar{k}_I = k \bar{a}_{LI}$, and the unit vector \bar{a}_{LI} has one component in the positive z -direction. This oblique incident acoustic plane wave will be reflected by the infinite plate in the form of an oblique reflected acoustic plane wave propagating in the direction \bar{k}_R , and be given by (15) in the region $z \leq 0$ in the form:

$$p_R(x, y, z, t) = P_R e^{i(\bar{k}_R \cdot \bar{r} - \omega t)} \quad (z \leq 0) \quad (31a)$$

$$\bar{u}_R(x, y, z, t) = \frac{P_R}{\rho c k} \bar{k}_R e^{i(\bar{k}_R \cdot \bar{r} - \omega t)} \quad (z \leq 0) \quad (31b)$$

where $\bar{k}_R = k \bar{a}_{LR}$, and the unit vector \bar{a}_{LR} has one component in the negative z -direction. The oblique incident acoustic plane wave will cause the infinite plate to vibrate harmonically in the lateral positive z -direction in the form:

$$\eta(x, y, t) = A e^{i(k_{Px}x + k_{Py}y - \omega t)} \quad (z = 0) \quad (32)$$

where η is the lateral displacement of the plate in the positive z-direction; the velocity of the plate in the positive z-direction may be found from (32) to give:

$$u_{pz} = \frac{d\eta}{dt} = -i\omega A e^{i(k_{Px}x + k_{Py}y - \omega t)} \quad (z = 0) \quad (33)$$

No plate boundary conditions are applied to (32) and (33) since the plate is of infinite dimensions in both x and y directions.

The vibrations of the plate given in (32) and (33) will generate on the other side of the plate $z \geq 0$ an oblique acoustic transmitted plane wave in the direction \bar{k}_T , which will be given by (16) in the region $z \geq 0$ in the form:

$$p_t(x, y, z, t) = P_T e^{i(\bar{k}_T \cdot \bar{r} - \omega t)} \quad (z \geq 0) \quad (34a)$$

$$\bar{u}_t(x, y, z, t) = \frac{P_T}{\rho c k} \bar{k}_T e^{i(\bar{k}_T \cdot \bar{r} - \omega t)} \quad (z \geq 0) \quad (34b)$$

where $\bar{k}_T = k \bar{a}_{LT}$, and the unit vector \bar{a}_{LT} has one component in the positive z-direction.

The total external force per unit area p_z on the plate at $z = 0$ in the positive z-direction by the incident oblique acoustic wave (30a), the reflected oblique acoustic wave (31a) and the transmitted oblique acoustic wave (34a) is given by:

$$\begin{aligned}
p_z(x,y,t) = & P_I e^{i(k_{Ix}x + k_{Iy}y - \omega t)} + \\
& + P_R e^{i(k_{Rx}x + k_{Ry}y - \omega t)} - P_T e^{i(k_{Tx}x + k_{Ty}y - \omega t)} \quad (35)
\end{aligned}$$

where the incident and the reflected oblique acoustic waves at $z < 0$ pressure the plate in the positive z -direction, and the transmitted oblique acoustic wave at $z > 0$ pressure the plate in the negative z -direction. Substituting (32) in (29b) one finds:

$$\begin{aligned}
\frac{\gamma^4}{\rho_p h \omega^2} p_z(x,y,t) = & [k_{Px}^4 + 2k_{Px}^2 k_{Py}^2 + k_{Py}^4 - \gamma^4] A e^{i(k_{Px}x + k_{Py}y - \omega t)} \\
= & [(k_{Px}^2 + k_{Py}^2)^2 - \gamma^4] A e^{i(k_{Px}x + k_{Py}y - \omega t)} \quad (36)
\end{aligned}$$

Substituting (35) on the left hand side of (36) one requires the identity to be correct for all (x,y) in the plane of the plate $z = 0$, and as a result one has:

$$k_x = k_{Ix} = k_{Rx} = k_{Tx} = k_{Px} \quad (37a)$$

$$k_y = k_{Iy} = k_{Ry} = k_{Ty} = k_{Py} \quad (37b)$$

Substituting (35) in (36) and using (37) one obtains:

$$[(k_x^2 + k_y^2)^2 - \gamma^4] A = \frac{\gamma^4}{\rho_p h \omega^2} [P_I + P_R - P_T] \quad (38)$$

where for the particular case of normal incidence of the acoustic plane wave on the plate one will have $k_x = k_y = 0$.

The plate velocity u_{pz} , and the fluid (air) velocity of the oblique acoustic waves in the z -direction \bar{a}_z on either side of the plate should be identical. On the positive side of the plate $z > 0$ at the plate $z = 0$, denoted by $z = 0_+$, the plate velocity u_{pz} in the positive z -direction should be identical with the transmitted acoustic wave velocity vector in the z -direction u_{tz} , as follows:

$$u_{pz}(z = 0_+) = u_{tz}(z = 0_+) \quad (39a)$$

Substituting (33) and (34b) in (39a) and using (37) one obtains:

$$-i\omega A = \frac{1}{\rho c k} (\bar{k}_T \cdot \bar{a}_z) P_T \quad (39b)$$

where for the particular case of normal incidence on the plate one will have $\bar{k}_T = k \bar{a}_z$. On the negative side of the plate $z < 0$ at the plate $z = 0$, denoted by $z = 0_-$, the plate velocity u_{pz} should be identical with the sum of the oblique incident acoustic wave velocity in the positive z -direction u_{iz} , and the oblique reflected acoustic wave velocity in the positive z -direction u_{rz} , as follows:

$$u_{pz}(z = 0_-) = u_{iz}(z = 0_-) + u_{rz}(z = 0_-) \quad (40a)$$

Substituting (30b), (31b) and (33) in (40a) and using (37) one obtains:

$$-i\omega A = \frac{1}{\rho c k} (\bar{k}_I \cdot \bar{a}_z) P_I + \frac{1}{\rho c k} (\bar{k}_R \cdot \bar{a}_z) P_R \quad (40b)$$

where for the particular case of normal incidence on the plate one will have $\bar{k}_I = k \bar{a}_z$ and $\bar{k}_R = -k \bar{a}_z$. From (39b) and (40b) one obtains:

$$(\bar{k}_I \cdot \bar{a}_z) P_I = (\bar{k}_T \cdot \bar{a}_z) P_T - (\bar{k}_R \cdot \bar{a}_z) P_R \quad (41)$$

where for the particular case of normal incidence one has $\bar{k}_I = \bar{k}_T = -\bar{k}_R = k \bar{a}_z$

From (6a), (9) and (37) one has:

$$\bar{k}_I = k_x \bar{a}_x + k_y \bar{a}_y + k_z \bar{a}_z \quad (42a)$$

$$\bar{k}_R = k_x \bar{a}_x + k_y \bar{a}_y - k_z \bar{a}_z \quad (42b)$$

$$\bar{k}_T = k_x \bar{a}_x + k_y \bar{a}_y + k_z \bar{a}_z \quad (42c)$$

$$k_z = \sqrt{k^2 - k_x^2 - k_y^2} = \sqrt{\left(\frac{\omega}{c}\right)^2 - k_x^2 - k_y^2} \quad (42d)$$

Using (42c) in (39b) one has:

$$-i\omega A = \frac{k_z}{\rho c k} P_T \quad (43a)$$

Using (42a) and (42b) in (40b) one has:

$$-i\omega A = \frac{k_z}{\rho c k} (P_I - P_R) \quad (43b)$$

Taking the angle of incidence θ to be the angle between the incident wave propagation vector \bar{k}_I and the positive z axis, as shown in Figure 1, one finds from (42a) and (42d):

$$k_z = \bar{k}_I \cdot \bar{a}_z = k \cos\theta \quad (44a)$$

$$\sqrt{k_x^2 + k_y^2} = \sqrt{k^2 - k_z^2} = k \sin\theta \quad (44b)$$

From (42b) and (42c) one finds, as shown in Figure 1, that the angle of transmission is also θ , and the angle of reflection is $\pi - \theta$ with the positive z -axis. Substituting (44) in (38), (43a) and (43b) one has:

$$\left(k^4 \sin^4 \theta - \gamma^4\right) A = \frac{\gamma^4}{\rho_p h \omega^2} \left(P_I + P_R - P_T\right) \quad (45a)$$

$$-i\omega A = \frac{\cos\theta}{\rho c} P_T \quad (45b)$$

$$-i\omega A = \frac{\cos\theta}{\rho c} (P_I - P_R) \quad (45c)$$

where for normal incidence one has $\theta = 0$ in (45).

From a given oblique acoustic incident plane wave P_I on the infinite plate, one obtains the unknown P_R , P_T and A by solving the three linear equations (45). From (45b) and (45c) one obtains:

$$P_I = P_R + P_T \quad (46a)$$

From (46a) one has:

$$P_I + P_R - P_T = 2P_I - 2P_T \quad (46b)$$

Substituting (45b) and (46b) in (45a) one obtains:

$$\left(k^4 \sin^4 \theta - \gamma^4 \right) \frac{i \cos \theta}{\omega \rho c} P_T = \frac{2\gamma^4}{\rho_p h \omega^2} \left(P_I - P_T \right) \quad (47a)$$

From (47a) one obtains:

$$\left[\left(\frac{k}{\gamma} \right)^4 \sin^4 \theta - 1 \right] \frac{\rho_p h \omega i \cos \theta}{2 \rho c} P_T = P_I - P_T \quad (47b)$$

The coupling parameter μ between the plate and the air is defined as follows:

$$\mu = \frac{2\rho}{\rho_p h} \quad (1/m)$$

where: ρ = air density (Kg/m^3).

ρ_p = plate material density (Kg/m^3).

h = thickness of plate (m).

By substituting the coupling parameter $\mu = \frac{2\rho}{\rho_p h}$ and the acoustic wave number $k = \frac{\omega}{c} = \frac{2\pi}{\lambda}$ one has:

$$\frac{\rho_p h \omega}{2 \rho c} = \frac{k}{\mu} \quad (48)$$

Substituting (48) in (47b) one obtains:

$$\left[\left(\frac{k}{\gamma} \right)^4 \sin^4 \theta - 1 \right] i \left(\frac{k}{\mu} \right) \cos \theta P_T = P_I - P_T \quad (49a)$$

Let us define:

$$Q(\theta) = \left[1 - \left(\frac{k}{\gamma}\right)^4 \sin^4 \theta \right] \frac{k}{u} \cos \theta \quad (49b)$$

Equation (49a) can be rewritten in the form:

$$-iQ(\theta)P_T = P_I - P_T \quad (49c)$$

From (49c) one obtains:

$$\frac{P_T}{P_I} = \frac{1}{1 - iQ(\theta)} \quad (50a)$$

Using (50a) in (46a) one has:

$$\frac{P_R}{P_I} = \frac{-iQ(\theta)}{1 - iQ(\theta)} \quad (50b)$$

Using (50a) in (45b) one obtains:

$$\frac{A}{P_I} = \frac{i(1/\rho c \omega) \cos \theta}{1 - iQ(\theta)} \quad (50c)$$

where (50) are the solutions of (45), and $Q(\theta)$ is defined in (49b).

By rotating the x and y coordinates around the z -axis one can obtain $k_y = 0$, and the plane of incidence will be located in the x - z plane, with no variation in the y direction. Taking $k_y = 0$ and substituting (44a) and (44b) in (30a), (31a), (32) and (34a) and using (37a) and (42), one obtains for the oblique acoustic waves:

$$P_I = P_I e^{ik(x \sin \theta + z \cos \theta)} e^{-i\omega t} \quad (51a)$$

$$P_r = P_R e^{ik(x\sin\theta - z\cos\theta)} e^{-i\omega t} \quad (51b)$$

$$P_t = P_T e^{ik(x\sin\theta + z\cos\theta)} e^{-i\omega t} \quad (51c)$$

$$\eta = A e^{ikx\sin\theta} e^{-i\omega t} \quad (51d)$$

where P_R , P_T and A are given in (50) in terms of P_I . For the particular case of normal incidence on the plate the corresponding results may be obtained by taking $\theta = 0$.

CHAPTER IV

NOISE REDUCTION FOR INFINITE PANEL

The Transmission Loss coefficient is defined as the ratio of the incident acoustic wave pressure power to the transmitted acoustic wave pressure power. From (51) one obtains the Transmission Loss coefficient TL_{db} in decibels in the form:

$$TL_{db} = 10 \log \frac{|P_i|^2}{|P_t|^2} = 10 \log \left| \frac{P_i}{P_t} \right|^2 \quad (52a)$$

Substituting (50a) for the present case in (52a) one has:

$$TL_{db} = 10 \log |1 - iQ|^2 = 10 \log[1 + Q^2] \quad (52b)$$

One has from (49b):

$$Q = [1 - \left(\frac{k}{\gamma}\right)^4 \sin^4 \theta] \frac{k}{\mu} \cos \theta \quad (53a)$$

where θ is the angle of incidence, and $\theta = 0$ represents the case of normal to the plate incidence of the acoustic wave. Substituting $\gamma^4 = \frac{\rho_p h \omega^2}{D}$,

$k = \omega/c$ and $\mu = \frac{2\rho}{\rho_p h}$ in (53a) one obtains:

$$Q = [1 - \frac{D\omega^2}{\rho_p hc^4} \sin^4 \theta] \frac{\rho_p h \omega}{2\rho c} \cos \theta \quad (53b)$$

where (53b) gives the functional variation of Q with respect to the angle of incidence θ and the wave frequency ω .

Usually the measurements are done by two microphones which measure the pressure power of the acoustic waves. One microphone is situated on the source side of the panel at $z = -d_1$ (the source microphone), and it measures the total acoustic wave pressure power at that point of both the incident and the reflected acoustic waves. The other microphone is situated on the other side of the panel at $z = +d_2$ (the receiver microphone), and it measures the total acoustic wave pressure power at that point of the transmitted acoustic wave. The Noise Reduction coefficient in decibels is defined as the ratio of the total acoustic wave pressure power measured by the source microphone at $z = -d_1$, to the acoustic wave pressure power measured by the receiver microphone at $z = +d_2$. From (51) one obtains the Noise Reduction coefficient NR_{db} in decibels in the form:

$$\begin{aligned}
 NR_{db} &= 10 \log \frac{|p_i + p_r|_{z = -d_1}^2}{|p_t|_{z = +d_2}^2} \\
 &= 10 \log \left| \frac{P_I e^{-ikd_1 \cos \theta} + P_R e^{+ikd_1 \cos \theta}}{P_T e^{ikd_2 \cos \theta}} \right|^2 \quad (54a)
 \end{aligned}$$

Substituting (50a) and (50b) for the present case in (54a) one obtains:

$$\begin{aligned}
 NR_{db} &= 10 \log \left| \frac{e^{-ikd_1 \cos \theta} - \frac{iQ}{1-iQ} e^{+ikd_1 \cos \theta}}{\frac{1}{1-iQ}} \right|^2 = \\
 &= 10 \log \left| (1 - iQ)e^{-ikd_1 \cos \theta} - iQe^{+ikd_1 \cos \theta} \right|^2 = \\
 &= 10 \log \left| e^{-ikd_1 \cos \theta} - iQ2\cos(kd_1 \cos \theta) \right|^2 = \\
 &= 10 \log \left| \cos(kd_1 \cos \theta) - i\sin(kd_1 \cos \theta) - i2Q\cos(kd_1 \cos \theta) \right|^2 \quad (54b)
 \end{aligned}$$

where (54b) may be rewritten in the form:

$$\begin{aligned} NR_{db} &= 10 \log \{ \cos^2(kd_1 \cos \theta) + [\sin(kd_1 \cos \theta) + 2Q \cos(kd_1 \cos \theta)]^2 \} = \\ &= 10 \log [1 + 4Q \sin(kd_1 \cos \theta) \cos(kd_1 \cos \theta) + 4Q^2 \cos^2(kd_1 \cos \theta)] \quad (54c) \end{aligned}$$

By using the trigonometric identities:

$$\begin{aligned} \sin 2\alpha &= 2 \sin \alpha \cos \alpha \\ 2 \cos^2 \alpha &= 1 + \cos 2\alpha \end{aligned}$$

Equation (54c) can be rewritten in the form:

$$NR_{db} = 10 \log [1 + 2Q^2 + 2Q \sin(2kd_1 \cos \theta) + 2Q^2 \cos(2kd_1 \cos \theta)] \quad (54d)$$

where the Noise Reduction coefficient NR_{db} depends on the position of the source microphone $z = -d_1$. One sees from (54d) that the Noise Reduction coefficient curve NR_{db} consists of an average value superimposed by oscillating component of sine and cosine which are functions of the distance of the source $z = -d_1$ and the frequency ω , since $k = \omega/c$. Denoting the average value of the Noise Reduction coefficient by \overline{NR}_{db} one obtains from (54d):

$$\overline{NR}_{db} = 10 \log [1 + 2Q^2] \quad (54e)$$

where \overline{NR}_{db} is the average Noise Reduction coefficient and the parameter Q is given in (53a) and (53b). For the particular case $kd_1 = 2\pi \frac{d_1}{\lambda} \ll 1$ (54d) will reduce to:

$$NR_{db} = 10 \log [1 + 4Q^2] \text{ for } |kd_1| \ll 1 \quad (54f)$$

For the case $|kd_1| \ll 1$ the Noise Reduction coefficient NR_{db} does not depend on the position of the source microphone $z = -d_1$. From (52b) and (54d) one finds that for $Q \gg 1$ one has:

$$\begin{aligned} NR_{db} - TL_{db} &= 10 \log(4Q^2) - 10 \log(Q^2) = \\ &= 10 \log 4 = 20 \log 2 = 20 \times 0.3010 = 6db \end{aligned}$$

which may be rewritten in the form:

$$NR_{db} = TL_{db} + 6db \text{ for } Q \gg 1 \text{ and } |kd_1| \ll 1 \quad (55)$$

For the case of $k \ll \mu$ one finds from (53a) that $Q \rightarrow 0$, and from (52b) and (54d) one has both the TL_{db} and the NR_{db} coefficients approach the values zero; the obliquely incident acoustic plane wave for $k \ll \mu$ will propagate through the infinite panel as if it is completely transparent to it. For the case $\omega \rightarrow 0$ one obtains from (53b) that $Q \rightarrow 0$. Thus for very low frequencies one finds from (52b) and (54d) that both TL_{db} and NR_{db} coefficients approach the zero value; for very low frequencies the obliquely incident acoustic plane wave will propagate through the infinite panel as if it is completely transparent to it. A similar result will be obtained for $\theta = \frac{\pi}{2}$, where from (53b) one has $Q = 0$. In this case the infinite plate is parallel to the direction of the acoustic wave propagation, and will not effect the acoustic wave propagation.

The Transmission Loss coefficient TL_{db} in (52b) and the Noise Reduction coefficient NR_{db} in (54d) both are functions of $Q^2(\omega)$, which may be found from (53b) in the form:

$$Q^2(\omega) = F\omega^2[1 - G\omega^2]^2 \quad (56a)$$

where one has:

$$F = \left(\frac{\rho_p h \cos \theta}{2\rho c}\right)^2 \quad (56b)$$

$$G = \frac{D \sin^4 \theta}{\rho_p h c^4} \quad (56c)$$

Taking the first two derivatives of (56a) with respect to ω one obtains:

$$\begin{aligned} \frac{1}{F} \frac{\partial Q^2(\omega)}{\partial \omega} &= 2\omega (1 - G\omega^2)^2 + \omega^2 2(1 - G\omega^2) (-2G\omega) = \\ &= 2\omega(1 - G\omega^2) (1 - 3G\omega^2) \end{aligned} \quad (57a)$$

$$\begin{aligned} \frac{1}{F} \frac{\partial^2 Q^2(\omega)}{\partial \omega^2} &= 2[1 - G\omega^2][1 - 3G\omega^2] + \\ &+ 2\omega[-2G\omega][1 - 3G\omega^2] + \\ &+ 2\omega[1 - G\omega^2][1 - 6G\omega] \end{aligned} \quad (57b)$$

Equating (57a) to zero $\frac{\partial Q^2(\omega)}{\partial \omega} = 0$ and solving for ω , one will obtain, using (56c), (57b) and the numerical values in the present case:

$$\omega_1 = 0 \qquad Q^2 = \min \qquad (58a)$$

$$\omega_2 = \frac{1}{\sqrt{3}\sqrt{G}} = \frac{1}{\sqrt{3}} \sqrt{\frac{\rho_p h}{D}} \frac{c^2}{\sin^2 \theta} \qquad Q^2 = \max \qquad (58b)$$

$$\omega_3 = \frac{1}{\sqrt{G}} = \sqrt{\frac{\rho_p h}{D}} \frac{c^2}{\sin^2 \theta} \qquad Q^2 = \min \qquad (58c)$$

Substituting (58a), (58b) and (58c) in (56a) one finds:

$$Q_1^2 = Q^2(\omega_1) = 0 \qquad Q_3^2 = Q^2(\omega_3) = 0 \qquad (59a)$$

$$Q_2^2 = Q^2(\omega_2) = \frac{1}{3} \left(\frac{2}{3}\right)^2 \frac{F}{G} \qquad (59b)$$

Using (56b), (56c), (58c) and $\mu = \frac{2\rho}{\rho_p h}$ one may rewrite (59b) in the form:

$$Q_2^2 = Q^2(\omega_2) = \frac{1}{27} \frac{\rho_p^3 h^3 c^2}{\rho^2 D} \frac{\cos^2 \theta}{\sin^4 \theta} = \left(\frac{2}{3} \frac{\omega_2 \cos \theta}{c\mu}\right)^2 \qquad (59c)$$

Substituting (59a), (59b) and (59c) in (52b) one obtains:

$$TL_{db}(\omega = \omega_1 = 0) = TL_{db}(\omega = \omega_3) = 0 \qquad (60a)$$

$$\begin{aligned} TL_{db}(\omega = \omega_2) &= 10 \log \left[1 + \frac{1}{3} \left(\frac{2}{3}\right)^2 \frac{F}{G} \right] = \\ &= 10 \log \left[1 + \left(\frac{2}{3} \frac{\omega_2 \cos \theta}{c\mu}\right)^2 \right] \end{aligned} \qquad (60b)$$

Substituting (59a), (59b) and (59c) in (54d) one obtains:

$$NR_{db}(\omega = \omega_1 = 0) = NR_{db}(\omega = \omega_3) = 0 \quad (61a)$$

$$\begin{aligned} NR_{db}(\omega = \omega_2) &= 10 \log \left[1 + \frac{4}{3} \left(\frac{2}{3} \right)^2 \frac{F}{G} \right] = \\ &= 10 \log \left[1 + \left(\frac{4}{3} \frac{\omega_2 \cos \theta}{c_\mu} \right)^2 \right] \end{aligned} \quad (61b)$$

Thus one finds from (60a) and (61a) that for $\omega = \omega_1 = 0$, and for $\omega = \omega_3$ given in (58c), the infinite plate (panel) behaves as if it is transparent to the oblique acoustic waves incident on it.

For the case $A\omega^2 \gg 1$ or $\omega \gg \omega_3 = \frac{1}{\sqrt{A}}$, where ω_3 is given in (58c), one obtains from (56a):

$$Q^2(\omega \gg \omega_3 = \frac{1}{\sqrt{A}}) = FG^2 \omega^6 = (2\pi)^6 BA^2 f^6 \quad (62)$$

where $f = \frac{\omega}{2\pi}$ is the frequency of the oblique incident acoustic plane wave. For the present case the value of (62) is much larger than 1, and therefore, by substituting (62) in (52b) one obtains:

$$\begin{aligned} TL_{db}(\omega \gg \omega_3 = \frac{1}{\sqrt{A}}) &= 10 \log[(2\pi)^6 FG^2 f^6] = \\ &= 10 \log[(2\pi)^6 FG^2] + 60 \log f \end{aligned} \quad (63)$$

Similarly, by substituting (62) in (54d) one obtains:

$$\begin{aligned} NR_{db}(\omega \gg \omega_3 = \frac{1}{\sqrt{G}}) &= 10 \log [4(2\pi)^6 FG^2 f^6] = \\ &= 10 \log[4(2\pi)^6 FG^2] + 60 \log f \end{aligned} \quad (64)$$

From (63) and (64) one obtains, using (55):

$$TL_{db} = C + 60 \log f \quad (65a)$$

$$NR_{db} = C + 6db + 60 \log f \quad (65b)$$

when one has:

$$C = 10 \log [(2\pi)^6 FG^2] \quad (66a)$$

From (56b) and (56c) one has:

$$\begin{aligned} BA^2 &= \left(\frac{\rho_p h \cos \theta}{2\rho c}\right)^2 \left(\frac{D \sin^4 \theta}{\rho_p h c^4}\right)^2 = \left(\frac{D}{2\rho c^5} \cos \theta \sin^4 \theta\right)^2 = \\ &= \left(\frac{D \cos \theta}{2\rho c}\right)^2 \left(\frac{\sin \theta}{c}\right)^8 \end{aligned} \quad (66b)$$

Substituting (66b) in (66a) one has:

$$C = 60 \log (2\pi) + 20 \log \left(\frac{D \cos \theta}{2\rho c}\right) + 80 \log \left(\frac{\sin \theta}{c}\right) \quad (66c)$$

One can see from (65a) and (65b) that by drawing TL_{db} and NR_{db} on a log paper, where the x-axis expressed in terms of $\log f$, one will obtain a straight line for $\omega \gg \omega_3 = \frac{1}{\sqrt{G}}$, with the constant C given in (66c). A doubling of the frequency (= raising the frequency by one octave) in this case will raise the Transmission Loss coefficient TL_{db} and the Noise Reduction coefficient NR_{db} by 18 db.

For the particular case of normal incidence $\theta = 0$ one obtains from (58a), (58b) and (58c):

$$\omega_1 = 0, \omega_2 = \infty, \omega_3 = \infty \quad (67)$$

Thus for the case of normal incidence the above phenomena of maximum (at $\omega = \omega_2$) and minimum (at $\omega = \omega_3$) in the TL_{db} and NR_{db} curves does not exist. Of course ω_2 and ω_3 in (67) will not be infinite, but will be limited by the critical frequency f_c to be discussed in the following.

Assuming in (29b) that there is no external force density $p_z = 0$, and there is a variation only in x-direction $\eta = \eta(x)$, one will obtain:

$$\frac{d^4 \eta}{dx^4} - \gamma^4 \eta = 0 \quad (68a)$$

which will be solved to give the following free motion elastic plate waves of the lateral displacement of the plate propagating along the plate:

$$\eta = \eta_0 e^{\pm \gamma x - i \omega t} \quad \text{Attenuated plate elastic waves} \quad (68b)$$

$$\eta = \eta_0 e^{i(\pm \gamma x - \omega t)} \quad \text{propagating plate elastic waves} \quad (68c)$$

where for the propagating plate elastic waves in (68c), the plate wave number γ can be given from (29c) in the form:

$$\gamma = \frac{\omega}{c_p} = \frac{2\pi f}{f\lambda_p} = \frac{2\pi}{\lambda_p} = \sqrt[4]{\frac{\rho_p h \omega^2}{D}} = \sqrt[4]{\frac{12(1-\nu^2)\rho_p}{E}} p \sqrt{\frac{\omega}{h}} \quad (1/m) \quad (69a)$$

where: c_p = wave velocity of the elastic plate waves (m/sec)

λ_p = wavelength of the elastic plate waves (m)

$\omega = 2\pi f$ = circular frequency of the wave (1/sec)

From (69a) one obtains:

$$c_p = \frac{\omega}{\gamma} = \sqrt[4]{\frac{D}{\rho_p h}} \sqrt{\omega} = \sqrt[4]{\frac{E}{12(1-\nu^2)\rho_p}} \sqrt{2\pi h f} \quad (\text{m/sec}) \quad (69b)$$

$$\lambda_p = \frac{2\pi}{\gamma} = 2\pi \sqrt[4]{\frac{D}{\rho_p h}} \frac{1}{\sqrt{\omega}} = \sqrt[4]{\frac{E}{12(1-\nu^2)\rho_p}} \sqrt{\frac{2\pi h}{f}} \quad (\text{m}) \quad (69c)$$

where $c_p = f\lambda_p$ and $c_p = c_p(f)$, with f being the frequency of the elastic wave along the infinite plate.

Assuming that an oblique acoustic plane wave is incident on the infinite plate in the x - z plane of incidence in an angle θ_I with the normal to the plate \bar{a}_z , as shown in Figure 1, the oblique acoustic plane wave propagation vector is given by \bar{k}_I , found for the present case from (20a):

$$\bar{k}_I = k_x \bar{a}_x + \sqrt{k^2 - k_x^2} \bar{a}_z = k \sin \theta_I \bar{a}_x + k \cos \theta_I \bar{a}_z \quad (70)$$

where $k = \omega/c$, c being the velocity of the acoustic wave in infinite space. Denoting the phase velocity of the oblique acoustic wave along the plate by c_x , one has $k_x = \omega/c_x$, and one obtains from (70):

$$c_x = \frac{\omega}{k_x} = \frac{\omega}{k \sin \theta_I} = \frac{c}{\sin \theta_I} \quad (71)$$

The critical frequency of radiation f_c of the infinite plate is defined by $c_p = c$ or by $\gamma = k$, and one obtains from (69b) for $f = f_c$:

$$c_p = \sqrt[4]{\frac{D}{\rho_p h}} \sqrt{2\pi f_c} \quad (72a)$$

From (72a) one may obtain the critical frequency of radiation f_c in the form:

$$f_c = \frac{c^2}{2\pi} \sqrt{\frac{\rho_p h}{D}} \quad (72b)$$

Substituting $D = Eh^3/12(1-\nu^2)$ in (72b) one obtains from (72b):

$$f_c = \frac{c^2}{2\pi h} \sqrt{\frac{12\rho_p(1-\nu^2)}{E}} \quad (72c)$$

Substituting the Poisson ratio ν for aluminum, one may obtain from (72c):

$$f_c = \frac{c^2}{1.9h} \sqrt{\frac{\rho_p}{E}} \quad \text{for } \nu = 0.3 \quad (72d)$$

When the velocity c_p of the elastic waves along the infinite plate is large than the phase velocity c of the acoustic waves in the air $c_p > c$, which implies $\gamma < k$ or $f > f_c$, the plate will radiate acoustic wave energy into the air, and it can be shown that the acoustic radiation ratio σ_{rad} , which is proportional to the acoustic power radiated by the plate, is given by:

$$\sigma_{\text{rad}} = \frac{1}{\sqrt{1 - (\frac{\gamma}{k})^2}} = \frac{1}{\sqrt{1 - \frac{f_c}{f}}} \quad \text{for } f > f_c \quad (73)$$

In the case of $f < f_c$ there is no acoustic wave power radiated from the infinite plate, provided that the plate behaves perfectly in accordance with (68a). For actual plates, which are not perfect, there is also some acoustic wave radiation even when $f < f_c$.

Comparing (58b) and (58c) with (72b) one finds for $f_2 = \omega_2/2\pi$ and $f_3 = \omega_3/2\pi$:

$$f_2 = \frac{f_c}{\sqrt{3} \sin^2 \theta} \quad f_3 = \frac{f_c}{\sin^2 \theta} \quad (74a)$$

From (74) one has $f_3 > f_c$, while $f_2 > f_c$ for $\theta < 49^\circ$ and $f_2 < f_c$ for $\theta > 49^\circ$. Thus the value of ω_3 in (58c) will be always affected by the radiated acoustic wave energy from the plate. The value of ω_2 in (58b) will be affected by the radiated acoustic wave energy from the plate only if $\theta < 49^\circ$.

In the experiments under discussion in the present report one has the numerical values:

$$\begin{aligned} h &= 0.025'' = 0.635 \text{ mm} = 0.635 \times 10^{-3} \text{ m} \\ \rho_p &= 2.7 \times 10^3 \text{ kg/m}^3 \\ E &= 7.0 \times 10^{10} \text{ N/m}^2 \\ c &= 343.8 \text{ m/sec} \end{aligned}$$

Substituting the above numerical values in (72d) one obtains:

$$f_c = 19,240 \text{ (1/sec)} \quad (74b)$$

where f_c is the critical frequency of radiation by the plate. Since the experiments discussed in the present report are in the frequency range $f \leq 5,000$ 1/sec, one has $f < f_c$, and the effect of acoustic wave radiation by the plate could be neglected, if one assumes a perfect plate.

CHAPTER V

OBLIQUE ACOUSTIC WAVE ON FINITE PANEL

In the present chapter the case of a plane acoustic wave incident on an oblique finite clamped panel (plate) in a rigid duct will be discussed.

It has been shown in a previous report that the fundamental mode of propagation of the acoustic waves propagating parallel to the axis of a rigid duct is identical with the plane acoustic wave propagating in the infinite fluid (air) limited by the walls of the rigid duct. The introduction of the walls of the rigid duct parallel to the direction of propagation does not affect the plane acoustic wave, since the boundary conditions of the walls of the rigid duct are obeyed; the fundamental mode of propagation of the acoustic wave in the duct propagates parallel to the axis of the duct as a plane acoustic wave, as if the duct rigid walls were not there. Thus, the introduction of the duct rigid walls parallel to the direction of propagation does not alter the behavior of the acoustic plane waves.

When one introduces a finite rectangular clamped panel (plate) in an oblique direction to the axis of the duct, one should apply the boundary conditions for a clamped rectangular plate. One is not able to use the solution for the infinite panel (plate) discussed in the previous two chapters without any boundary conditions. Thus, the introduction of the duct rigid walls parallel to the direction of propagation does not affect the incident plane acoustic waves, but it does introduce the effect of the clamped boundary conditions of the panel (plate), which is in

oblique direction to the axis of the duct, and is now clamped to the rigid walls of the duct. The solution given previously for the infinite panel (plate) for the lateral displacement η does not obey the boundary conditions for the clamped edges of the panel (plate). Therefore, the solution for the infinite panel (plate) given in the previous two chapters should be modified.

In order to simplify the analysis and limit it only to the fundamental resonance frequency of the oblique panel (plate) in the present chapter, it is assumed that the effect of the four clamped edges of the oblique plate in the duct is equivalent to a spring, forcing the plate to return to its position of equilibrium when no acoustic plane wave is incident on it. Thus, the oblique plate in the duct has been idealized by introducing the effect of the clamped edges' boundary conditions as an equivalent system of a single degree of freedom only. For small lateral displacements η of the oblique plate in the duct, the spring-like force per unit area is proportional to the lateral displacement of the plate, and can be expressed in the following form, by using the stiffness constant of the plate;

$$p_z^{\text{spring}} = -K\eta \quad (75)$$

where: p_z^{spring} = spring-like force density (N/m^2)

η = lateral displacement of the plate (m)

K = stiffness constant of the plate (N/m^3)

The formulation of the structural damping of the vibrating plate can be accomplished by expressing the damping force per unit area as a purely imaginary constant, being proportional to the small lateral displacement, as follows, taking $i = \sqrt{-1}$:

$$p_z^{\text{damping}} = -i\alpha K\eta \quad (76)$$

where: p_z^{damping} = damping force density (N/m^2)

η = lateral displacement of the plate (m)

K = stiffness constant of the plate (N/m^3)

α = the damping factor (non-dimensional)

Equation (76) has been employed extensively in the dynamic analysis of aerospace structures.

The inertial force density associated with the lateral translation $\eta(x,y)$ of a plate element has been given as follows:

$$p_z^{\text{inertial}} = -\rho_p h \frac{d^2\eta}{dt^2} \quad (77)$$

where: p_z^{inertial} = inertial force per unit area (N/m^2)

ρ_p = mass density of the plate material (kg/m^3)

h = thickness of the plate (m)

$\rho_p h$ = mass of plate per unit area (kg/m^2)

The natural fundamental circular resonance frequency ω_0 will be defined for a spring-like system of one degree of freedom of this type as follows, using (75) and (77):

$$\omega_0 = \sqrt{\frac{K}{\rho_p h}}, \quad f_0 = \frac{1}{2\pi} \sqrt{\frac{K}{\rho_p h}} \quad (\text{1/sec}) \quad (78)$$

Revising the differential equation for static equilibrium for the plate $D\nabla^4\eta = p_z$, by adding the spring force in (75), the damping force in (76), and the inertial force in (77), one obtains:

$$\begin{aligned}
 DV^4 \eta &= p_z + p_z^{\text{inertial}} + p_z^{\text{spring}} + p_z^{\text{damping}} \\
 &= p_z - \rho_p h \frac{d^2 \eta}{dt^2} - K\eta - i\alpha K\eta
 \end{aligned} \tag{79a}$$

which could be rewritten in the form:

$$DV^4 \eta + \rho_p h \frac{d^2 \eta}{dt^2} + K(1 + i\alpha)\eta = p_z \tag{79b}$$

Substituting $K = \rho_p h \omega_o^2$ from (78) and assuming harmonic time variation $e^{-i\omega t}$ in (79b) one obtains:

$$DV^4 \eta - \rho_p h \omega^2 \left[1 - \frac{\omega_o^2}{\omega^2} (1 + i\alpha)\right] \eta = p_z(x, y) \tag{80a}$$

which may be rewritten in the form:

$$\nabla^4 \eta - \gamma_o^4 \eta = \frac{1}{D} p_z = \frac{\gamma^4}{\rho_p h \omega^2} p_z \tag{80b}$$

where γ has been defined in (29c), and the plate wave number γ_o for the present case is defined by:

$$\gamma_o^4 = \frac{\rho_p h \omega^2}{D} \left[1 - \frac{\omega_o^2}{\omega^2} (1 + i\alpha)\right] = \gamma^4 \left[1 - \frac{\omega_o^2}{\omega^2} (1 + i\alpha)\right] (1/m^4) \tag{80c}$$

For the particular case of infinite unclamped plate $\omega_o = 0$, $\gamma_o = \gamma$, and (80b) reduces to (29b).

In the subsequent analysis the plate will be considered to be infinite. However, the effect of the plate being finite in extent, and clamped at the

edges, will be introduced by the resonance frequency ω_0 in (80c). Furthermore, instead of considering the plane acoustic wave (the fundamental mode) propagating along the axis of the duct and incident on an oblique panel (plate) in accordance with the experimental set up, we will consider an oblique plane acoustic wave in infinite space incident on an infinite plate situated at $z = 0$, and subject to inertial force, spring-like force and damping force.

Let an infinite panel (plate) be situated at $z = 0$ in the x-y plane. Let an oblique acoustic plane wave propagating in the direction \bar{k}_I be incident on the infinite plate, and be given by (14) in the region $z \leq 0$ in the form:

$$p_i(x,y,z,t) = P_I e^{i(\bar{k}_I \cdot \bar{r} - \omega t)} \quad (z \leq 0) \quad (81a)$$

$$\bar{u}_i(x,y,z,t) = \frac{P_I \bar{k}_I}{\rho c k} e^{i(\bar{k}_I \cdot \bar{r} - \omega t)} \quad (z \leq 0) \quad (81b)$$

where $\bar{k}_I = k \bar{a}_{LI}$, and the unit vector \bar{a}_{LI} has one component in the positive z-direction. This oblique incident acoustic plane wave will be reflected by the infinite plate in the form of an oblique reflected acoustic plane wave propagating in the direction \bar{k}_R , and be given by (15) in the region $z \leq 0$ in the form:

$$p_r(x,y,z,t) = P_R e^{i(\bar{k}_R \cdot \bar{r} - \omega t)} \quad (z \leq 0) \quad (82a)$$

$$\bar{u}_r(x,y,z,t) = \frac{P_R \bar{k}_R}{\rho c k} e^{i(\bar{k}_R \cdot \bar{r} - \omega t)} \quad (z \leq 0) \quad (82b)$$

where $\bar{k}_R = k\bar{a}_{LR}$, and the unit vector \bar{a}_{LR} has one component in the negative z-direction. The oblique incident acoustic plane wave will cause the infinite plate to vibrate harmonically in the lateral positive z-direction in the form:

$$\eta(x,y,t) = Ae^{i(k_{px}x + k_{py}y - \omega t)} \quad (z = 0) \quad (83)$$

where η is the lateral displacement of the plate in the positive z-direction; velocity of the plate in the positive z-direction may be found from (83) to give:

$$u_{pz} = \frac{d\eta}{dt} = -i\omega Ae^{i(k_{px}x + k_{py}y - \omega t)} \quad (z = 0) \quad (84)$$

No plate boundary conditions are applied to (83) and (84) since the plate is assumed to be of infinite extent in both x- and y-direction. The effect of the clamped finite plate is introduced by the resonance frequency ω_0 in (80c).

The vibrations of the plate given in (83) and (84) will generate on the other side of the plate $z \geq 0$ an oblique acoustic transmitted plane wave in the direction \bar{k}_T , which will be given by (16) in the region $z \geq 0$ in the form:

$$p_t(x,y,z,t) = P_T e^{i(\bar{k}_T \cdot \bar{r} - \omega t)} \quad (z \geq 0) \quad (85a)$$

$$\bar{u}_t(x,y,z,t) = \frac{P_T \bar{k}_T}{\rho c k} e^{i(\bar{k}_T \cdot \bar{r} - \omega t)} \quad (z \geq 0) \quad (85b)$$

where $\bar{k}_T = k\bar{a}_{LT}$, and the unit vector \bar{a}_{LT} has one component in the positive z-direction.

The total external force per unit area p_z on the plate at $z = 0$ in the positive z-direction by the incident oblique acoustic wave (81a), the reflected oblique acoustic wave (82a) and the transmitted oblique acoustic wave (85a) is given by:

$$p_z(x,y,t) = P_I e^{i(k_{Ix}x + k_{Iy}y - \omega t)} + P_R e^{i(k_{Rx}x + k_{Ry}y - \omega t)} - P_T e^{i(k_{Tx}x + k_{Ty}y - \omega t)} \quad (86)$$

where the incident and the reflected oblique acoustic waves at $z < 0$ pressure the plate in the positive z-direction, and the transmitted oblique acoustic wave at $z > 0$ pressure the plate in the negative z-direction. Substituting (83) in (80b) one finds:

$$\frac{\gamma}{\rho_p h \omega^2} p_z(x,y,t) = [(k_{px}^2 + k_{py}^2)^2 - \gamma_0^4] A e^{i(k_{px}x + k_{py}y - \omega t)} \quad (87)$$

Substituting (86) on the left hand side of (87) one requires the identity to be correct for all (x,y) in the plane of the plate $z = 0$, and as a result one has:

$$k_x = k_{Ix} = k_{Rx} = k_{Tx} = k_{px} \quad (88a)$$

$$k_y = k_{Iy} = k_{Ry} = k_{Ty} = k_{py} \quad (88b)$$

Substituting (86) in (87) and using (88) one obtains:

$$[(k_x^2 + k_y^2)^2 - \gamma_0^4]A = \frac{\gamma^4}{\rho_p h \omega^2} [P_I + P_R - P_T] \quad (89)$$

where (89) reduces to (38) for the particular case of $\omega_0 = 0$ and $\gamma_0 = \gamma$.

The plate velocity u_{pz} and the fluid (air) velocity of the oblique acoustic waves in the z -direction \bar{a}_z on either side of the plate should be identical. On the positive side of the plate $z \geq 0$ at the plate $z = 0$, denoted by $z = 0_+$, the plate velocity u_{pz} in the positive z -direction should be identical with the transmitted acoustic wave velocity vector in the positive z -direction u_{tz} as follows:

$$u_{pz}(z = 0_+) = u_{tz}(z = 0_+) \quad (90a)$$

Substituting (84) and (85b) in (90a) and using (88) one obtains:

$$-i\omega A = \frac{1}{\rho c k} (\bar{k}_T \cdot \bar{a}_z) P_T \quad (90b)$$

On the negative side of the plate $z \leq 0$ at the plate $z = 0$, denoted by $z = 0_-$, the plate velocity u_{pz} should be identical with the sum of the oblique incident acoustic wave velocity in the positive z -direction u_{iz} and the oblique reflected acoustic wave velocity in the positive z -direction u_{rz} , as follows:

$$u_{pz}(z = 0_-) = u_{iz}(z = 0_-) + u_{rz}(z = 0_-) \quad (91a)$$

Substituting (81b), (82b) and (84) in (91a) and using (88) one obtains:

$$-i\omega A = \frac{1}{\rho c k} (\bar{k}_I \cdot \bar{a}_z) P_I + \frac{1}{\rho c k} (\bar{k}_R \cdot \bar{a}_z) P_R \quad (91b)$$

From (90b) and (91b) one obtains:

$$(\bar{k}_I \cdot \bar{a}_z)P_I = (\bar{k}_T \cdot \bar{a}_z)P_T - (\bar{k}_R \cdot \bar{a}_z)P_R \quad (92)$$

where for the particular case of normal incidence one has $\bar{k}_I = \bar{k}_T = -\bar{k}_R = k\bar{a}_z$.

From (6a), (9) and (88) one has:

$$\bar{k}_I = k_x \bar{a}_x + k_y \bar{a}_y + k_z \bar{a}_z \quad (93a)$$

$$\bar{k}_R = k_x \bar{a}_x + k_y \bar{a}_y - k_z \bar{a}_z \quad (93b)$$

$$\bar{k}_T = k_x \bar{a}_x + k_y \bar{a}_y + k_z \bar{a}_z \quad (93c)$$

$$k_z = \sqrt{k^2 - k_x^2 - k_y^2} = \sqrt{\left(\frac{\omega}{c}\right)^2 - k_x^2 - k_y^2} \quad (93d)$$

Using (93c) in (90b) one has:

$$-i\omega A = \frac{k_z}{\rho c k} P_T \quad (94a)$$

Using (93a) and (93b) in (91b) one has:

$$-i\omega A = \frac{k_z}{\rho c k} (P_I - P_R) \quad (94b)$$

Taking the angle of incidence θ to be the angle between the incident wave propagation vector \bar{k}_I and the positive z axis, one finds from (93a) and (93d):

$$k_z = \bar{k}_I \cdot \bar{a}_z = k \cos \theta \quad (95a)$$

$$\sqrt{k_x^2 + k_y^2} = \sqrt{k^2 - k_z^2} = k \sin \theta \quad (95b)$$

From (42b) and (42c) one finds that the angle of transmission is also θ , and the angle of reflection is $\pi - \theta$. Substituting (95) in (89), (94a) and (94b) one obtains:

$$[k^4 \sin^4 \theta - \gamma_0^4] A = \frac{\gamma^4}{\rho_p h \omega^2} (P_I + P_R - P_T) \quad (96a)$$

$$-i\omega A = \frac{\cos \theta}{\rho c} P_T \quad (96b)$$

$$-i\omega A = \frac{\cos \theta}{\rho c} (P_I - P_R) \quad (96c)$$

where (96a) will reduce to (45a) for $\omega_0 = 0$ and $\gamma = \gamma_0$, and (96b) and (96c) are identical with (45b) and (45c). From (96b) and (96c) one obtains:

$$P_I = P_R + P_T \quad (97a)$$

From (97a) one will obtain:

$$P_I + P_R - P_T = 2P_I - 2P_T \quad (97b)$$

Substituting (96b) and (97b) in (96a) one obtains:

$$[k^4 \sin^4 \theta - \gamma_0^4] \frac{i \cos \theta}{\omega \rho c} P_T = \frac{2\gamma^4}{\rho_p h \omega^2} [P_I - P_T] \quad (98a)$$

From (98a) one obtains:

$$\left[\left(\frac{k}{\gamma} \right)^4 \sin^4 \theta - \left(\frac{\gamma_0}{\gamma} \right)^4 \right] \frac{\rho_p h \omega \cos \theta}{2 \rho c} P_T = P_I - P_T \quad (98b)$$

where for the case $\omega_0 = 0$ and $\gamma = \gamma_0$ (98b) reduces to (47b).

The coupling parameter μ between the plate and the air is defined as follows:

$$\mu = \frac{2\rho}{\rho_p h} \quad (99a)$$

Taking the acoustic wave number $k = \omega/c$ and (99a) one obtains:

$$\frac{k}{\mu} = \frac{\rho_p h \omega}{2 \rho c} \quad (99b)$$

Substituting (99b) in (98b) one obtains:

$$\left[\left(\frac{k}{\gamma} \right)^4 \sin^4 \theta - \left(\frac{\gamma_0}{\gamma} \right)^4 \right] i \left(\frac{k}{\mu} \right) \cos \theta P_T = P_I - P_T \quad (100a)$$

Let us define:

$$Q_0(\theta) = \left[\left(\frac{\gamma_0}{\gamma} \right)^4 - \left(\frac{k}{\gamma} \right)^4 \sin^4 \theta \right] \frac{k}{\mu} \cos \theta \quad (100b)$$

where one has from (80c):

$$\left(\frac{\gamma_0}{\gamma} \right)^4 = 1 - \frac{\omega_0^2}{\omega^2} (1 + ia) \quad (100c)$$

Using definition (100b) in (100a) one obtains:

$$-i Q_0(\theta) P_T = P_I - P_T \quad (101)$$

From (101) one obtains:

$$\frac{P_T}{P_I} = \frac{1}{1 - iQ_o(\theta)} \quad (102a)$$

Using (102a) in (97a) one has:

$$\frac{P_R}{P_I} = \frac{-iQ_o(\theta)}{1 - iQ_o(\theta)} \quad (102b)$$

Using (102a) in (96b) one obtains:

$$\frac{A}{P_I} = \frac{i(1/\rho c \omega) \cos \theta}{1 - iQ_o(\theta)} \quad (102c)$$

where (102) are the solutions of (96) and $Q_o(\theta)$ is defined in (100b). For the particular case of $\omega_c = 0$, one obtains from (100c) $\gamma_o = \gamma$, equation (100b) becomes identical with (49b) for $Q_o(\theta) = Q(\theta)$, and the results (101) are identical with (50).

Using the solutions (102) in (51) one obtains the corresponding oblique acoustic waves, where P_R , P_T and A are given in (102) in terms of P_I of the incident oblique acoustic wave. For the particular case of normal incidence on the plate, the corresponding results may be obtained by taking $\theta = 0$.

CHAPTER VI

NOISE REDUCTION FOR FINITE PANEL

The Transmission Loss coefficient is defined as the ratio of the incident acoustic wave pressure power to the transmitted acoustic wave pressure power. From (81) and (85) one obtains the Transmission Loss coefficient TL_{db} in decibels in the form:

$$TL_{db} = 10 \log \frac{|P_i|^2}{|P_t|^2} = 10 \log \left| \frac{P_I}{P_T} \right|^2 \quad (103a)$$

Substituting (102a) for the present case, one has:

$$TL_{db} = 10 \log |1 - iQ_o|^2 \quad (103b)$$

Substituting (100c) in (100b) one obtains:

$$Q_o(\theta) = \left[1 - \frac{\omega_o^2}{\omega^2} (1 + i\alpha) - \left(\frac{k}{\gamma}\right)^4 \sin^4 \theta \right] \frac{k}{\mu} \cos \theta \quad (104a)$$

Substituting (104a) in (103b), and separating into real and imaginary parts, one obtains:

$$TL_{db} = 10 \log \left| \left[1 - \frac{\omega_o^2 \alpha k}{\omega^2 \mu} \cos \theta \right] - i \left[1 - \frac{\omega_o^2}{\omega^2} - \left(\frac{k}{\gamma}\right)^4 \sin^4 \theta \right] \frac{k}{\mu} \cos \theta \right|^2 \quad (104b)$$

From (104b) one has:

$$\begin{aligned}
TL_{db} = 10 \log \left\{ \left[1 - \frac{\alpha k \omega_o^2}{\mu \omega^2} \cos \theta \right]^2 + \right. \\
\left. + \left[1 - \frac{\omega_o^2}{\omega^2} - \left(\frac{k}{\gamma} \right)^4 \sin^4 \theta \right]^2 \left(\frac{k}{\mu} \cos \theta \right)^2 \right\} \quad (104c)
\end{aligned}$$

where one has from (80c) and (99b):

$$\frac{k}{\mu} = \frac{\omega}{c\mu} = \frac{\rho_p h \omega}{2\rho c} \quad (105a)$$

$$\left(\frac{k}{\gamma} \right)^4 = \left(\frac{\omega}{c} \right)^4 \frac{D}{\rho_p h \omega^2} = \frac{D \omega^2}{\rho_p h c^4} \quad (105b)$$

Substituting (105) in (104c) one has:

$$\begin{aligned}
TL_{db} = 10 \log \left\{ \left[1 - \frac{\alpha \omega_o^2}{c\mu \omega} \cos \theta \right]^2 + \right. \\
\left. + \left[1 - \frac{\omega_o^2}{\omega^2} - \frac{D \omega^2}{\rho_p h c^4} \sin^4 \theta \right]^2 \left[\frac{\omega}{c\mu} \cos \theta \right]^2 \right\} \quad (106)
\end{aligned}$$

For the particular case of $\omega_o = 0$ (106) reduces to (52b).

The Noise Reduction coefficient is defined as the ratio of the total acoustic wave pressure power measured by the source microphone at $z = -d_1$, to the acoustic wave pressure measured by the receiver microphone at $z = +d_2$. From (51) one obtains the Noise Reduction coefficient NR_{db} in decibels in the form:

$$\begin{aligned}
NR_{db} = 10 \log \frac{|p_i + p_r|_{z = -d_1}^2}{|p_t|_{z = +d_2}^2} = \\
= 10 \log \left| \frac{P_I e^{-ikd_1 \cos \theta} + P_R e^{+ikd_1 \cos \theta}}{P_T e^{ikd_2 \cos \theta}} \right|^2 \quad (107a)
\end{aligned}$$

Substituting (102a) and (102b) for the present case in (107a) one obtains:

$$\begin{aligned} NR_{db} &= 10 \log \left| (1 - iQ_o) e^{-ikd_1 \cos \theta} - iQ_o e^{+ikd_1 \cos \theta} \right|^2 = \\ &= 10 \log \left| e^{-ikd_1 \cos \theta} - iQ_o 2 \cos(kd_1 \cos \theta) \right|^2 \end{aligned} \quad (107b)$$

Equation (104a) may be rewritten in the form:

$$Q_o(\theta) = Q_o^R - iQ_o^I \quad (108a)$$

$$Q_o^R = \left[1 - \frac{\omega_o^2}{\omega^2} - \left(\frac{k}{\gamma}\right)^4 \sin^4 \theta \right] \frac{k}{\mu} \cos \theta \quad (108b)$$

$$Q_o^I = \alpha \frac{\omega_o^2}{\omega^2} \frac{k}{\mu} \cos \theta \quad (108c)$$

where $\frac{k}{\mu}$ and $\left(\frac{k}{\gamma}\right)^4$ are given in (105a) and (105b). Substituting (108a) in (107b) one obtains:

$$\begin{aligned} NR_{db} &= 10 \log \left| \cos(kd_1 \cos \theta) - i \sin(kd_1 \cos \theta) - \right. \\ &\quad \left. - i 2Q_o^R \cos(kd_1 \cos \theta) - 2Q_o^I \cos(kd_1 \cos \theta) \right|^2 = \\ &= 10 \log \left| (1 - 2Q_o^I) \cos(kd_1 \cos \theta) - i [\sin(kd_1 \cos \theta) + \right. \\ &\quad \left. + 2Q_o^R \cos(kd_1 \cos \theta)] \right|^2 \end{aligned} \quad (109a)$$

Equation (109a) can be rewritten in the form:

$$NR_{db} = 10 \log \{ (1 - 2Q_o^I)^2 \cos^2(kd_1 \cos \theta) + \\ + [\sin(kd_1 \cos \theta) + 2Q_o^R \cos(kd_1 \cos \theta)]^2 \} \quad (109b)$$

By opening the brackets (109b) may be rewritten as follows:

$$NR_{db} = 10 \log \{ 1 + 4Q_o^I(Q_o^I - 1) \cos^2(kd_1 \cos \theta) + \\ + 4Q_o^R \sin(kd_1 \cos \theta) \cos(kd_1 \cos \theta) + 4(Q_o^R)^2 \cos^2(kd_1 \cos \theta) \} \quad (110a)$$

By using the trigonometric identities

$$\sin 2\alpha = 2 \sin \alpha \cos \alpha$$

$$2 \cos^2 \alpha = 1 + \cos 2\alpha$$

equation (110a) may be rewritten in the form:

$$NR_{db} = 10 \log \{ 1 + 2(Q_o^R)^2 + 2Q_o^I(Q_o^I - 1) + \\ + 2Q_o^R \sin(2kd_1 \cos \theta) + 2(Q_o^R)^2 \cos(2kd_1 \cos \theta) + \\ + 2Q_o^I(Q_o^I - 1) \cos(2kd_1 \cos \theta) \} \quad (110b)$$

where Q_o^R and Q_o^I are given in (108b) and (108c). The Noise Reduction coefficient NR_{db} in (110b) depends on the position of the source at $z = -d_1$. For the particular case $kd_1 = 2\pi \frac{d_1}{\lambda} \ll 1$ (110b) will reduce to:

$$NR_{db} = 10 \log [1 + (2Q_o^R)^2 + 4Q_o^I(Q_o^I - 1)] \text{ for } |kd_1| \ll 1 \quad (111)$$

For $|kd_1| \ll 1$ the Noise Reduction coefficient NR_{db} does not depend on the position of the source microphone $z = -d_1$.

For the case where the values of kd_1 are not small, the last three terms of (110b), which include the trigonometric functions, will oscillate very much by a small change of frequency, especially at the high frequency region. The average non oscillating part of the Noise Reduction coefficient \overline{NR}_{db} may be found from (110b) by eliminating the oscillating terms:

$$\overline{NR}_{db} = 10 \log [1 + 2(Q_o^R)^2 + 2Q_o^I(Q_o^I - 1)] \quad (112)$$

From (105) and (108) one has:

$$Q_o^R = \left[1 - \frac{\omega_o^2}{\omega^2} - \frac{D\omega^2}{\rho_p hc^4} \sin^4 \theta \right] \frac{\omega}{c\mu} \cos \theta \quad (113a)$$

$$Q_o^I = \alpha \frac{\omega_o^2}{\omega^2} \frac{\rho_p h\omega}{2\rho c} \cos \theta = \frac{\alpha}{c\mu} \frac{\omega_o^2}{\omega^2} \cos \theta \quad (113b)$$

Substituting (113) in (112) one has:

$$\begin{aligned} \overline{NR}_{db} = 10 \log \{ & 1 + 2 \left[1 - \frac{\omega_o^2}{\omega^2} - \frac{D\omega^2}{\rho_p hc^4} \sin^4 \theta \right]^2 \left(\frac{\omega}{c\mu} \cos \theta \right)^2 + \\ & + 2 \left[\frac{\alpha}{c\mu} \frac{\omega_o^2}{\omega^2} \cos \theta \right] \left[\frac{\alpha}{c\mu} \frac{\omega_o^2}{\omega^2} \cos \theta - 1 \right] \} \quad (114) \end{aligned}$$

For the case where $\alpha = 0$ and $Q_o^I = 0$ (110b) will become:

$$\begin{aligned} \text{NR}_{\text{db}} = & 10 \log [1 + 2(Q_o^R)^2 + 2Q_o^R \sin(2kd_1 \cos\theta) + \\ & + 2(Q_o^R)^2 \cos(2kd_1 \cos\theta)] \end{aligned} \quad (115)$$

where Q_o^R is defined in (113a). Equation (115) has the same form as (54d). The Noise Reduction coefficient NR_{db} in (115) depends on the position of the source $z = -d_1$. The average non-oscillating part of the Noise Reduction coefficient $\overline{\text{NR}}_{\text{db}}$ may be found from (115) in the form:

$$\overline{\text{NR}}_{\text{db}} = 10 \log [1 + 2(Q_o^R)^2] \quad (116a)$$

Equation (116a) has the same form as (54e). Substituting (113a) in (116a) one has:

$$\overline{\text{NR}}_{\text{db}} = 10 \log \left[1 + 2 \left(1 - \frac{\omega_o^2}{\omega^2} - \frac{D\omega^2}{\rho_p hc^4} \sin^4 \theta \right)^2 \left(\frac{\omega}{c\mu} \cos\theta \right)^2 \right] \quad (116b)$$

where $\overline{\text{NR}}_{\text{db}}$ is the average value of the Noise Reduction coefficient NR_{db} over the local oscillations of the curve due to a finite value of the source position $z = -d_1$. For $\omega_o = 0$ (116b) becomes identical with (54e). For the case where $\frac{D\omega^2}{\rho_p hc^4} \sin^4 \theta \ll 1$ equation (116b) will have the form:

$$\overline{\text{NR}}_{\text{db}} = 10 \log \left\{ 1 + 2 \left[\frac{\omega}{c\mu} \cos\theta \right]^2 \left[1 - \frac{\omega_o^2}{\omega^2} \right]^2 \right\} \quad (117)$$

where $\mu = \frac{2\rho}{\rho_p h}$. Equation (117) gives the local average of the Noise Reduction coefficient $\overline{\text{NR}}_{\text{db}}$ for the case of an infinite plate, subject to stiffness, expressed in the form of a resonance frequency ω_o . For the

case $\omega = \omega_0$ one finds from (117) that the local average Noise Reduction coefficient $\overline{NR}_{db} = 0$. Some additional discussion of the results in the present chapter will be found in a later chapter on the experimental results.

CHAPTER VII

FREE VIBRATIONS OF THE FINITE PANEL

In the present chapter the characteristic resonance frequencies of the free vibrations of the clamped oblique finite panel (plate) in the rigid duct will be discussed. Other possible resonance effects will be also considered and a general formulation of the Noise Reduction coefficient will be given.

Let the clamped rectangular plate of dimensions "d" and "b" be situated obliquely in the rigid rectangular duct of cross-section dimensions "a" and "b." The angle between the axis of the duct and the normal to the plate will be θ . Thus, one dimension of the rectangular plate will be the same as one dimension of the rectangular duct, while the other dimension will be related as follows:

$$a = d \cos\theta \qquad b = b \qquad (118)$$

For the plate normal to the axis of the duct one will have $\theta = 0$ and $a = d$.

Let the coordinates (ξ, y, η) be associated with the oblique plate, where $\xi = 0$, $\xi = d$, $y = 0$, $y = b$ describe the clamped edges of the plate, with η being the coordinate normal to the plate. The boundary conditions of the clamped plate (panel) will be given by:

$$\eta = 0 \qquad \text{at } \xi = 0 \qquad \text{and } \xi = d \qquad (119a)$$

$$\frac{\partial \eta}{\partial \xi} = 0 \qquad \text{at } \xi = 0 \qquad \text{and } \xi = d \qquad (119b)$$

$$\eta = 0 \qquad \text{at } y = 0 \qquad \text{and } y = b \qquad (119c)$$

$$\frac{\partial \eta}{\partial y} = 0 \qquad \text{at } y = 0 \qquad \text{and } y = b \qquad (119d)$$

The motion of the free vibrations of the clamped oblique finite panel (plate) in the rigid duct as a function of time could be described in the form:

$$\eta(\xi, y, t) = A_{m,n} \cos \frac{m\pi\xi}{d} \cos \frac{n\pi y}{b} e^{-i\omega t} \quad (120)$$

The value of the lateral displacement $\eta(\xi, y, t)$ in (120) obeys the boundary conditions (119b) and (119d) of the clamped plate at the edges, but does not obey the boundary conditions (119a) and (119c). Equation (120) has been chosen in this form, since for normal plate (panel) in the rigid duct $\theta = 0$, $d = a$, and $\xi = x$, it has the same form as the acoustic wave mode (m, n) propagating in the rigid duct. The boundary conditions requirement in (119a) and (119c) that $\eta = 0$ at the edges of the clamped plate will introduce interaction between the different vibration modes (m, n) of the clamped plate. The amplitude $A_{m,n}$ in (120) of one vibrational mode of the clamped plate (panel) will be related to the amplitudes of all the other vibrational modes (m, n) of the clamped plate (panel). However, in the present case we are interested in finding the values of the characteristic frequencies of the free vibrations of the plate and not their amplitudes. One is able to find these characteristic frequencies of the free vibrations of the plate by using (120) in the following.

Taking $p_z = 0$ in (29a) one will have for the case of harmonic time variation:

$$\nabla^4 \eta - \frac{\rho h \omega^2}{D} \eta = 0 \quad (121)$$

where $\nabla^4 = \left(\frac{\partial^2}{\partial \xi^2} + \frac{\partial^2}{\partial y^2} \right)^2$ for the present case. Substituting (120) in (121) one will obtain:

$$\left[\left(\frac{m\pi}{d} \right)^2 + \left(\frac{n\pi}{b} \right)^2 \right]^2 - \frac{\rho_p h \omega^2}{D} = 0 \quad (122)$$

From (122) one obtains the resonance frequencies of the oblique clamped plate in the form:

$$\omega = \sqrt{\frac{D}{\rho_p h}} \left[\left(\frac{m\pi}{d} \right)^2 + \left(\frac{n\pi}{b} \right)^2 \right] \quad (123)$$

where (123) gives the resonance frequencies of the oblique clamped panel (plate) in the duct, which will cause acoustic waves of the same frequency. Substituting (118) in (123) one obtains:

$$\omega = \sqrt{\frac{D}{\rho_p h}} \left[\left(\frac{m\pi \cos \theta}{a} \right)^2 + \left(\frac{n\pi}{b} \right)^2 \right] \quad (124)$$

where (124) gives the resonance frequencies of the oblique plate (panel) in terms of the dimensions of the cross-section of the duct. For a clamped plate perpendicular to the axis of the duct one takes in (124) $\theta = 0$.

For a rigid duct with a square cross section $a = b$ one could rewrite (124) in the form:

$$\omega = \frac{\pi^2}{a^2} \sqrt{\frac{D}{\rho_p h}} \left[(m \cos \theta)^2 + n^2 \right] \quad a = b \quad (125)$$

The resonance frequency f of the oblique plate (panel) in the duct may be found from (125) in the form:

$$f = \frac{\omega}{2\pi} = \frac{\pi}{2a^2} \sqrt{\frac{D}{\rho_p h}} \left[m^2 \cos^2 \theta + n^2 \right] \quad (126a)$$

using the trigonometric identity $\sin^2 \theta + \cos^2 \theta = 1$ (126a) may be rewritten in the form:

$$f = \frac{\pi}{2a^2} \sqrt{\frac{D}{\rho_p h}} [m^2 + n^2 - m^2 \sin^2 \theta] \quad (126b)$$

Where (126b) gives the resonance frequencies of the oblique plate for mode (m,n) which will produce acoustic waves of the same frequency.

For the particular case of a plate (panel) perpendicular to the axis of the duct $\theta = 0$, one has from (126b):

$$f = \frac{\pi}{2a^2} \sqrt{\frac{D}{\rho_p h}} [m^2 + n^2] \quad \text{for } \theta = 0 \quad (127)$$

For each mode of vibration (m,n) or (n,m), one will have one resonance frequency of the normal plate given in (127), but two resonance frequencies of the oblique plate given in (126). Thus, for the square rigid duct the number of the plate resonance frequencies for the oblique plate will be doubled of that of the normal to the axis plate.

Let a uniform plane wave of the fundamental mode in the rectangular duct be propagating in the positive z-direction in the form:

$$p_1 = p_I e^{i(kz - \omega t)} \quad (128a)$$

$$u_{z1} = \frac{p_I}{\rho c} e^{i(kz - \omega t)} \quad (128b)$$

where $k = \omega/c$, and the losses in the lossy duct have been neglected. Let the uniform plane wave be reflected by the back wooden panel of the rectangular duct, and the reflected uniform plane wave will propagate in the negative z-direction in the form:

$$p_r = p_R e^{-i(kz + \omega t)} \quad (129a)$$

$$u_{zr} = -\frac{p_R}{\rho c} e^{-i(kz + \omega t)} \quad (129b)$$

Taking the back wooden panel to be rigid and situated at $z = L$, one has the boundary condition $u_n = 0$, and from (128b) and (129b) one obtains:

$$u_n = 0 = u_{z1} \Big|_{z=L} + u_{zr} \Big|_{z=L} = \frac{P_I}{\rho c} e^{i(kL-\omega t)} - \frac{P_R}{\rho c} e^{-i(kL+\omega t)} \quad (130a)$$

From (130a) one has:

$$P_R = P_I e^{i2kL} \quad (130b)$$

If one assumes that the back wooden panel is not rigid, but is a purely reactive surface, which will cause phase shift -2ϕ during the reflection, one will obtain (130b) in the form:

$$P_R = P_I e^{i2(kL-\phi)} \quad (130c)$$

The total pressure field of the incident and reflected waves may be found from (128a), (129a) and (130c) in the form:

$$p = p_I + p_r = p_I e^{+ikz} + p_I e^{i2(kL-\phi)} e^{-ikz} \quad (131)$$

The magnitude of the total pressure at any point $z = z_0$ may be found from (131) in the form:

$$\begin{aligned} |p|_{z=z_0} &= p_I | e^{ikz_0} + e^{i2(kL-\phi)} e^{-ikz_0} | \\ &= p_I | e^{i(kL-\phi)} | | e^{i[kz_0-(kL-\phi)]} + e^{-i[kz_0-(kL-\phi)]} | \end{aligned} \quad (132a)$$

From (132a) one obtains:

$$\begin{aligned}
 |p|_{z=z_0} &= 2p_I |\cos[k(z_0-L) + \phi]| = \\
 &= 2p_I |\cos[k(L-z_0) - \phi]| \quad (132b)
 \end{aligned}$$

If the acoustic impedance of the wall is a function of the frequency, one has $\phi = \phi(\omega)$. For the case $|p|_{z=z_0} = 0$ one requires in (132b):

$$k(L - z_0) - \phi = (2n + 1) \frac{\pi}{2} \quad (n = 0, 1, 2, 3, \dots) \quad (133)$$

Taking $k = \omega/c = 2\pi f/c$ one obtains from (133) the characteristic frequencies for minimum magnitude of the pressure at the receiver microphone situated at $z = z_0$.

$$\begin{aligned}
 f_n &= \frac{c}{2\pi(L - z_0)} [(2n + 1) \frac{\pi}{2} + \phi] = \\
 &= \frac{c}{L - z_0} \left[\frac{2n + 1}{4} + \frac{\phi}{2\pi} \right] \quad (134)
 \end{aligned}$$

For $\phi = 0$ (134) will become

$$f_n = \frac{c}{L - z_0} \frac{2n + 1}{4} = \frac{c}{L - z_0} \left(\frac{n}{2} + \frac{1}{4} \right) \quad (\phi = 0) \quad (135a)$$

For $\phi = -\frac{\pi}{2}$ (134) will become

$$f_n = \frac{c}{L - z_0} \frac{n}{2} \quad (\phi = -\frac{\pi}{2}) \quad (135b)$$

For $\phi = +\frac{\pi}{2}$ (134) will become

$$f_n = \frac{c}{L - z_0} \left(\frac{n}{2} + \frac{1}{2} \right) \quad (\phi = +\frac{\pi}{2}) \quad (135c)$$

Other possible cases could be found from (134).

When a plane acoustic wave propagating in the rigid duct parallel to its axis, is incident on the oblique plate (panel), there will be an oblique reflected acoustic wave. This reflected acoustic wave will be reflected obliquely back and forth from the duct walls and will travel back to the transmitter microphone. In addition, the incident plane acoustic wave will cause the oblique plate to vibrate at the same frequency. These vibrations of the plate will produce a transmitted acoustic plane wave which will propagate parallel to the duct axis to the receiver microphone. This transmitted acoustic plane wave will also propagate as the fundamental mode in the rigid duct and will be reflected by the wooden back panel. The Noise Reduction coefficient NR_{db} may be found in the following form for the present case by using (54b):

$$NR_{db} = 10 \log \left| (1 - iQ) e^{-ikd_1 \cos \theta} - iQ e^{i\psi(f)} \right|^2 \quad (136)$$

In (136) it has been assumed that the phases and amplitudes of the incident and transmitted acoustic plane waves of the fundamental acoustic mode in the rigid duct are the same as in the infinite plate. However, since the reflected acoustic plane wave will be reflected obliquely back and forth among the duct walls until it reaches the transmitter microphone, it has been assumed that its amplitude remains the same as before in the rigid duct, while

its phase $\psi(f)$ will be a function of the frequency f of the wave. The phase delay $\psi(f)$ in the case of the reflected oblique acoustic wave will be caused by the additional length it transverses, as well as the phase difference caused by its oblique reflection each time from the duct walls. From (136) one obtains:

$$NR_{db} = 10 \log |(1 - iQ) [\cos(kd_1 \cos\theta) - i \sin(kd_1 \cos\theta)] - iQ [\cos\psi + i \sin\psi]|^2 \quad (137a)$$

where the phase delay of the reflected wave from the oblique plate (panel) in the duct to the transmitter microphone is given by $\psi = \psi(f)$. From (137a) one obtains:

$$NR_{db} = 10 \log |[\cos(kd_1 \cos\theta) - Q \sin(kd_1 \cos\theta) + Q \sin\psi] - i[\sin(kd_1 \cos\theta) + Q \cos(kd_1 \cos\theta) + Q \cos\psi]|^2 \quad (137b)$$

From (137b) one has:

$$NR_{db} = 10 \log \{ [\cos(kd_1 \cos\theta) - Q \sin(kd_1 \cos\theta) + Q \sin\psi]^2 + [\sin(kd_1 \cos\theta) + Q \cos(kd_1 \cos\theta) + Q \cos\psi]^2 \} \quad (138a)$$

Opening the brackets in (138a) and using the trigonometric identities:

$$\cos^2 \alpha + \sin^2 \alpha = 1$$

$$\cos(\beta + \gamma) = \cos\beta \cos\gamma - \sin\beta \sin\gamma$$

$$\sin(\beta + \gamma) = \sin\beta \cos\gamma + \cos\beta \sin\gamma$$

one obtains:

$$\begin{aligned} NR_{db} = 10 \log [1 + 2Q^2 + 2Q\sin(kd_1\cos\theta + \psi) + \\ + 2Q^2\cos(kd_1\cos\theta + \psi)] \end{aligned} \quad (138b)$$

where $\psi = \psi(f)$ is the phase delay of the oblique reflected wave. For the particular case of $\psi = \psi(f) = kd_1\cos\theta$ Eqn. (138b) is identical with (54d). Denoting the average value of the Noise Reduction coefficient by \overline{NR}_{db} one obtains from (138b):

$$\overline{NR}_{db} = 10 \log [1 + 2Q^2] \quad (139)$$

where (139) is identical with (54e). One sees from (138b) that the Noise Reduction coefficient NR_{db} , found as a function of the wave frequency f , will oscillate around the average value \overline{NR}_{db} given in (139).

CHAPTER VIII

EXPERIMENTAL AND NUMERICAL RESULTS

In the present chapter the theory, which has been given in this report, will be applied in order to analyze and calculate some of the outstanding aspects of the experimental results. Figure 2 and Figure 3 give the experimental set up for the oblique aluminum plates (panels) in the duct. Figure 4 gives for reference the experimental Noise Reduction curve NR_{db} when the panel is perpendicular to the axis of the duct, i.e. the angle between the normal to the panel and the axis of the duct is $\theta = 0^\circ$. Figures 5, 6, 7 and 8 give the experimental Noise Reduction curve NR_{db} when the angles between the normal to the panel and the axis of the duct are, respectively, $\theta = 15^\circ$, $\theta = 30^\circ$, $\theta = 40^\circ$ and $\theta = 60^\circ$. The basic dimensions of the cross-section of the duct are:

$$\text{Length x Axis: } a = 18'' = 0.4572 \text{ m}$$

$$\text{Width y Axis: } b = 18'' = 0.4572 \text{ m}$$

In the Beranek tube the boundaries of the square duct are given by hardwood, which could be considered to be rigid for the present. As can be seen from Figure 2 and Figure 3, the dimensions of the special test section are larger than the rest of the duct, and the walls of the special test section are covered by absorbing material. However, the dimensions of the cross-section of the air part in the special section are the same as above. The main effect of the absorbing material as a

boundary of the special test section of the duct will be to cause additional phase shift, and some attenuation, in the reflected wave, as it is reflected back and forth between the boundaries of the special test section of the duct. The aluminum panels, which give the Noise Reduction curves in Figures 4, 5, 6, 7 and 8 have the following dimensions:

$$\text{Thickness: } h = 0.025'' = 0.635 \text{ mm} = 0.635 \times 10^{-3} \text{ m}$$

$$\text{Length x Axis: } d = \frac{a}{\cos\theta} = \frac{18''}{\cos\theta} = \frac{0.4572 \text{ m}}{\cos\theta}$$

$$\text{Width y Axis: } b = 18'' = 0.4572 \text{ m}$$

where $\theta = 0^\circ, 15^\circ, 30^\circ, 40^\circ, 60^\circ$ for the different cases in the corresponding Figures 4, 5, 6, 7, and 8.

The material and the mechanical properties of the aluminum panels are as follows:

Material: Alclad 2024T3 Aluminum

$$\text{Density} = \rho_p = 2.7 \times 10^3 \text{ kg/m}^3$$

$$\text{Young Modulus of Elasticity} = E = 7.0 \times 10^{10} \text{ N/m}^2$$

$$\text{Poisson's Ratio} = \nu = 0.3 \quad 1 - \nu^2 = 0.91$$

The experiments were done in Lawrence, Kansas at about 1,000 ft above sea level, under the following conditions of the air:

$$\text{Temperature} = T = 21^{\circ}\text{C} \approx 70^{\circ}\text{F} = 294.15^{\circ}\text{K}$$

$$\text{Pressure} = P = 0.97735 \text{ atmosphere} = 97,735 \text{ N/m}^2$$

$$\text{Density} = \rho = 1.1575 \text{ Kg/m}^3$$

$$\text{Velocity of Acoustic Waves} = c = 343.8 \text{ m/sec}$$

The coupling parameter μ between the aluminum panel and the air may be calculated from the above:

$$\mu = \frac{2\rho}{\rho_p h} = \frac{2 \times 1.1575}{2.7 \times 0.635} = 1.350 \text{ 1/m}$$

The analysis of the experimental results will be divided into several parts according to the particular aspect of the physical phenomena to be discussed.

A. The Average Noise Reduction Coefficient $\overline{\text{NR}}_{\text{db}}$: The average Noise Reduction coefficient $\overline{\text{NR}}_{\text{db}}$ for the infinite plate is given in (54e) in the form:

$$\overline{\text{NR}}_{\text{db}} = 10 \log [1 + 2Q^2] \quad (140)$$

where one has from (53a) and (53b):

$$Q = [1 - (\frac{k}{\gamma})^4 \sin^4 \theta] \frac{k}{\mu} \cos \theta = [1 - \frac{D\omega^2}{\rho_p hc^4} \sin^4 \theta] \frac{k}{\mu} \cos \theta \quad (141a)$$

where $D = \frac{Eh^3}{12(1-\nu^2)}$. It should be pointed out that the average Noise Reduction coefficient $\overline{\text{NR}}_{\text{db}}$ for the infinite panel given in (140) is identical with $\overline{\text{NR}}_{\text{db}}$ for the finite panel given in (116b) for the case

$\omega_0 \ll \omega$. This is the case for most of the frequency range under consideration in Figures 5, 6, 7 and 8, except in the lowest range of frequencies. It should be also pointed out that \overline{NR}_{db} given in (140) is identical with (139), where the multiple oblique reflection of the reflected wave from the oblique plate has been taken into account.

One may rewrite (141a) in the form:

$$Q = [1 - (\frac{f}{f_4})^2 \sin^4 \theta] \frac{k}{\mu} \cos \theta \quad (141b)$$

where the frequency f_4 is defined in the following form upon comparing (141b) with (141a) and is evaluated by using the above numerical values:

$$f_4 = \frac{c}{2\pi} \sqrt{\frac{\rho_p h}{D}} = \frac{c}{2\pi h} \sqrt{\frac{12\rho_p (1 - \nu^2)}{E}} = 19,227 \text{ 1/sec} \quad (141c)$$

Since for the experiments under consideration $f \ll f_4$, one obtains from (141b) for the present case:

$$Q \approx \frac{k}{\mu} \cos \theta = \frac{\omega}{\mu c} \cos \theta = (\frac{2\pi}{\mu c}) f \cos \theta \quad (142)$$

Substituting the numerical values one obtains from (142):

$$2Q^2 \approx 2(\frac{2\pi}{\mu c})^2 f^2 \cos^2 \theta = 3.6653 \cos^2 \theta (\frac{f}{100})^2 \quad (143)$$

From (143) one has the following numerical values for the different angles:

$$2Q^2 = 3.6653 \left(\frac{f}{100}\right)^2 \quad \text{for } \theta = 0^\circ \quad (144a)$$

$$2Q^2 = 3.4198 \left(\frac{f}{100}\right)^2 \quad \text{for } \theta = 15^\circ \quad (144b)$$

$$2Q^2 = 2.7490 \left(\frac{f}{100}\right)^2 \quad \text{for } \theta = 30^\circ \quad (144c)$$

$$2Q^2 = 2.1509 \left(\frac{f}{100}\right)^2 \quad \text{for } \theta = 40^\circ \quad (144d)$$

$$2Q^2 = 0.9163 \left(\frac{f}{100}\right)^2 \quad \text{for } \theta = 60^\circ \quad (144e)$$

Using the numerical results in equations (144) for the different angles in (140), one obtains the numerical values in Table A for the average Noise Reduction coefficient \overline{NR}_{db} . The numerical results in Table A are represented in Figures 5, 6, 7 and 8 by the lower oblique straight line for high frequencies. The upper oblique straight line for high frequencies in the same figures, which is 2-3 decibels higher, represents the theoretical result, when the impedance of the absorbing material of the Beranek tube is taken into account, as derived and calculated in a previous report by Grosveld, which is listed in the Bibliography. It should be pointed out that the results in (140) and Table A are 3 decibels higher for the high frequency region (the oblique straight line region in Figures 5, 6, 7 and 8) than the relationship given in (52b) for the Transmission Loss coefficient TL_{db} , which is also given by Beranek in his book. The slope of all the straight lines in Figures 5, 6, 7 and 8 at the higher frequency region is the same, namely, increase of the average Noise Reduction coefficient \overline{NR}_{db} by 6 decibels for every octave (= doubling of the frequency). The same slope appears also in the straight lines in Figure 4, for the case of a panel perpendicular to the axis of the duct $\theta = 0^\circ$.

TABLE A
 AVERAGE NOISE REDUCTION COEFFICIENT \overline{NR}_{db} (DECIBELS)

f	$\theta = 15^\circ$	$\theta = 30^\circ$	$\theta = 40^\circ$	$\theta = 60^\circ$
20	0.557	0.418	0.358	0.157
50	2.683	2.271	1.870	0.895
100	6.454	5.739	4.984	2.825
200	11.667	10.790	9.824	6.689
500	19.370	18.433	17.386	13.786
1000	25.353	24.409	23.346	19.668
2000	31.364	30.414	29.520	25.653
5000	39.320	38.370	37.306	33.602

Theoretical values calculated from (140) and (144).

B. The Noise Reduction Coefficient NR_{db} : When a plane acoustic wave in the rigid duct parallel to its axis is incident on the oblique plate (panel), the transmitted acoustic wave will be in the same direction towards the receiver microphone. The reflected acoustic wave will be reflected obliquely back and forth from the duct walls towards the transmitter microphone. Because of its several oblique reflections, and its additional path length, the phase of the reflected wave $\psi(f)$ when it reaches the transmitter microphone will be a function of the frequency. The corresponding Noise Reduction coefficient NR_{db} is given in (138b) in the form:

$$NR_{db} = 10 \log [1 + 2Q^2 + 2Q\sin(kd_1\cos\theta + \psi) + 2Q^2\cos(kd_1\cos\theta + \psi)] \quad (145)$$

where the phase of the reflected wave is a function of the frequency $\psi = \psi(f)$. The values of the distance d_1 from the center of the oblique panel to the transmitter microphone are given as follows:

$\theta = 15^\circ$	$d_1 = 1.42 \text{ m}$
$\theta = 30^\circ$	$d_1 = 1.32 \text{ m}$
$\theta = 40^\circ$	$d_1 = 1.26 \text{ m}$
$\theta = 60^\circ$	$d_1 = 0.94 \text{ m}$

Comparing (145) with (140) one finds that, because the trigonometric functions in (145), the value of the Noise Reduction coefficient NR_{db} in (145)

will oscillate around the average Noise Reduction coefficient \overline{NR}_{db} . These oscillations of the curve will be a function of the frequency of the incident acoustic wave, since $\psi = \psi(f)$ and $k = \omega/c = (2\pi/c)f$ in (145), and $Q = Q(f)$ in (144). This trend of the Noise Reduction coefficient NR_{db} to oscillate around the average Noise Reduction coefficient \overline{NR}_{db} is seen very clearly in Figure 5 ($\theta = 15^\circ$), Figure 6 ($\theta = 30^\circ$), Figure 7 ($\theta = 40^\circ$) and Figure 8 ($\theta = 60^\circ$), and is marked in those figures by a heavy black line.

This trend of oscillation does not appear in Figure 4 ($\theta = 0^\circ$) for the panel perpendicular to the axis. The reason is that in this case $\psi(f) = kd_1 \cos\theta$ in (145), the result being given in (54d) for $\theta = 0^\circ$ and $kd_1 \ll 1$. The reflected wave for $\theta = 0^\circ$ propagates along the duct axis and does not bounce from the walls of the duct, and the transmitter microphone $z = -d_1$ is located very close to the panel. The oscillation trend of NR_{db} around \overline{NR}_{db} will similarly disappear in the case of the different oblique panels in Figures 5, 6, 7, and 8 if the transmitter microphone was to be located very close to the center of the oblique panel. However, in the present experimental set up this has not been possible to do.

From studying the oscillation trends, marked by heavy lines in Figures 5, 6, 7 and 8, one finds that in Figure 5 ($\theta = 15^\circ$) one has only three peaks, in Figure 6 ($\theta = 30^\circ$) one has seven peaks, in Figure 7 ($\theta = 40^\circ$) one has six peaks, and in Figure 8 ($\theta = 60^\circ$) one has only two peaks. These results can be explained in the following way. In Figure 5 ($\theta = 15^\circ$) the panel is very close to being perpendicular to the axis ($\theta = 0^\circ$), and the reflected wave bounce only once from the absorbing material in

the special test section as can be seen from Figure 9. As a result $\psi(f)$ does not vary with the frequency as much as in other cases, and one has only the peaks in Figures 5 ($\theta = 15^\circ$). In Figure 6 ($\theta = 30^\circ$) and Figure 7 ($\theta = 40^\circ$) the reflected wave bounces several times from the absorbing material in the special test section as can be seen from Figure 9. As a result $\psi(f)$ in (145) varies very much with the frequency, and one has six or seven peaks in Figure 6 ($\theta = 30^\circ$) and Figure 7 ($\theta = 40^\circ$). Of particular interest is Figure 8 ($\theta = 60^\circ$), where one has only two peaks. As can be seen from Figure 9 for $\theta = 60^\circ$, in this case the reflected acoustic wave returns along the same ray as the incident acoustic wave, and bounces only twice from the absorbing material at the special test section, both times from the same place. This explains why the oscillation trend in Figure 8 ($\theta = 60^\circ$) has only two peaks, the number of peaks being closer to $\theta = 15^\circ$ (three peaks) than either to $\theta = 30^\circ$ (7 peaks) or to $\theta = 40^\circ$ (6 peaks). Thus the oscillation trends of the Noise Reduction coefficient for the different oblique panels have been explained qualitatively reasonably well by using acoustic ray theory. It has been found experimentally that the above oscillation trends of the Noise Reduction coefficient is independent of the thickness h of the panel, and panels with different thickness h exhibit essentially identical oscillation trends.

C. The Cavity Resonance: From the experimental results for the Noise Reduction coefficient given in Figures 5, 6, 7 and 8 one finds that at the lowest range of the frequencies there are several peaks, both upward and downward. The resonance frequencies $f_R < 100$ Hz are listed in Table B.

TABLE B
 CAVITY RESONANCE FREQUENCIES ($f_R^{\text{cavity}} < 100 \text{ Hz}$)
 Experimental values

$\theta = 15^\circ$	$\theta = 30^\circ$	$\theta = 40^\circ$	$\theta = 60^\circ$
35	32	35,41	33,38
42	45,48	45,48	45
	57,66	53	
80,86	79,85	86	72,85

The resonance effect of the standing plane wave along the length of the Beranek tube will be called the cavity resonance effect and will be discussed in the present section. The cavity resonance effect is described by (134) in the form:

$$f_s^{\text{cavity}} = \frac{c}{L - z_0} \left[\frac{2s + 1}{4} + \frac{\phi}{2\pi} \right] \quad (s = 0, 1, 2, 3) \quad (146)$$

where $(L - z_0)$ represents the distance transversed by the reflected wave from the wooden back panel and $\phi = \phi(\omega)$ represents the phase shift of the reflected wave at the wooden back panel and any other possible reflections.

In our experimental set up the distance of the wooden back panel from the receiver microphone is:

$$L - z_0 = 99.5'' = 2.527 \text{ m}$$

Taking the acoustic wave velocity for $T = 21^{\circ}\text{C} \approx 70^{\circ}\text{F}$ to be $c = 343.8$ m/sec one obtains in (146):

$$f_s^{\text{cavity}} = \frac{68.0}{\tau} \left[s + \frac{1}{2} + \frac{\phi}{\pi} \right] \quad \text{1/sec} \quad (147)$$

where τ represents the additional distance factor transversed by the reflected acoustic wave after additional reflections, to be discussed later. If one takes $\tau = 1$, $\phi = 0$ and $s = 0$ in (147) one obtains:

$$f_{\substack{s=0 \\ \tau=1}}^{\text{cavity}} = 34.0 \quad \text{1/sec} \quad (148)$$

where the theoretical result (148) agrees well with the first row of experimental resonance frequencies given in Table B.

As can be seen from Figure 2, the reflected acoustic wave from the back wooden panel will have additional reflection from the oblique aluminum panel, as well as the absorbing side walls of the special test section, which will cause it a phase shift. It will also transverse additional distance after oblique reflection from the aluminum panel before it reaches to the receiver microphone. Taking, for example, the additional distance transversed by the reflected wave to be 50% longer, one will be required to divide (147) by a factor $\tau = 1.5$ in accordance with (146). Assuming in addition that $\phi = -\frac{\pi}{2}$ and taking $s = 1$, one will obtain from (147):

$$f_{\substack{s=1 \\ \tau=1.5}}^{\text{cavity}} = 45.0 \quad \text{1/sec} \quad (149)$$

where the result (149) agrees well with the second row of experimental resonance frequencies given in Table B.

While the additional distance transversed by the reflected wave can be calculated exactly for each case of reflection, there is not enough experimental data available for the phase shift associated with each reflection. However, within the order of magnitude, it is found that the resonance frequencies listed in Table B result from (147), and therefore are the result of the cavity resonance phenomena, if one includes the possible additional multiple reflections by the reflected wave in the Beranek tube.

D. The Acoustic Resonance: The acoustic resonance frequencies have been discussed in detail in a previous report by the present author listed in the Bibliography. It was found that for the case of normal incidence on the plate in the square duct, the acoustic resonance frequencies are given by:

$$f_{m,n}^{\text{acoustic}} = \frac{c}{2a} \sqrt{m^2 + n^2} \quad (\theta = 0^\circ) \quad (150)$$

comparing (150) with (126b) one may find the acoustic resonance frequencies for the oblique plate to be in the form:

$$f_{m,n}^{\text{acoustic}} = \frac{c}{2a} \sqrt{m^2 + n^2 - m^2 \sin^2 \theta} \quad (151)$$

In order to use the numerical results of the previous report one could take $m = 0$ in (151), and substituting the corresponding numerical values, one obtains:

TABLE C
ACOUSTIC RESONANCE FREQUENCIES

m-n	Theoretical	Experimental			
		$\theta = 15^\circ$	$\theta = 30^\circ$	$\theta = 40^\circ$	$\theta = 60^\circ$
0-1	376.0	366	365	380	363
0-2	752.0	x	740	x	x
0-3	1,127.9	1,150	x	1,120	x
0-4	1,503.9	1,520	1,500	1,490	1,540
0-5	1,879.9	1,890	1,850	1,900	x
0-6	2,255.9	2,250	2,250	2,220	2,260
0-7	2,631.9	2,630	2,630	2,650	x
0-8	3,007.8	2,980	3,000	2,970	2,980
0-9	3,383.8	3,340	3,400	x	
0-10	3,759.8	3,760	x	3,820	3,700
0-11	4,135.8	4,200	4,100	4,080	x
0-12	4,511.8	4,560	4,480	4,580	x
0-13	4,887.7	4,800	4,840	x	x

Theoretical values calculated from (152).
 Experimental numerical values represent spikes.
 x represents a break in the experimental curves.

$$f_{o,n}^{\text{acoustic}} = 375.98 n \approx 376.0 n \quad (m = 0) \quad (152)$$

where for mode (o,n) the resulting acoustic resonance frequencies are independent of the angle θ .

In Table C one finds the theoretical numerical values derived from (152), as well as the corresponding experimental results values found from Figures 5, 6, 7 and 8. The experimental numerical values in Table C represent a major or a minor spike, upward or downward, while the x in Table C represents a break in the experimental curve.

While the acoustic resonance frequencies may be calculated for every mode (m,n) in (151), they are almost impossible to identify experimentally in Figures 5, 6, 7 and 8, because of the large number and the close proximity of the plate resonance spikes, to be discussed later. The acoustic resonance frequencies for every mode (m,n) have been identified separately for the case of normal incidence on the panel (plate) for $\theta = 0^\circ$ given in Figure 4, and the results are given in a previous report by the present author listed in the bibliography.

E. The Wooden Back Panel Resonance: Although the wooden back panel is relatively massive, it can act as a resonator under the influence of the plane acoustic wave incident upon it. Thus, the wooden back panel excites reflected plane acoustic waves at frequencies of its own wooden "plate" resonance. It was found in a previous report by the present author listed in the Bibliography that for the wooden back panel one has:

$$f_{m,n}^{\text{wood}} = 155 (m^2 + n^2) \quad (153)$$

Table D gives the theoretical numerical values for the different modes, together with the corresponding experimental resonance spikes in Figures 5, 6, 7, and 8. All the listed experimental numbers in Table D are of large or small separate upward or downward spikes, while the x represents corresponding breaks in the curve or minor spikes. While the experimental and theoretical results in Table D indicate that the back wooden panel is a source of numerous spikes, both upward and downward, it can be tested further if this is really the case. A repetition of the same experiments without the back wooden panel, and a comparison of the spike formation in the present experimental results given in Figures 5, 6, 7 and 8 and the proposed experiments will hopefully decide the issue.

TABLE D
WOOD RESONANCE FREQUENCIES

m-n	m^2+n^2	Theoretical	Experimental			
			$\theta = 15^\circ$	$\theta = 30^\circ$	$\theta = 40^\circ$	$\theta = 60^\circ$
1-0	1	155	159	150	151	144
1-1	2	310	327	300	320	311
2-0	4	620	625	610	620	640
2-1	5	775	x	800	800	x
2-2	8	1,240	1,210	x	1,220	1,280
3-0	9	1,395	1,400	1,400	1,440	1,370
3-1	10	1,550	1,540	1,600	1,570	1,540
3-2	13	2,015	2,000	2,050	2,000	2,000
4-0	16	2,480	2,440	2,540	2,520	2,480
4-1	17	2,635	2,630	2,620	x	x
3-3	18	2,790	2,820	x	2,750	2,800
4-2	20	3,100	3,150	3,010	3,080	3,100
4-3	25	3,875	3,830	3,800	3,860	3,910
5-0	25	3,875	3,830	3,800	3,860	3,910
5-1	26	4,030	4,020	4,040	4,080	4,090
5-2	29	4,495	4,410	4,450	4,500	4,500
4-4	32	4,960	4,950	5,000	5,000	5,000

Theoretical values calculated from (153).
 Experimental numerical values represent spikes.
 x represents a break or a minor spike in the experimental curves.

F. The Plate Resonance: It has been shown in the previous chapter that the free vibrations of the panel (plate) will establish plate acoustic wave resonance modes (m,n) of the clamped oblique plate in the rigid duct, as given by (126a) or (126b). These acoustic wave plate resonance modes have a frequency which is much below the cut off frequency of the corresponding higher order modes of the acoustic waves in the duct, and therefore will not propagate at all in the duct. Their effect is primarily a near zone effect near the plate and thus will effect the receiver microphone near the oblique panel. These panel resonance frequencies will also interact with the plane acoustic wave excited by the plate, and the plane acoustic wave of the fundamental mode of the acoustic wave in the duct will propagate in the duct at all frequencies, since its cut off frequency in the rigid duct is zero. By these two aspects the plate (panel) resonance modes will affect the microphones. The incident acoustic plane wave of the fundamental mode in the duct and the oblique reflected acoustic wave will be superimposed in the transmitter microphone. The phase of the oblique reflected acoustic wave will be determined by the length of its path, as given in Figure 9, and by the phase change at the various oblique reflections from the oblique plate and the duct walls. The transmitted acoustic plane wave of the fundamental mode in the duct and the plate acoustic resonance mode will be superimposed in the receiver microphone, as well as the reflected acoustic wave from the wooden back panel. An upward spike (= large noise reduction) in the experimental curves of Figures 5, 6, 7 and 8 will mean that the waves are added in phase in the transmitter microphone, but out of phase in the receiver microphone. A downward spike (= small noise reduction or even "amplification") in the experimental curves of Figures 5, 6, 7 and 8 will mean that the

waves are added out of phase in the transmitter microphone, but in phase in the receiver microphone.

Equation (126b) gives the oblique plate resonance frequencies in the following form for a square duct $a = b$:

$$f_{\text{plate}} = \frac{\pi}{2a^2} \sqrt{\frac{D}{\rho_p h}} [m^2 + n^2 - m^2 \sin^2 \theta] \quad (154a)$$

Substituting the value of $D = \frac{Eh^3}{12(1 - \nu^2)}$ in (154a) one obtains:

$$f_{m,n}^{\text{plate}} = \frac{\pi h}{2a^2} \sqrt{\frac{E}{12\rho_p(1 - \nu^2)}} [m^2 + n^2 - m^2 \sin^2 \theta] \quad (154b)$$

Using the numerical values for the present case from the beginning of this chapter, one obtains for the plate resonance frequencies:

$$f_{m,n}^{\text{plate}} = 7.353 [m^2 + n^2 - m^2 \sin^2 \theta] \quad (154c)$$

All the calculated theoretical plate resonance frequencies for the range of frequencies under consideration and for the angles $\theta = 0^\circ, 15^\circ, 30^\circ, 40^\circ, \text{ and } 60^\circ$ of the inclined panel are listed in Appendix A.

For the case $\theta = 0^\circ$ the last term in (154) will become zero. Thus for $\theta = 0^\circ$ the plate resonance frequency for mode (m,n) is the same as the plate resonance frequency for mode (n,m) for the square duct, and the two plate resonance modes are degenerate for $\theta = 0^\circ$. This is not the case for $\theta \neq 0^\circ$, where the two plate resonance frequencies for mode (m,n) and mode (n,m) are different. This explains why the number of the spikes in the experimental curves in Figure 5 ($\theta = 15^\circ$), Figure 6 ($\theta = 30^\circ$), Figure 7 ($\theta = 40^\circ$) and Figure 8 ($\theta = 60^\circ$) is so

much larger than the number of spikes in Figure 4 ($\theta = 0^\circ$) for the case of the plate perpendicular to the axis.

For the case of a clamped plate perpendicular ($\theta = 0^\circ$) to the axis of a rectangular duct one has from (120):

$$\eta(x,y,t) = A_{m,n} \cos \frac{m\pi x}{a} \cos \frac{n\pi y}{b} \quad (155)$$

where the plate edges are given by $x = 0$, $x = a$, $y = 0$, $y = b$. One could transform the origin to the center of the plate by using a new set of rectangular coordinates (x' , y') as follows:

$$x' = x - \frac{a}{2} \quad y' = y - \frac{b}{2} \quad (156)$$

where the clamped plate edges are given by $x' = \pm \frac{a}{2}$ and $y' = \pm \frac{b}{2}$. Substituting (156) into (155) one obtains:

$$\eta(x',y',t) = A_{m,n} \cos \frac{m\pi}{a} \left(x' + \frac{a}{2}\right) \cos \frac{n\pi}{b} \left(y' + \frac{b}{2}\right) \quad (157a)$$

which could be rewritten as follows:

$$\eta(x',y',t) = A_{m,n} \cos \left(\frac{m\pi x'}{a} + \frac{m\pi}{2}\right) \cos \left(\frac{n\pi y'}{b} + \frac{n\pi}{2}\right) \quad (157b)$$

From trigonometric identities one has:

$$\cos \left(\frac{m\pi x'}{a} + \frac{m\pi}{2}\right) = \cos \frac{m\pi x'}{a} \cos \frac{m\pi}{2} - \sin \frac{m\pi x'}{a} \sin \frac{m\pi}{2} \quad (158)$$

Since the incident plane acoustic wave of the fundamental mode in the duct has an even symmetry around the axis of the duct, one allows only even functions in (158) for the plate displacement. This will require in (158) that the second term on the right hand side will disappear, i.e. the characteristic mode number m should be an even number. For the same reason, the characteristic mode number n should be also an even number. Taking both (m,n) to be even numbers, one will obtain from (158) and (157b):

$$\eta(x',y';t) = \pm A_{m,n} \cos \frac{m\pi x'}{a} \cos \frac{n\pi y'}{b} \quad (159)$$

This explains why only the even-even plate resonance modes, where both (m,n) are even numbers, should be considered for the plate perpendicular to the axis $\theta = 0^\circ$.

When the plate is oblique in the x - z plane to the axis of the duct ($\theta \neq 0^\circ$), the even symmetry consideration is not valid in the x -direction, and both even and odd numbers should be taken for m , while n should include even numbers only. This is another reason why the number of spikes in Figures 5, 6, 7 and 8 is so much larger than in Figure 4 for normal incidence ($\theta = 0^\circ$). Of course under the experimental set up the even symmetry is not perfect, and some odd symmetry is introduced in both directions. For completeness sake, both odd and even numbers will be considered for both (m,n) in all the following tables.

In the following tables all the frequencies of the distinct experimental resonance spikes, both downward and upward, are listed from Figure 4 ($\theta = 0^\circ$), Figure 5 ($\theta = 15^\circ$), Figure 6 ($\theta = 30^\circ$), Figure 7

($\theta = 40^\circ$) and Figure 8 ($\theta = 60^\circ$). Next to each experimental resonance spike frequency the theoretical plate resonance modes (m,n), which have approximately the same frequency, are identified and are also listed. These theoretical results are taken from Appendix A, there the theoretical plate resonance frequency for each mode (m,n) has been calculated.

TABLE E-1
 PLATE RESONANCE FREQUENCIES ($\theta = 0^\circ$, DOWNWARD SPIKES)

Spike Frequency Experimental	Theoretical Plate Resonance Modes (m-n)
62	(2-2), (3-0), (0-3)
220	(4-4), (5-2), (2-5)
380	(6-4), (4-6), (7-2), (2-7)
620	(9-2), (2-9), (7-6), (6-7)
920	(8-8), (10-5), (5-10), (11-2), (2-11)
1280	(12-6), (6-12), (13-2), (2-13)
1650	(12-9), (9-12), (15-1), (1-15), (15-0), (0-15)
2400	(18-0), (0-18), (18-2), (2-18), (15-10), (10-15)
3000	(20-2), (2-20), (17-11), (11-17), (19-7), (7-19)
3300	(16-14), (14-16), (15-13), (21-3), (3-21)
3800	(18-14), (14-18), (22-6), (6-22), (17-15), (15-17)
4300	(22-10), (10-22), (19-15), (15-19)
4600	(22-12), (12-22), (25-1), (1-25)

TABLE E-2

PLATE RESONANCE FREQUENCIES ($\theta = 0^\circ$, UPWARD SPIKES)

Spike Frequency Experimental	Theoretical Plate Resonance Modes (m-n)
192	(5-1), (1-5)
370	(6-4), (4-6), (7-1), (1-7)
430	(7-3), (3-7), (7-4), (4-7)
590	(8-4), (4-8), (9-0), (0-9)
760	(10-2), (2-10), (9-5), (5-9), (10-1) (1-10)
1000	(10-6), (6-10), (11-4), (4-11)
1080	(12-2), (2-12), (9-8), (8-9), (10-7), (7-10), (11-5), (5-11), (12-1), (1-12)
1300	(12-6), (6-12), (10-9), (9-10), (13-3), (3-13)
1720	(14-6), (6-14), (13-8), (8-13), (15-3), (3-15)
2080	(16-5), (5-16)
2900	(14-14), (15-13), (13-15)
3200	(20-6), (6-20)
3500	(16-15), (15-16), (19-11), (11-19)
4000	(20-12), (12-20), (23-5), (5-23)
4500	(24-6), (6-24), (21-13), (13-21), (23-9), (9-23)

TABLE F-1

PLATE RESONANCE FREQUENCIES ($\theta = 15^\circ$, DOWNWARD SPIKES)

Spike Frequency Experimental	Theoretical Plate Resonance Modes (m-n)
42	
86	
280	(6-2),(2-6), (5-4), (1-6)
327	(3-6), (7-0)
366	(6-4), (0-7), (1-7), (7-2)
430	(8-0), (6-5), (5-6), (3-7)
487	(2-8), (1-8)
650	(5-8), (3-9)
1080	(2-12), (7-10), (11-6), (1-12)
1290	(6-12), (10-9), (9-10), (11-8), (13-4)
2000	(4-16), (16-6), (9-14), (7-15), (15-8), (17-1)
2250	(18-2), (12-13), (14-11), (15-10), (7-16)
2630	(6-18), (12-15), (16-11)
2820	(8-18),(16-12), (13-15), (5-19), (19-7)
3150	
3600	(2-22), (10-20), (16-16), (22-6), (17-15), (7-21), (21-9)
4250	(0-24), (2-24), (21-13), (7-23), (23-9)
4630	(8-24), (18-18), (20-16), (17-19), (21-15), (1-25), (3-25), (25-7), (7-25)
4800	(15-21)

TABLE F-2

PLATE RESONANCE FREQUENCIES ($\theta = 15^\circ$, UPWARD SPIKES)

Spike Frequency Experimental	Theoretical Plate Resonance Modes (m-n)
35	(0-2), (2-1)
80	
160	
187	(0-5), (1-5)
270	(0-6), (6-2), (1-6)
291	(2-6), (4-5)
356	(6-4), (5-5), (0-7)
404	(7-3)
475	(0-8), (4-7), (1-8)
520	(6-6), (7-5)
550	(8-4), (9-0)
825	(9-6), (11-0), (11-1)
1040	(0-12), (12-2), (8-9), (10-7), (12-3)
1150	(4-12), (10-8), (9-9), (6-11), (13-1), (13-0)
1210	(7-11), (5-12), (13-3)
1640	(9-12), (13-8), (0-15)
1810	(14-8), (9-13), (5-15), (15-6), (16-3)
2120	(6-16), (10-14), (15-9), (16-7), (1-17)
2440	(12-14), (13-13), (15-11), (9-16), (7-17)
3070	(4-20), (10-18), (13-16), (19-9), (21-3)
3480	(20-10), (11-19)

TABLE F-2 (Continued)

Spike Frequency Experimental	Theoretical Plate Resonance Modes ()
3920	(12-20), (21-11), (3-23)
4130	(16-18), (17-17), (19-15)
4410	(24-8), (13-21), (9-23)
4800	(15-21)

TABLE G-1

PLATE RESONANCE FREQUENCIES ($\theta = 30^\circ$, DOWNWARD SPIKES)

Spike Frequency Experimental	Theoretical Plate Resonance Modes (m-n)
32	(0-2), (2-1), (1-2)
48	(2-2), (3-0)
66	(0-3)
85	(4-0), (2-3)
163	(3-4), (5-2)
193	(6-0), (1-5)
258	(0-6), (5-4), (6-3)
350	(4-6), (8-0)
380	(8-2), (6-5), (2-7), (7-4)
430	(4-7), (8-3), (9-0)
500	(2-8), (5-7), (9-3)
610	(8-6), (5-8), (0-9), (1-9), (2-9), (10-3)
800	(10-6), (6-9), (9-7), (3-10), (12-1)
1020	(10-8), (7-10), (5-11), (11-7)
1440	(0-14), (16-2), (10-11), (6-13), (1-14), (14-7), (15-5)
1600	(10-12), (8-13), (15-7), (16-5), (17-1)
2100	(6-16), (11-14), (9-15)
2390	(0-18), (2-18), (13-14), (7-17)
3000	(4-20), (21-9), (23-3)
3780	(6-22), (16-18), (26-2), (25-7)
4450	(6-24), (15-21)

c-2

TABLE G-2

PLATE RESONANCE FREQUENCIES ($\theta = 30^\circ$, UPWARD SPIKES)

Spike Frequency Experimental	Theoretical Plate Resonance Modes (m-n)
45	(3-0)
57	(2-2), (3-1)
79	(4-0), (3-2)
150	(4-3)
179	(0-5)
300	(6-4), (3-6), (7-2)
365	(4-6), (8-0), (0-7), (1-7), (8-1)
412	(5-6), (3-7), (8-3)
464	(6-6), (8-4), (7-5), (1-8), (9-1)
643	(10-4), (7-7), (3-9), (9-5)
1400	(8-12), (16-0), (11-10), (12-9), (5-13), (13-8), (16-1)
1500	(4-14), (12-10), (9-12), (7-13), (15-6)
1850	(12-12), (6-15), (15-9)
2190	(20-0), (13-13), (10-15), (17-9), (19-5)
2530	(14-14), (18-10)
3500	(10-20), (7-21), (23-9), (25-3)
4040	(14-20), (21-15), (5-23)
4700	(5-25)

TABLE H-1

PLATE RESONANCE FREQUENCIES ($\theta = 40^\circ$, DOWNWARD SPIKES)

Spike Frequency Experimental	Theoretical Plate Resonance Modes (m-n)
35	(0-2), (1-2)
45	(2-2), (3-1)
53	
100	(3-3), (5-0)
163	(6-0), (3-4), (6-1)
210	(2-5), (6-3), (7-0), (7-1)
320	(4-6), (7-4)
400	(8-4), (3-7), (7-5)
575	(7-7), (5-8), (11-3)
690	(10-6), (7-8), (12-3)
800	(4-10), (7-9), (10-7), (11-6), (12-5), (13-3)
900	(6-10), (10-8), (0-11), (1-11), (2-11), (13-5), (14-3)
1100	(12-8), (14-6), (16-0), (9-10), (7-11), (3-12), (13-7), (15-4), (16-1)
1220	(6-12), (16-4), (9-11), (12-9), (14-7), (15-6)
1680	(12-12), (18-6), (10-13), (14-11), (2-15), (16-9)
1900	(0-16), (2-16), (14-12), (1-16), (19-7), (21-1)
2380	(0-18), (2-18), (13-15), (11-16)
2500	(12-16), (24-2), (14-15), (17-13), (21-9)
2750	(14-16), (24-6), (16-15), (5-19), (25-3)
3080	(6-20), (15-17), (25-7)

TABLE H-1 (Continued)

Spike Frequency Experimental	Theoretical Plate Resonance Modes (m-n)
3400	(10-20), (17-17), (13-19)
3620	(4-22), (20-16), (15-19)
4080	(16-20), (7-23)
4750	(7-25)

TABLE H-2

PLATE RESONANCE FREQUENCIES ($\theta = 40^\circ$, UPWARD SPIKES)

Spike Frequency Experimental	Theoretical Plate Resonance Modes (m-n)
41	(3-0)
48	(2-2), (3-1)
86	(2-3)
119	(0-4), (1-4), (5-1)
151	(6-0), (3-4)
200	(2-5), (7-0)
279	(2-6), (6-4), (8-0), (7-3), (8-1)
354	(0-7), (1-7), (9-0)
382	(5-6), (2-7), (9-2)
540	(4-8), (8-6), (10-4), (9-5), (11-1), (11-2)
620	(6-8), (12-0), (2-9), (9-6), (10-5), (12-1)
1030	(10-9), (6-11), (15-3)
1120	(4-12), (14-6), (16-2), (11-9), (16-1)
1490	(10-12), (3-14)
1600	(6-14), (14-10), (9-13), (17-7)
1870	(0-16), (10-14), (18-8), (7-15), (15-11), (1-16)
2150	(8-16), (16-12), (18-10), (13-14), (3-17), (17-11), (19-9)
2590	(24-4), (13-16)
3200	(8-20), (14-18), (11-19), (19-15), (23-11)
3770	(14-20), (18-18), (11-21)
4380	(6-24), (14-22), (11-23)
5000	(2-26)

TABLE I-1

PLATE RESONANCE FREQUENCIES ($\theta = 60^\circ$, DOWNWARD SPIKES)

Spike Frequency Experimental	Theoretical Plate Resonance Modes (m-n)
33	(0-2), (2-2), (4-0), (1-2), (4-1)
45	(3-2), (5-0), (5-1)
85	(3-3), (7-0)
119	(0-4), (2-4), (8-0), (1-4), (5-3), (7-2), (8-1)
144	(4-4), (8-2), (9-0)
180	(6-4), (10-0), (0-5), (1-5), (8-3), (9-2)
225	(10-2), (5-5), (9-3)
244	(10-3), (11-2)
325	(6-6), (12-3), (13-1)
350	(14-0), (0-7), (7-6), (11-4), (13-2)
398	(14-2), (4-7), (5-7), (11-5)
464	(0-8), (14-4), (16-0), (1-8)
530	(6-8), (12-6), (15-4), (16-3), (17-1)
640	(10-8), (14-6), (18-2), (5-9)
1170	(8-12), (12-11), (21-7), (23-5), (25-1)
1280	(26-2), (11-12), (4-13), (5-13)
1460	(2-14), (4-14), (20-10), (11-13), (3-14)
1900	(2-16), (4-16), (16-14), (3-16), (19-13)
2180	(20-14), (13-16), (5-17), (17-15)
2800	(9-19), (19-17)
3000	(6-20), (18-18)
3240	(1-21)

TABLE I-1 (Continued)

Spike Frequency Experimental	Theoretical Plate Resonance Modes (m-n)
3970	(7-23)
4600	(1-25)
4780	
4950	(0-26), (2-26)

TABLE I-2

PLATE RESONANCE FREQUENCIES ($\theta = 60^\circ$, UPWARD SPIKES)

Spike Frequency Experimental	Theoretical Plate Resonance Modes (m-n)
38	(2-2), (1-2), (4-1)
72	(6-0), (0-3), (1-3), (2-3), (5-2), (6-1)
113	(0-4), (8-0), (1-4), (5-3), (7-2)
132	(2-4), (3-4), (6-3), (8-1)
183	(6-4), (10-0), (0-5), (1-5), (8-3), (9-2), (10-1)
235	(8-4), (5-5), (11-1)
311	(10-4), (5-6), (8-5), (13-1)
347	(14-0), (7-6), (11-4)
363	(0-7), (1-7), (2-7), (14-1)
410	(5-7), (9-6), (11-5), (15-0), (15-1)
500	(4-8), (9-7), (11-6), (13-5)
560	(7-8), (10-7)
990	(12-10), (16-2), (20-6), (22-4), (7-11), (21-5), (23-1)
1370	(22-8), (8-13), (13-12), (16-11)
1540	(8-14), (16-12), (24-8), (13-13), (7-14), (19-11)
2000	(8-16), (14-15)
2260	(14-16), (9-17)
2840	(16-18)
3100	(10-20)
3500	(11-21)

TABLE I-2 (Continued)

Spike Frequency Experimental	Theoretical Plate Resonance Modes (m-n)
3700	(8-22)
4300	(6-24)
4600	(1-25), (3-25)

CHAPTER IX

SUMMARY

In the present report the theoretical background has been given and the theory has been developed for acoustic plane waves obliquely incident on a clamped panel in a rectangular duct. The coupling theory between the elastic vibrations of the panel (plate) and the oblique acoustic waves propagating in infinite space and in the duct have been considered in detail. The coupling theory developed in this report is based on the theory of acoustic wave propagation and the dynamic theory of elasticity and the plate vibrations. This theory has been applied for the experimental results of the Noise Reduction curves measured for oblique plates of $\theta = 15^\circ, 30^\circ, 40^\circ, 60^\circ$, which are discussed in detail.

In Chapter I the basic general theoretical considerations are introduced.

In Chapter II the partial differential equations which govern the propagation of acoustic waves in three dimensions are given, and some basic concepts of the theory of propagation of oblique acoustic waves are introduced.

In Chapter III the boundary value problem of an acoustic plane wave obliquely incident on an infinite plate is solved rigorously, and the transmission and reflection coefficients of the corresponding oblique acoustic waves are found.

In Chapter IV the Transmission Loss coefficient and the Noise Reduction coefficient for oblique incidence on the infinite plate are defined and derived in detail. It is found that the Noise Reduction coefficient in this case consists of an average value, superimposed by an oscillating component. The average Noise Reduction coefficient is defined and derived. The theoretical behavior of the above coefficients is discussed.

In Chapter V the boundary value problem of an acoustic plane wave obliquely incident on a finite clamped panel is solved. The partial differential equation which governs the vibrations of the plate (panel) is modified by adding to it stiffness (spring) forces and damping forces, and the fundamental resonance frequency is defined. The transmission and the reflection coefficients of the corresponding oblique acoustic waves are derived.

In Chapter VI the Transmission Loss coefficient and the Noise Reduction coefficient are evaluated for the finite clamped oblique panel, using the results of the previous chapter. The average Noise Reduction coefficient is found for different cases.

In Chapter VII the resonance frequencies excited by the free vibrations of the oblique finite clamped plate (panel) are derived. The reflection of the acoustic wave from the wooden back panel is discussed and the corresponding resonance frequencies are found. The Noise Reduction coefficient and the average Noise Reduction coefficient are discussed in general, when the reflected oblique acoustic wave is reflected obliquely back and forth from the duct walls.

In Chapter VIII the experimental results are discussed in detail in view of the theory presented in this report, and the corresponding numerical values are calculated from this theory. The following aspects of the experimental results for the oblique plates of $\theta = 15^\circ, 30^\circ, 40^\circ, 60^\circ$ are discussed with reference to the theories previously presented in this report:

- A. The average Noise Reduction coefficient.
- B. The Noise Reduction coefficient.
- C. The Cavity Resonance.
- D. The Acoustic Resonance.
- E. The Wooden Back Panel Resonance.
- F. The Plate Resonance.

The detailed features and the trends of the experimental curves in Figures 5, 6, 7, 8 for $\theta = 15^\circ, 30^\circ, 40^\circ, 60^\circ$ have been explained, and almost all the experimental resonance spikes have been identified, by using the above listed theoretical considerations, and the theoretical results agree very well with the experimental results.

BIBLIOGRAPHY

1. Beranek, L. L., Noise and Vibration Control (McGraw-Hill, 1971).
2. Kinsler, L. E. and A. R. Frey, Fundamentals of Acoustics (Wiley, 1962).
3. Poges, G., Applied Acoustics (Wiley, 1977).
4. Morse, P. M. and K. U. Ingard, Theoretical Acoustics (McGraw-Hill, 1968).
5. Ramo, S., J. R. Whinnery and T. Van-Duzer, Fields and Waves in Communication Electronics (Wiley, 1965).
6. Szilard, R., Theory and Analysis of Plates (Prentice Hall, 1974).
7. Timoshenko, S. and S. Woinowsky-Krieger, Theory of Plates and Shells (McGraw-Hill, 1959).
8. Grosveld, F., J. Lameris and D. Dunn, "The Effect of Oblique Angle of Sound Incidence, Realistic Edge Conditions, Curvature and In-Plane Panel Stresses on the Noise Reduction Characteristics of General Aviation Type Panels," Report KU-FRL-417-10 (July, 1979).
9. Unz, H., "Acoustic Plane Waves Normally Incident on a Clamped Panel in a Rectangular Duct," Report KU-FRL-417-10 (August, 1979).

APPENDIX A

PLATE RESONANCE FREQUENCIES

The plate resonance frequencies are given in (154c) in the form:

$$f_{m,n}^{\text{plate}} = 7.353 [m^2 + n^2 - m^2 \sin^2 \theta] \quad (160)$$

where one can define:

$$g_m(\theta) = (m \sin \theta)^2 = m^2 \sin^2 \theta \quad (161)$$

In the present appendix the calculated values of the plate resonance frequencies from (160) will be listed for the different plate modes (m-n).

Table J gives the calculated values of $g_m(\theta)$ from (161). Table K gives the calculated values of the plate resonance frequencies from (160) for all the modes (m-n). It is arranged by the order of the increasing parameter $(m^2 + n^2)$.

TABLE J

CALCULATED VALUES FOR EQUATION (161)

$$g_m(\theta) = (m \sin\theta)^2 = m^2 \sin^2 \theta$$

m	$\theta = 15^\circ$	$\theta = 30^\circ$	$\theta = 40^\circ$	$\theta = 60^\circ$
1	0.0670	0.2500	0.4132	0.7500
2	0.2680	1.0000	1.6527	3.0000
3	0.6030	2.2500	3.7186	6.7500
4	1.0718	4.0000	6.6109	12.0000
5	1.6747	6.2500	10.3295	18.7500
6	2.4116	9.0000	14.8740	27.0000
7	3.2824	12.2500	20.2458	36.7500
8	4.2872	16.0000	26.4430	48.0000
9	5.4260	20.2500	33.4675	60.7500
10	6.6988	25.0000	41.3180	75.0000
11	8.1055	30.2500	49.9947	90.7500
12	9.6462	36.0000	59.4978	108.0000
13	11.3209	42.2500	60.8272	126.7500
14	13.1296	49.0000	80.9830	147.0000
15	15.0722	56.2500	92.9653	168.7500
16	17.1489	64.0000	105.7740	192.0000
17	19.3594	72.2500	119.4087	216.7500
18	21.7040	81.0000	133.8700	243.0000
19	24.1826	90.2500	149.1576	270.7500
20	26.7951	100.0000	165.2720	300.0000
21	29.5416	110.2500	182.2119	330.7500

TABLE J (Continued)

m	$\theta = 15^\circ$	$\theta = 30^\circ$	$\theta = 40^\circ$	$\theta = 60^\circ$
22	32.4220	121.0000	199.9800	363.0000
23	35.4365	132.2500	218.5717	396.7500
24	38.5850	144.0000	237.9900	432.0000
25	41.8674	156.2500	258.2369	468.7500
26	45.2837	169.0000	279.3100	507.0000
27	48.8341	182.2500	301.2075	546.7500

TABLE K

THEORETICAL PLATE RESONANCE FREQUENCIES

$$f_{m,n}^{\text{plate}} = 7.353 [m^2 + n^2 - m^2 \sin^2 \theta]$$

m-n	m^2+n^2	$\theta=0^\circ$	$\theta=15^\circ$	$\theta=30^\circ$	$\theta=40^\circ$	$\theta=60^\circ$
1-0	1	7.4	6.9	5.5	4.3	1.8
0-1	1	7.4	7.4	7.4	7.4	7.4
1-1	2	14.7	14.2	12.9	11.7	9.2
2-0	4	29.4	27.4	22.1	17.3	7.4
0-2	4	29.4	29.4	29.4	29.4	29.4
2-1	5	36.8	34.8	29.4	24.6	14.7
1-2	5	36.8	36.3	34.9	33.7	31.3
2-2	8	58.8	56.9	51.5	46.7	36.8
3-0	9	66.2	61.7	49.6	38.8	16.5
0-3	9	66.2	66.2	66.2	66.2	66.2
3-1	10	73.5	69.1	57.0	46.2	23.9
1-3	10	73.5	73.0	71.7	70.5	68.0
3-2	13	95.6	91.2	79.0	68.2	46.0
2-3	13	95.6	93.6	88.2	83.4	73.5
4-0	16	117.6	109.8	88.2	69.0	29.4
0-4	16	117.6	117.6	117.6	117.6	117.6
4-1	17	125.0	117.1	95.6	76.4	36.8
1-4	17	125.0	124.5	123.2	122.0	119.5
3-3	18	132.4	127.9	115.8	105.0	82.7
4-2	20	147.1	139.2	117.6	98.5	58.8
2-4	20	147.1	145.1	139.7	134.9	125.0
5-0	25	183.8	171.5	137.9	107.9	46.0
4-3	25	183.8	175.9	154.4	135.2	95.6
3-4	25	183.8	179.4	167.3	156.5	134.2
0-5	25	183.8	183.8	183.8	183.8	183.8
5-1	26	191.2	178.9	145.2	115.2	53.3
1-5	26	191.2	190.7	189.3	188.1	185.7
5-2	29	213.2	200.9	167.3	137.3	75.4
2-5	29	213.2	211.3	205.9	201.1	191.2

TABLE K (CONTINUED)

$m-n$	m^2+n^2	$\theta=0^\circ$	$\theta=15^\circ$	$\theta=30^\circ$	$\theta=40^\circ$	$\theta=60^\circ$
4-4	32	235.3	227.4	205.9	186.7	147.1
5-3	34	250.0	237.7	204.0	174.0	112.1
3-5	34	250.0	245.6	233.5	222.7	200.4
6-0	36	264.7	247.0	198.5	155.3	66.2
0-6	36	264.7	264.7	264.7	264.7	264.7
6-1	37	272.1	254.3	205.9	162.7	73.5
1-6	37	272.1	271.6	270.2	269.0	266.5
6-2	40	294.1	276.4	227.9	184.8	95.6
2-6	40	294.1	292.1	286.8	282.0	272.1
5-4	41	301.5	289.2	255.5	225.5	163.6
4-5	41	301.5	293.6	272.1	252.9	213.2
6-3	45	330.9	313.2	264.7	221.5	132.4
3-6	45	330.9	326.5	314.3	303.5	281.3
7-0	49	360.3	336.2	270.2	211.4	90.1
0-7	49	360.3	360.3	360.3	360.3	360.3
7-1	50	367.7	343.5	277.6	218.8	97.4
5-5	50	367.7	355.3	321.7	291.7	229.8
1-7	50	367.7	367.2	365.8	364.6	362.1
6-4	52	382.4	364.6	316.2	273.0	183.8
4-6	52	382.4	374.5	352.9	333.8	294.1
7-2	53	389.7	365.6	299.6	240.8	119.5
2-7	53	389.7	387.7	382.4	377.6	367.7
7-3	58	426.5	402.3	336.4	277.6	156.3
3-7	58	426.5	422.0	409.9	399.1	376.8
6-5	61	448.5	430.8	382.4	339.2	250.0
5-6	61	448.5	436.2	402.5	372.6	310.7
8-0	64	470.6	439.1	352.9	276.2	117.6
0-8	64	470.6	470.6	470.6	470.6	470.6
8-1	65	477.9	446.4	360.3	283.5	125.0
7-4	65	477.9	453.8	387.9	329.1	207.7

TABLE K (CONTINUED)

m-n	m^2+n^2	$\theta=0^\circ$	$\theta=15^\circ$	$\theta=30^\circ$	$\theta=40^\circ$	$\theta=60^\circ$
4-7	65	477.9	470.1	448.5	429.3	389.7
1-8	65	477.9	477.5	476.1	474.9	472.4
8-2	68	500.0	468.5	382.4	305.6	147.1
2-8	68	500.0	498.0	492.7	487.9	477.9
6-6	72	529.4	511.7	463.2	420.0	330.9
8-3	73	536.8	505.2	419.1	342.3	183.8
3-8	73	536.8	532.3	520.2	509.4	487.1
7-5	74	544.1	520.0	454.0	395.3	273.9
5-7	74	544.1	531.8	498.2	468.2	406.3
8-4	80	588.2	556.7	470.6	393.8	235.3
4-8	80	588.2	580.4	558.8	539.6	500.0
9-0	81	595.6	555.7	446.7	349.5	148.9
0-9	81	595.6	595.6	595.6	595.6	595.6
9-1	82	602.9	563.0	454.0	356.9	156.3
1-9	82	602.9	602.5	601.1	599.9	597.4
9-2	85	625.0	585.1	476.1	378.9	178.3
7-6	85	625.0	600.9	534.9	476.1	354.8
6-7	85	625.0	607.3	558.8	515.6	426.5
2-9	85	625.0	623.0	617.7	612.9	602.9
8-5	89	654.4	622.9	536.8	460.0	301.5
5-8	89	654.4	642.1	608.5	578.5	516.5
9-3	90	661.8	621.9	512.9	415.7	215.1
3-9	90	661.8	657.3	645.2	634.4	612.1
9-4	97	713.2	673.3	564.3	467.2	266.5
4-9	97	713.2	705.4	683.8	664.6	625.0
7-7	98	720.6	696.5	630.5	571.7	450.4
10-0	100	735.3	686.0	551.5	431.5	183.8
8-6	100	735.3	703.8	617.7	540.9	382.4
6-8	100	735.3	717.6	669.1	625.9	536.8
0-10	100	735.3	735.3	735.3	735.3	735.3

TABLE K (CONTINUED)

m-n	m^2+n^2	$\theta=0^\circ$	$\theta=15^\circ$	$\theta=30^\circ$	$\theta=40^\circ$	$\theta=60^\circ$
10-1	101	742.7	693.4	558.8	438.8	191.2
1-10	101	742.7	742.2	740.8	739.6	737.1
10-2	104	764.7	715.4	580.9	460.9	213.2
2-10	104	764.7	762.7	757.4	752.6	742.7
9-5	106	779.4	739.5	630.5	533.3	332.7
5-9	106	779.4	767.1	733.5	703.5	641.5
10-3	109	801.5	752.2	617.7	497.7	250.0
3-10	109	801.5	797.0	784.9	774.1	751.8
8-7	113	830.9	799.4	713.2	636.5	477.9
7-8	113	830.9	806.8	740.8	682.0	560.7
10-4	116	852.9	803.7	669.1	549.1	301.5
4-10	116	852.9	845.1	823.5	804.3	764.7
9-6	117	860.3	820.4	711.4	614.2	413.6
6-9	117	860.3	842.6	794.1	750.9	661.8
11-0	121	889.7	830.1	667.3	522.1	222.4
0-11	121	889.7	889.7	889.7	889.7	889.7
11-1	122	897.1	837.5	674.6	529.4	229.8
1-11	122	897.1	896.6	895.2	894.0	891.6
11-2	125	919.1	859.5	696.7	551.5	251.8
10-5	125	919.1	869.8	735.3	615.3	367.7
5-10	125	919.1	906.8	873.2	843.2	781.3
2-11	125	919.1	917.2	911.8	907.0	897.1
8-8	128	941.2	909.7	823.5	746.7	588.2
11-3	130	955.9	896.3	733.5	588.2	288.6
9-7	130	955.9	916.0	807.0	709.8	509.2
7-9	130	955.9	931.8	865.8	807.0	685.7
3-11	130	955.9	951.5	939.3	928.5	906.3
10-6	136	1000.0	950.7	816.2	696.2	448.5
6-10	136	1000.0	982.3	933.8	890.6	801.5
11-4	137	1007.4	947.8	784.9	639.7	340.1

TABLE K (CONTINUED)

m-n	m^2+n^2	$\theta=0^\circ$	$\theta=15^\circ$	$\theta=30^\circ$	$\theta=40^\circ$	$\theta=60^\circ$
4-11	137	1007.4	999.5	977.9	958.8	919.1
12-0	144	1058.8	987.9	794.1	621.3	264.7
0-12	144	1058.8	1058.8	1058.8	1058.8	1058.8
12-1	145	1066.2	995.3	801.5	628.7	272.1
9-8	145	1066.2	1026.3	917.3	820.1	619.5
8-9	145	1066.2	1034.7	948.5	871.7	713.2
1-12	145	1066.2	1065.7	1064.3	1063.1	1060.7
11-5	146	1073.5	1013.9	851.1	705.9	406.3
5-11	146	1073.5	1061.2	1027.6	997.6	935.7
12-2	148	1088.2	1017.3	823.5	650.7	294.1
2-12	148	1088.2	1086.3	1080.9	1076.1	1066.2
10-7	149	1095.6	1046.3	911.8	791.8	544.1
7-10	149	1095.6	1071.5	1005.5	946.7	825.4
12-3	153	1125.0	1054.1	860.3	687.5	330.9
3-12	153	1125.0	1120.6	1108.5	1097.7	1075.4
11-6	157	1154.4	1094.8	932.0	786.8	487.1
6-11	157	1154.4	1136.7	1088.2	1045.1	955.9
12-4	160	1176.5	1105.6	911.8	739.0	382.4
4-12	160	1176.5	1168.6	1147.1	1127.9	1088.2
9-9	162	1191.2	1151.3	1042.3	945.1	744.5
10-8	164	1205.9	1156.6	1022.1	902.1	654.4
8-10	164	1205.9	1174.4	1088.2	1011.5	852.9
13-0	169	1242.7	1159.4	932.0	729.2	310.7
12-5	169	1242.7	1171.7	977.9	805.2	448.5
5-12	169	1242.7	1230.3	1196.7	1166.7	1104.8
0-13	169	1242.7	1242.7	1242.7	1242.7	1242.7
13-1	170	1250.0	1166.8	939.3	736.6	318.0
11-7	170	1250.0	1190.4	1027.6	882.4	582.7
7-11	170	1250.0	1225.9	1159.9	1101.1	979.8
1-13	170	1250.0	1249.5	1248.2	1247.0	1244.5

TABLE K (CONTINUED)

m-n	m^2+n^2	$\theta=0^\circ$	$\theta=15^\circ$	$\theta=30^\circ$	$\theta=40^\circ$	$\theta=60^\circ$
13-2	173	1272.1	1188.8	961.4	758.6	340.1
2-13	173	1272.1	1270.1	1264.7	1259.9	1250.0
13-3	178	1308.8	1225.6	998.2	795.4	376.8
3-13	178	1308.8	1304.4	1292.3	1281.5	1259.2
12-6	180	1323.5	1252.6	1058.8	886.0	529.4
6-12	180	1323.5	1305.8	1257.4	1214.2	1125.0
10-9	181	1330.9	1281.6	1147.1	1027.1	779.4
9-10	181	1330.9	1291.0	1182.0	1084.8	884.2
13-4	185	1360.3	1277.1	1049.6	846.8	428.3
11-8	185	1360.3	1300.7	1137.9	992.7	693.0
8-11	185	1360.3	1328.8	1242.7	1165.9	1007.4
4-13	185	1360.3	1352.4	1330.9	1311.7	1272.1
12-7	193	1419.1	1348.2	1154.4	981.6	625.0
7-12	193	1419.1	1395.0	1329.1	1270.3	1148.9
13-5	196	1426.5	1343.2	1115.8	913.0	494.5
5-13	196	1426.5	1414.2	1380.5	1350.5	1288.6
14-0	196	1441.2	1344.6	1080.9	845.7	360.3
0-14	196	1441.2	1441.2	1441.2	1441.2	1441.2
14-1	197	1448.5	1352.0	1088.2	853.1	367.7
1-14	197	1448.5	1448.0	1446.7	1445.5	1443.0
14-2	200	1470.6	1374.1	1110.3	875.1	389.7
10-10	200	1470.6	1421.3	1286.8	1166.8	919.1
2-14	200	1470.6	1468.6	1463.2	1458.4	1448.5
11-9	202	1485.3	1425.7	1262.9	1117.7	818.0
9-11	202	1485.3	1445.4	1336.4	1239.2	1038.6
14-3	205	1507.4	1410.8	1147.1	911.9	426.5
13-6	205	1507.4	1424.1	1196.7	993.9	575.4
6-13	205	1507.4	1489.6	1441.2	1398.0	1308.8
3-14	205	1507.4	1502.9	1490.8	1480.0	1457.7
12-8	208	1529.4	1458.5	1264.7	1091.9	735.3
8-12	208	1529.4	1497.9	1411.8	1335.0	1176.48

TABLE K (CONTINUED)

$m-n$	m^2+n^2	$\theta=0^\circ$	$\theta=15^\circ$	$\theta=30^\circ$	$\theta=40^\circ$	$\theta=60^\circ$
14-4	212	1558.8	1462.3	1198.5	963.4	477.9
4-14	212	1558.8	1551.0	1529.4	1510.2	1470.6
13-7	218	1603.0	1519.7	1292.3	1089.5	671.0
7-13	218	1603.0	1578.8	1512.9	1454.1	1332.7
14-5	221	1625.0	1528.5	1264.7	1029.5	544.1
11-10	221	1625.0	1565.4	1402.6	1257.4	957.7
10-11	221	1625.0	1575.7	1441.2	1321.2	1073.5
5-14	221	1625.0	1612.7	1579.1	1549.1	1487.1
15-0	225	1654.4	1543.6	1240.8	970.9	413.6
12-9	225	1654.4	1583.5	1389.7	1216.9	860.3
9-12	225	1654.4	1614.5	1505.5	1408.3	1207.7
0-15	225	1654.4	1654.4	1654.4	1654.4	1654.4
15-1	226	1661.8	1551.0	1248.2	978.2	421.0
1-15	226	1661.8	1661.3	1659.9	1658.7	1656.3
15-2	229	1683.8	1573.0	1270.2	1000.3	443.0
2-15	229	1683.8	1681.9	1676.5	1671.7	1661.8
14-6	232	1705.9	1609.4	1345.6	1110.4	625.0
6-14	232	1705.9	1688.2	1639.7	1596.5	1507.4
13-8	233	1713.2	1630.0	1402.6	1199.8	781.3
8-13	233	1713.2	1681.7	1595.6	1518.8	1360.3
15-3	234	1720.6	1609.8	1307.0	1037.0	479.8
3-15	234	1720.6	1716.2	1704.1	1693.3	1671.0
15-4	241	1772.1	1661.2	1358.5	1088.5	531.3
4-15	241	1772.1	1764.2	1742.7	1723.5	1683.8
11-11	242	1779.4	1719.8	1557.0	1411.8	1112.1
12-10	244	1794.1	1723.2	1529.4	1356.6	1000.0
10-12	244	1794.1	1744.9	1610.3	1490.3	1242.7
14-7	245	1801.5	1704.9	1441.2	1206.0	720.6
7-14	245	1801.5	1777.3	1711.4	1652.6	1531.3
15-5	250	1838.3	1727.4	1424.6	1154.7	597.4
13-9	250	1838.3	1755.0	1527.6	1324.8	906.3

TABLE K (CONTINUED)

m-n	m^2+n^2	$\theta=0^\circ$	$\theta=15^\circ$	$\theta=30^\circ$	$\theta=40^\circ$	$\theta=60^\circ$
9-13	250	1838.3	1798.4	1689.4	1592.2	1391.6
5-15	250	1838.3	1825.9	1792.3	1762.3	1700.4
16-0	256	1882.4	1756.3	1411.8	1104.6	470.6
0-16	256	1882.4	1882.4	1882.4	1882.4	1882.4
16-1	257	1889.7	1763.6	1419.1	1112.0	477.9
1-16	257	1889.7	1889.2	1887.9	1886.7	1884.2
16-2	260	1911.8	1785.7	1441.2	1134.0	500.0
14-8	260	1911.8	1815.2	1551.5	1316.3	830.9
8-14	260	1911.8	1880.3	1794.1	1717.3	1558.8
2-16	260	1911.8	1909.8	1904.4	1899.6	1889.7
15-6	261	1919.1	1808.3	1505.5	1235.6	678.3
6-15	261	1919.1	1901.4	1853.0	1809.8	1720.6
16-3	265	1948.5	1822.4	1478.0	1170.8	536.8
12-11	265	1948.5	1877.6	1683.8	1511.0	1154.4
11-12	265	1948.5	1888.9	1726.1	1580.9	1281.3
3-16	265	1948.5	1944.1	1932.0	1921.2	1898.9
13-10	269	1978.0	1894.7	1667.3	1464.5	1046.0
10-13	269	1978.0	1928.7	1794.1	1674.1	1426.5
16-4	272	2000.0	1873.9	1529.4	1222.3	588.2
4-16	272	2000.0	1992.1	1970.6	1951.4	1911.8
15-7	274	2014.7	1903.9	1601.1	1331.2	773.9
7-15	274	2014.7	1990.6	1924.6	1865.9	1744.5
14-9	277	2036.8	1940.2	1676.5	1441.3	955.9
9-14	277	2036.8	1996.9	1887.9	1790.7	1590.1
16-5	281	2066.2	1940.1	1595.6	1288.5	654.4
5-16	281	2066.2	2053.9	2020.2	1990.2	1928.3
12-12	288	2117.7	2046.7	1853.0	1680.2	1323.5
15-8	289	2125.0	2014.2	1711.4	1441.4	884.2
8-15	289	2125.0	2093.5	2007.4	1930.6	1772.1
17-1	290	2132.4	1990.0	1601.1	1254.3	538.6
13-11	290	2132.4	2049.1	1321.7	1618.9	1200.4

TABLE K (CONTINUED)

m-n	m^2+n^2	$\theta=0^\circ$	$\theta=15^\circ$	$\theta=30^\circ$	$\theta=40^\circ$	$\theta=60^\circ$
11-13	290	2132.4	2072.8	1909.9	1764.7	1465.1
1-17	290	2132.4	2131.9	2130.5	2129.3	2126.9
16-6	292	2147.1	2021.0	1676.5	1369.3	735.3
6-16	292	2147.1	2129.3	2080.9	2037.7	1948.5
14-10	296	2176.5	2079.9	1816.2	1581.0	1905.6
10-14	296	2176.5	2127.2	1992.7	1872.7	1625.0
17-3	298	2191.2	2048.8	1659.9	1313.2	597.4
3-17	298	2191.2	2186.8	2174.6	2163.8	2141.6
16-7	305	2242.7	2116.6	1772.1	1464.9	830.9
7-16	305	2242.7	2218.5	2152.6	2093.8	1972.4
15-9	306	2250.0	2139.2	1836.4	1566.4	1009.2
9-15	306	2250.0	2210.1	2101.1	2003.9	1803.3
13-12	313	2301.5	2218.2	1990.8	1788.1	1369.5
12-13	313	2301.5	2230.6	2036.8	1864.0	1507.4
17-5	314	2308.8	2166.5	1777.6	1430.8	715.1
5-17	314	2308.8	2296.5	2262.9	2232.9	2171.0
14-11	317	2330.9	2234.4	1970.6	1735.4	1250.0
11-14	317	2330.9	2271.3	2108.5	1963.3	1663.6
16-8	320	2353.0	2226.9	1882.4	1575.2	941.2
8-16	320	2353.0	2321.4	2235.3	2158.5	2000.0
18-0	324	2382.4	2222.8	1786.8	1398.0	595.6
0-18	324	2382.4	2382.4	2382.4	2382.4	2382.4
15-10	325	2389.7	2278.9	1976.1	1706.2	1148.9
10-15	325	2389.7	2340.5	2205.9	2085.9	1838.3
18-2	328	2411.8	2252.2	1816.2	1427.4	625.0
2-18	328	2411.8	2409.8	2404.4	2399.6	2389.7
16-9	337	2478.0	2351.9	2007.4	1700.2	1066.2
9-16	337	2478.0	2438.1	2329.1	2231.9	2031.3
17-7	338	2485.3	2343.0	1954.1	1607.3	891.6
13-13	338	2485.3	2402.1	2174.6	1971.9	1553.3

TABLE K (CONTINUED)

m-n	m^2+n^2	$\theta=0^\circ$	$\theta=15^\circ$	$\theta=30^\circ$	$\theta=40^\circ$	$\theta=60^\circ$
7-17	338	2485.3	2461.2	2395.2	2336.4	2215.1
18-4	340	2500.0	2340.5	1904.4	1515.7	713.2
14-12	340	2500.0	2403.5	2139.7	1904.6	1419.1
12-14	340	2500.0	2429.1	2235.3	2062.5	1705.9
4-18	340	2500.0	2492.1	2470.6	2451.4	2411.8
15-11	346	2544.1	2433.3	2130.5	1860.6	1303.3
11-15	346	2544.1	2484.5	2321.7	2176.5	1876.9
16-10	356	2617.7	2491.6	2147.1	1839.9	1205.9
10-16	356	2617.7	2568.4	2433.8	2313.9	2066.2
18-6	360	2647.1	2487.5	2051.5	1662.7	860.3
6-18	360	2647.1	2629.3	2580.9	2537.7	2448.5
19-1	362	2661.8	2484.0	1998.2	1565.0	671.0
1-19	362	2661.8	2661.3	2659.9	2658.7	2656.3
14-13	365	2683.8	2587.3	2323.5	2088.4	1603.0
13-14	365	2683.8	2600.6	2373.2	2170.4	1751.9
15-12	369	2713.3	2602.4	2299.7	2029.7	1472.4
12-15	369	2713.3	2642.3	2448.5	2275.8	1919.1
19-3	370	2720.6	2542.8	2057.0	1623.8	729.8
17-9	370	2720.6	2578.3	2189.4	1842.6	1126.8
9-17	370	2720.6	2680.7	2571.7	2474.5	2273.9
3-19	370	2720.6	2716.2	2704.1	2693.3	2671.0
16-11	377	2772.1	2646.0	2301.5	1994.4	1360.3
11-16	377	2772.1	2712.5	2549.7	2404.4	2104.8
19-5	386	2838.3	2660.5	2174.6	1741.5	847.4
5-19	386	2838.3	2825.9	2792.3	2762.3	2700.4
18-8	388	2853.0	2693.4	2257.4	1868.6	1066.2
8-18	388	2853.0	2821.4	2735.3	2658.5	2500.0
14-14	392	2882.4	2785.8	2522.1	2286.9	1801.5
15-13	394	2897.1	2786.3	2483.5	2213.5	1656.3
13-15	394	2897.1	2813.8	2586.4	2383.6	1965.1

TABLE K (CONTINUED)

$m-n$	m^2+n^2	$\theta=0^\circ$	$\theta=15^\circ$	$\theta=30^\circ$	$\theta=40^\circ$	$\theta=60^\circ$
20-0	400	2941.2	2744.1	2205.9	1726.0	735.3
16-12	400	2941.2	2815.1	2470.6	2163.4	1529.4
12-16	400	2941.2	2870.3	2676.4	2503.7	2147.1
0-20	400	2941.2	2941.2	2941.2	2941.2	2941.2
20-2	404	2970.6	2773.6	2235.3	1755.4	764.7
2-20	404	2970.6	2968.6	2963.3	2958.5	2948.6
19-7	410	3014.7	2836.9	2351.1	1918.0	1023.9
17-11	410	3014.7	2872.4	2483.5	2136.7	1421.0
11-17	410	3014.7	2955.1	2792.3	2647.1	2347.4
7-19	410	3014.7	2990.6	2924.7	2865.9	2744.5
20-4	416	3058.8	2861.8	2323.5	1843.6	852.9
4-20	416	3058.8	3051.0	3029.4	3010.2	2970.6
15-14	421	3095.6	2984.8	2682.0	2412.0	1854.8
14-15	421	3095.6	2999.1	2735.3	2500.1	2014.7
18-10	424	3117.7	2958.1	2522.1	2133.3	1330.9
10-18	424	3117.7	3068.4	2933.8	2813.9	2566.2
16-13	425	3125.0	2998.9	2654.4	2347.3	1713.2
13-16	425	3125.0	3041.8	2814.4	2611.6	2193.0
20-6	436	3205.9	3008.8	2470.6	1990.7	1000.0
6-20	436	3205.9	3188.3	3139.7	3096.5	3007.4
21-1	442	3250.0	3032.8	2439.4	1910.3	818.0
19-9	442	3250.0	3072.2	2586.4	2153.3	1259.2
9-19	442	3250.0	3210.1	3101.1	3003.9	2803.3
1-21	442	3250.0	3249.5	3248.2	3247.0	3244.5
21-3	450	3308.9	3091.6	2498.2	1969.1	876.8
15-15	450	3308.9	3198.0	2895.2	2625.3	2068.0
3-21	450	3308.9	3304.4	3292.3	3281.5	3259.2
16-14	452	3323.6	3197.5	2853.0	2545.8	1911.8
14-16	452	3323.6	3227.0	2963.3	2728.1	2242.7
17-13	458	3367.7	3225.3	2836.4	2489.7	1773.9
13-17	458	3367.7	3284.4	3057.0	2854.2	2435.7

TABLE K (CONTINUED)

m-n	m^2+n^2	$\theta=0^\circ$	$\theta=15^\circ$	$\theta=30^\circ$	$\theta=40^\circ$	$\theta=60^\circ$
20-8	464	3411.8	3214.7	2676.4	2196.5	1205.9
8-20	464	3411.8	3380.3	3294.1	3217.4	3058.8
21-5	466	3426.5	3209.3	2615.8	2086.8	994.5
5-21	466	3426.5	3414.2	3380.5	3350.5	3288.6
18-12	468	3441.2	3281.6	2845.6	2456.9	1654.4
12-18	468	3441.2	3370.3	3176.5	3003.7	2647.1
16-15	481	3536.8	3410.7	3066.2	2759.1	2125.0
15-16	481	3536.8	3426.0	3123.2	2853.2	2296.0
19-11	482	3544.1	3366.4	2880.5	2447.4	1553.3
11-19	482	3544.1	3484.5	3321.7	3176.5	2876.9
22-0	484	3558.9	3320.6	2669.1	2088.3	889.7
0-22	484	3558.9	3558.9	3558.9	3558.9	3558.8
22-2	488	3588.3	3350.0	2698.6	2117.7	919.1
2-22	488	3588.3	3586.3	3580.9	3576.1	3566.2
21-7	490	3603.0	3385.8	2792.3	2263.3	1171.0
7-21	490	3603.0	3578.8	3512.9	3454.1	3332.7
22-4	500	3676.5	3438.3	2786.8	2205.9	1007.4
20-10	500	3676.5	3479.4	2941.2	2461.3	1470.6
10-20	500	3676.5	3627.2	3492.6	3372.7	3125.0
4-22	500	3676.5	3668.6	3647.1	3627.9	3588.3
16-16	512	3764.7	3638.6	3294.1	2987.0	2353.0
17-15	514	3779.4	3637.1	3248.2	2901.4	2185.7
15-17	514	3779.4	3668.6	3365.8	3095.9	2538.6
22-6	520	3823.6	3585.3	2933.8	2353.0	1154.4
18-14	520	3823.6	3664.0	3228.0	2839.2	2036.8
14-18	520	3823.6	3727.0	3463.3	3228.1	2742.7
6-22	520	3823.6	3805.9	3757.4	3714.2	3625.0
21-9	522	3838.3	3621.0	3027.6	2498.5	1406.3
9-21	522	3838.3	3798.4	3689.4	3592.2	3391.6
23-1	530	3897.1	3636.5	2924.7	2289.9	979.8

TABLE K (CONTINUED)

m-n	m^2+n^2	$\theta=0^\circ$	$\theta=15^\circ$	$\theta=30^\circ$	$\theta=40^\circ$	$\theta=60^\circ$
19-13	530	3897.1	3719.3	3233.5	2800.3	1906.3
13-19	530	3897.1	3813.8	3586.4	3383.7	2965.1
1-23	530	3897.1	3896.6	3895.3	3894.1	3891.6
23-3	538	3955.9	3695.3	2983.5	2348.8	1038.6
3-23	538	3955.9	3951.5	3939.4	3928.6	3906.3
20-12	544	4000.0	3803.0	3264.7	2784.8	1794.1
12-20	544	4000.0	3929.1	3735.3	3562.5	3205.9
22-8	548	4029.4	3791.2	3139.7	2558.8	1360.3
8-22	548	4029.4	3997.9	3911.8	3835.0	3676.5
23-5	554	4073.6	3813.0	3101.1	2466.4	1156.3
5-23	554	4073.6	4061.2	4027.6	3997.6	3935.7
21-11	562	4132.4	3915.2	3321.7	2792.7	1700.4
11-21	562	4132.4	4072.8	3910.0	3764.7	3465.1
24-0	576	4235.3	3951.6	3176.5	2485.3	1058.8
0-24	576	4235.3	4235.3	4235.3	4235.3	4235.3
23-7	578	4250.0	3989.5	3277.6	2642.9	1332.7
17-17	578	4250.0	4107.7	3718.8	3372.0	2656.3
7-23	578	4250.0	4225.9	4160.0	4101.2	3979.8
24-2	580	4264.7	3981.0	3205.9	2514.7	1088.2
18-16	580	4264.7	4105.2	3669.1	3280.4	2478.0
16-18	580	4264.7	4138.6	3794.1	3487.0	2853.0
2-24	580	4264.7	4262.7	4257.4	4252.6	4242.7
22-10	584	4294.2	4055.8	3404.4	2823.6	1625.0
10-22	584	4294.2	4244.9	4110.3	3990.3	3742.7
19-15	586	4308.9	4131.1	3645.2	3212.1	2318.0
15-19	586	4308.9	4198.0	3895.3	3625.3	3068.0
24-4	592	4353.0	4069.3	3294.1	2603.0	1176.5
4-24	592	4353.0	4345.1	4323.6	4304.4	4264.7
20-14	596	4382.4	4185.3	3647.1	3167.1	2176.5
14-20	596	4382.4	4285.8	4022.1	3786.9	3301.5

TABLE K (CONTINUED)

m-n	m^2+n^2	$\theta=0^\circ$	$\theta=15^\circ$	$\theta=30^\circ$	$\theta=40^\circ$	$\theta=60^\circ$
23-9	610	4485.3	4224.8	3512.9	2878.2	1568.0
21-13	610	4485.3	4268.1	3674.7	3145.6	2053.3
13-21	610	4485.3	4402.1	4174.7	3971.9	3553.3
9-23	610	4485.3	4445.4	4336.4	4239.2	4038.6
24-6	612	4500.0	4216.3	3441.2	2750.0	1323.5
6-24	612	4500.0	4482.3	4433.9	4390.7	4301.5
25-1	626	4603.0	4295.1	3454.1	2704.1	1156.3
1-25	626	4603.0	4602.5	4601.1	4599.9	4597.5
22-12	628	4617.7	4379.3	3728.0	3147.1	1948.5
12-22	628	4617.7	4546.8	4353.0	4180.2	3823.6
25-3	634	4661.8	4354.0	3512.9	2763.0	1215.1
3-25	634	4661.8	4657.4	4645.3	4634.4	4612.2
24-8	640	4705.9	4422.2	3647.1	2955.9	1529.4
8-24	640	4705.9	4674.4	4588.3	4511.5	4353.0
18-18	648	4764.7	4605.2	4169.2	3780.4	2978.0
25-5	650	4779.5	4471.6	3630.5	2880.6	1332.7
23-11	650	4779.5	4518.9	3807.0	3172.3	1862.1
19-17	650	4779.5	4601.7	4115.8	3682.7	2788.6
17-19	650	4779.5	4637.1	4248.2	3901.5	3185.7
11-23	650	4779.5	4719.9	4557.0	4411.8	4112.2
5-25	650	4779.5	4767.1	4733.5	4703.5	4641.6
20-16	656	4823.6	4626.5	4088.3	3608.3	2617.7
16-20	656	4823.6	4697.5	4353.0	4045.8	3411.8
21-15	666	4897.1	4679.9	4086.4	3557.4	2465.1
15-21	666	4897.1	4786.3	4483.5	4213.5	3656.3
25-7	674	4955.9	4648.1	3807.0	3057.1	1509.2
7-25	674	4955.9	4931.8	4865.8	4807.1	4685.7
26-0	676	4970.6	4637.7	3728.0	2916.9	1242.7
24-10	676	4970.6	4686.9	3911.8	3220.6	1794.1

TABLE K (CONCLUDED)

m-n	m^2+n^2	$\theta=0^\circ$	$\theta=15^\circ$	$\theta=30^\circ$	$\theta=40^\circ$	$\theta=60^\circ$
10-24	676	4970.6	4921.4	4786.8	4666.8	4419.2
0-26	676	4970.6	4970.6	4970.6	4970.6	4970.6
26-2	680	5000.0	4667.1	3757.4	2946.3	1272.1
22-14	680	5000.0	4761.6	4110.3	3529.4	2330.9
14-22	680	5000.0	4903.5	4639.7	4404.6	3919.1
2-26	680	5000.0	4998.1	4992.7	4987.9	4948.6

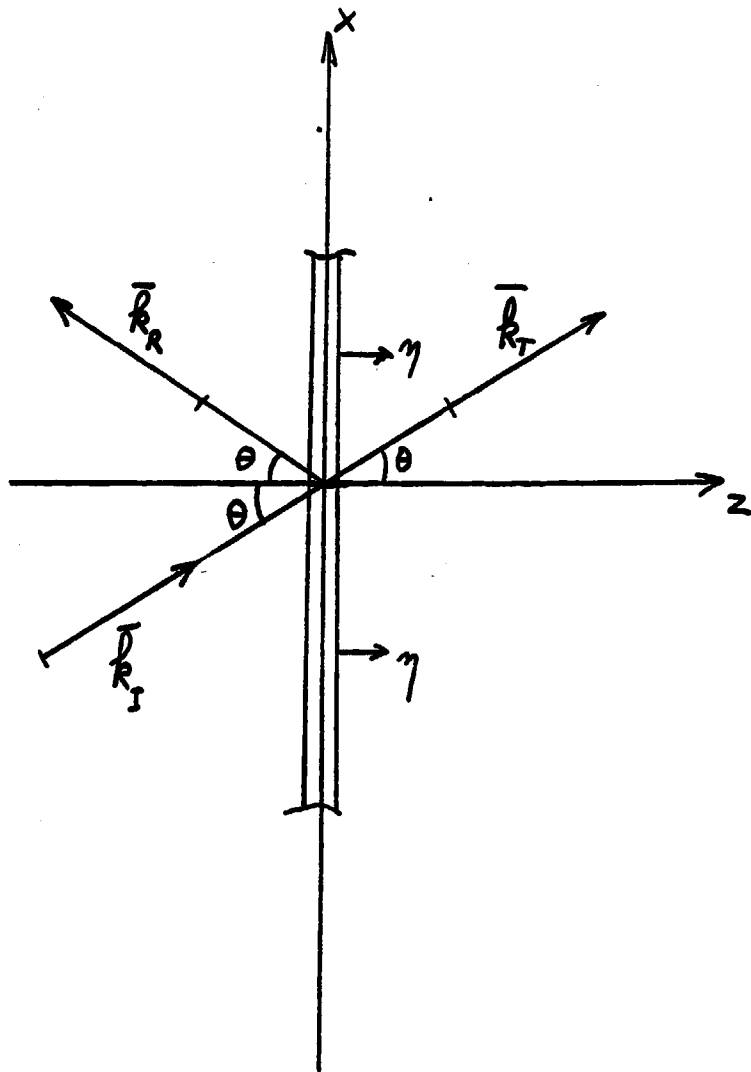
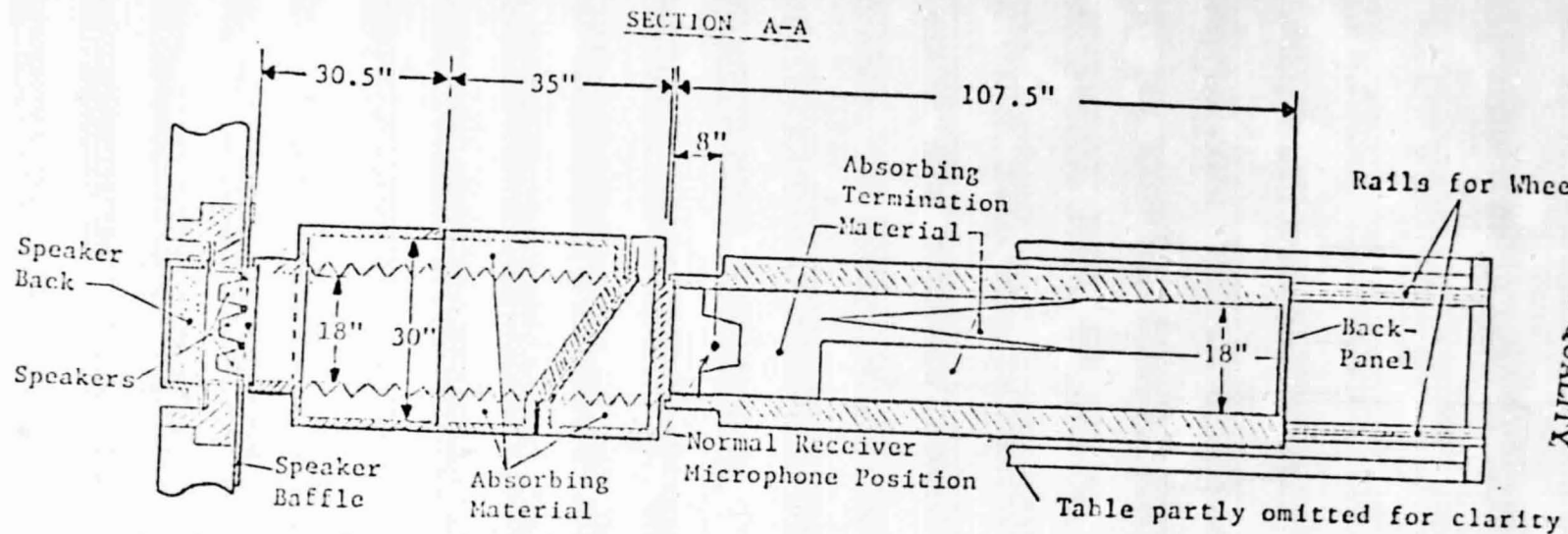


FIGURE 1

Geometrical Configuration for Oblique Incidence



ORIGINAL PAGE IS OF POOR QUALITY

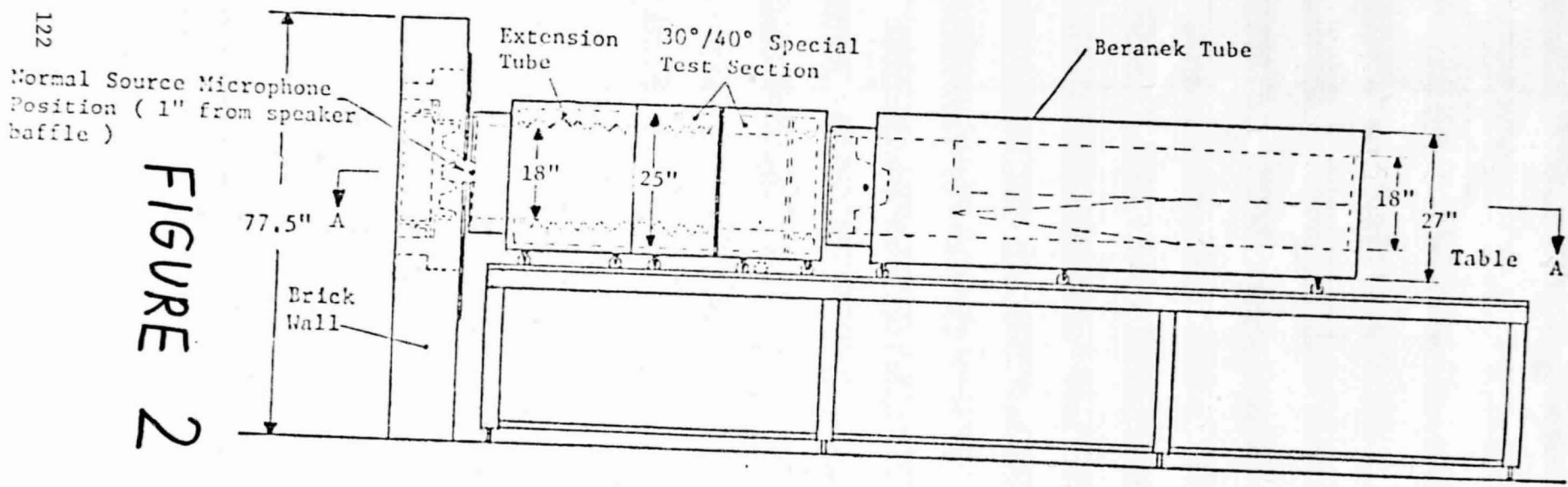


FIGURE 2

KU-FRL Acoustic Panel Test Facility Showing Extension Tube and 30°/40° Special Test Section.

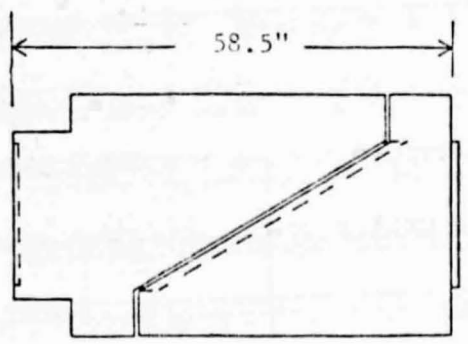
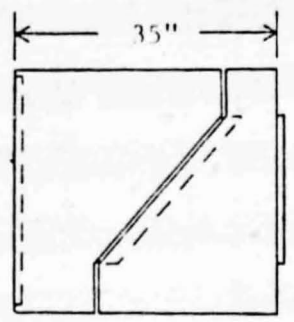
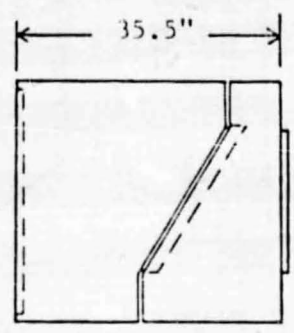
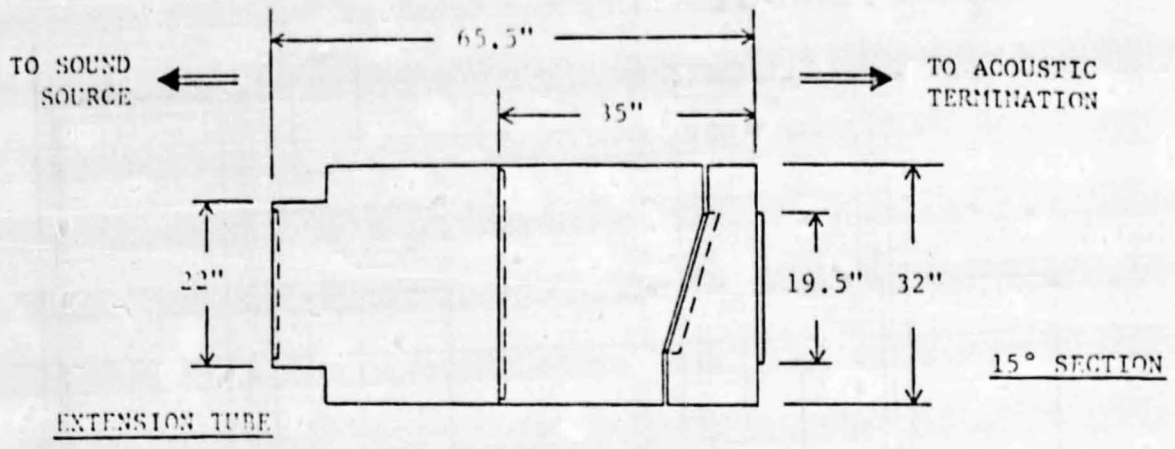
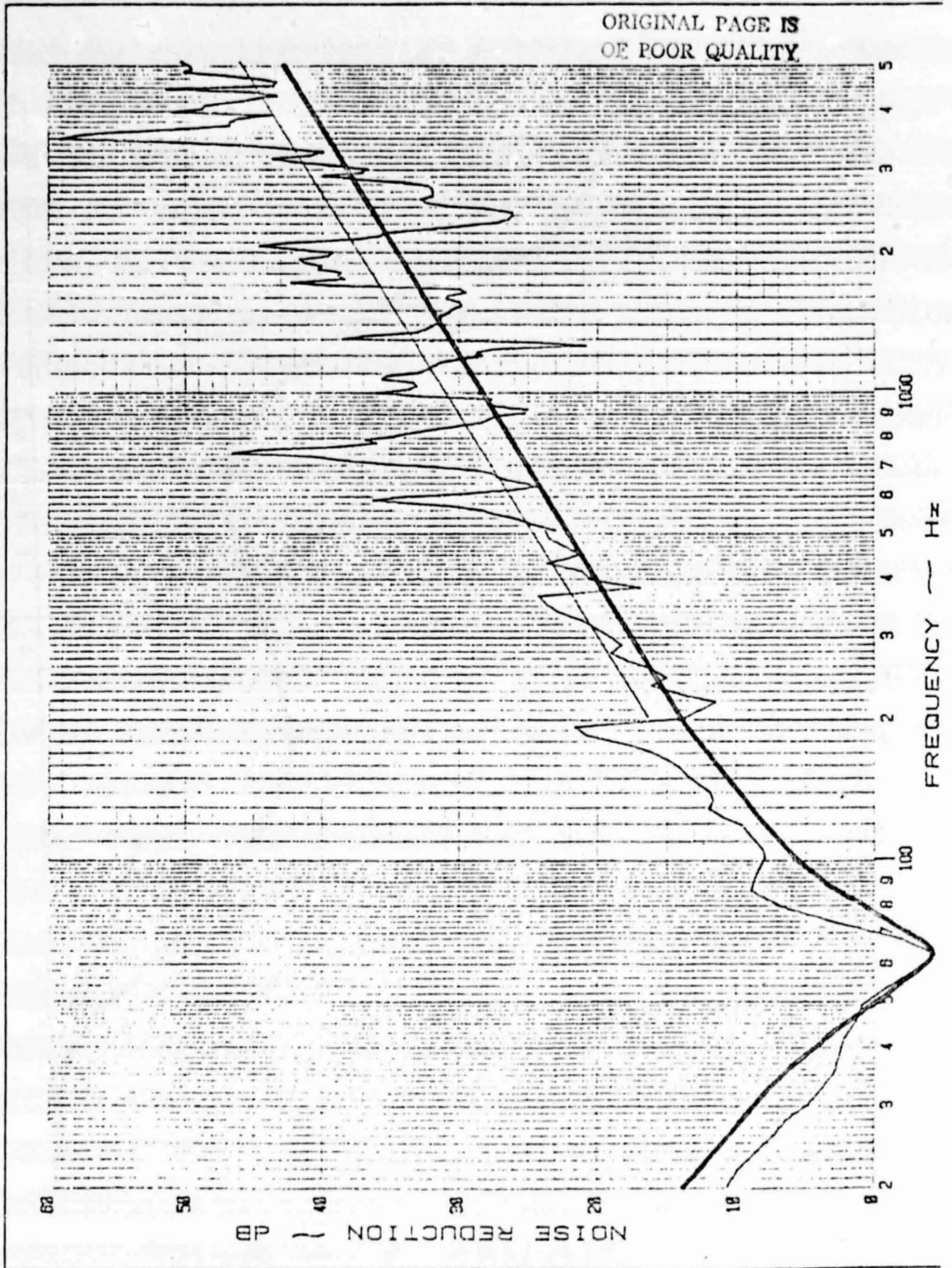


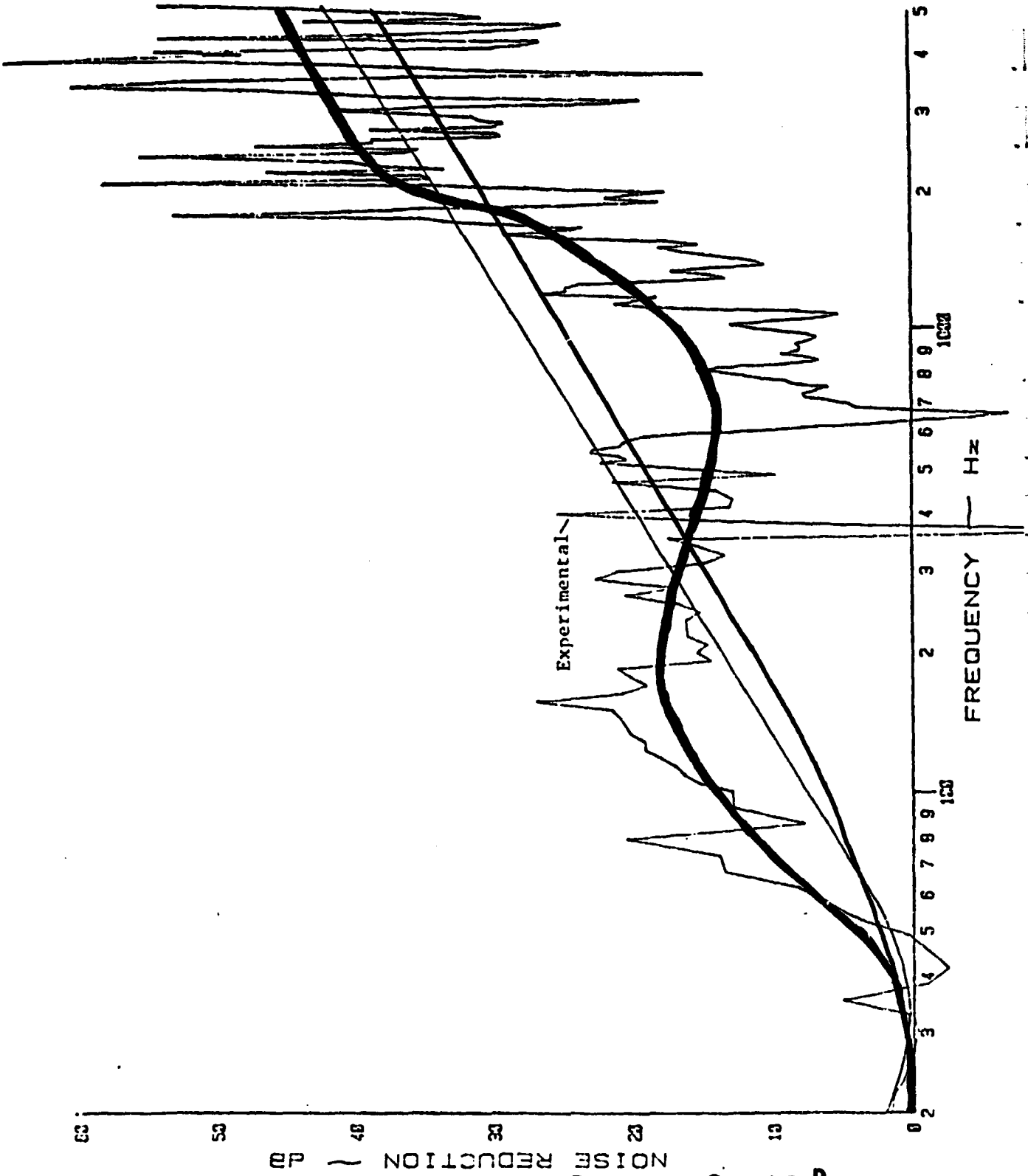
FIGURE 3

Top Views of the Special Test Sections

ORIGINAL PAGE IS
OF POOR QUALITY



CALC		REVISED	DATE	<p>FIGURE 4 - $\theta = 0^\circ$</p>	
CHECK					
APPD					
APPD					
				124	UNIVERSITY OF KANSAS
					PAGE



NOISE REDUCTION - dB

FIGURE 5 - $\theta = 15^\circ$

Experimental and Theoretical Noise Reduction Characteristics of a .025 Inch Thick Aluminum Panel Under 15° Angle of Sound Incidence.

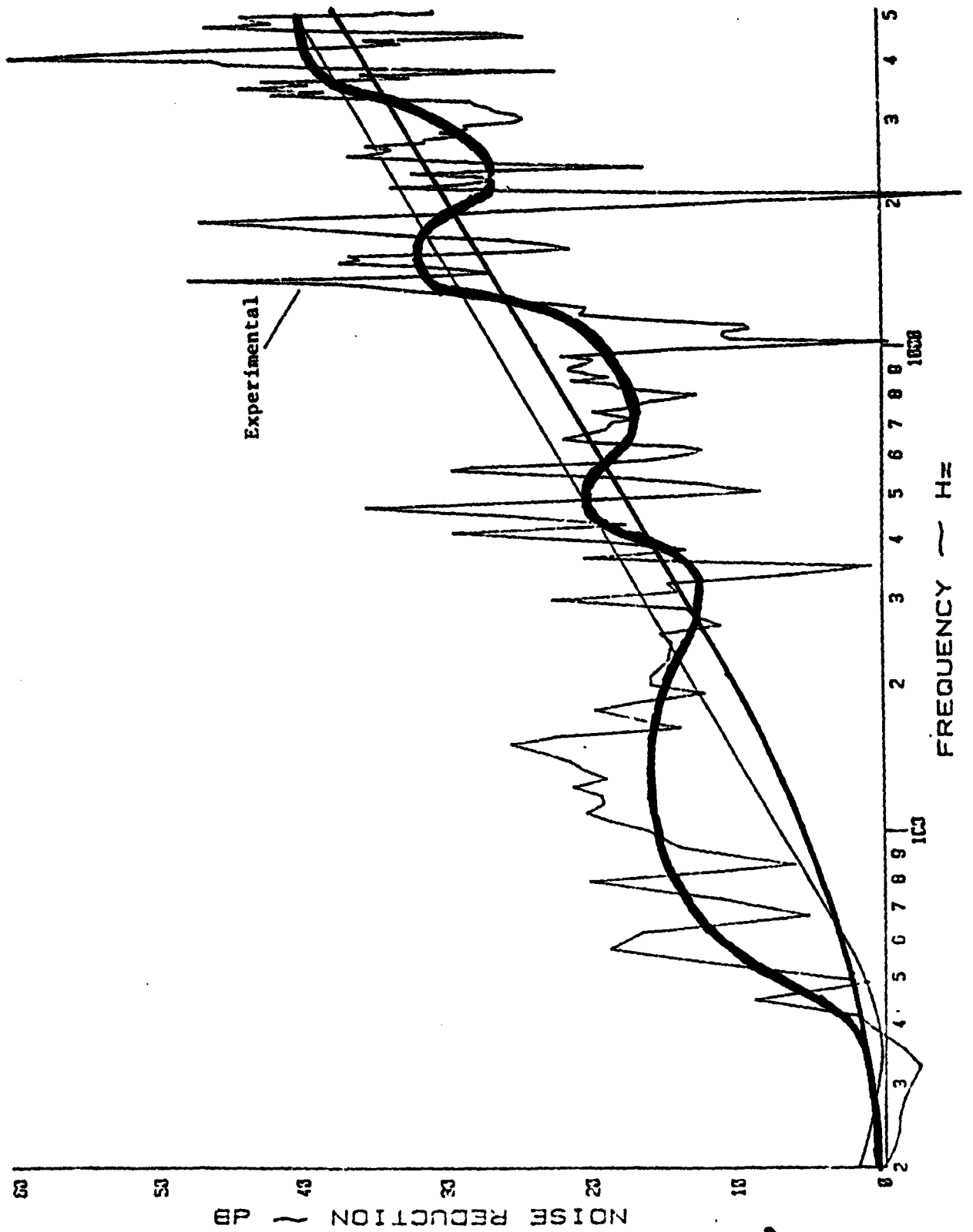


FIGURE 6 - $\theta=30^\circ$

Experimental and Theoretical Noise Reduction Characteristics of a .025 Inch Thick Aluminum Panel Under 30° Angle of Sound Incidence.

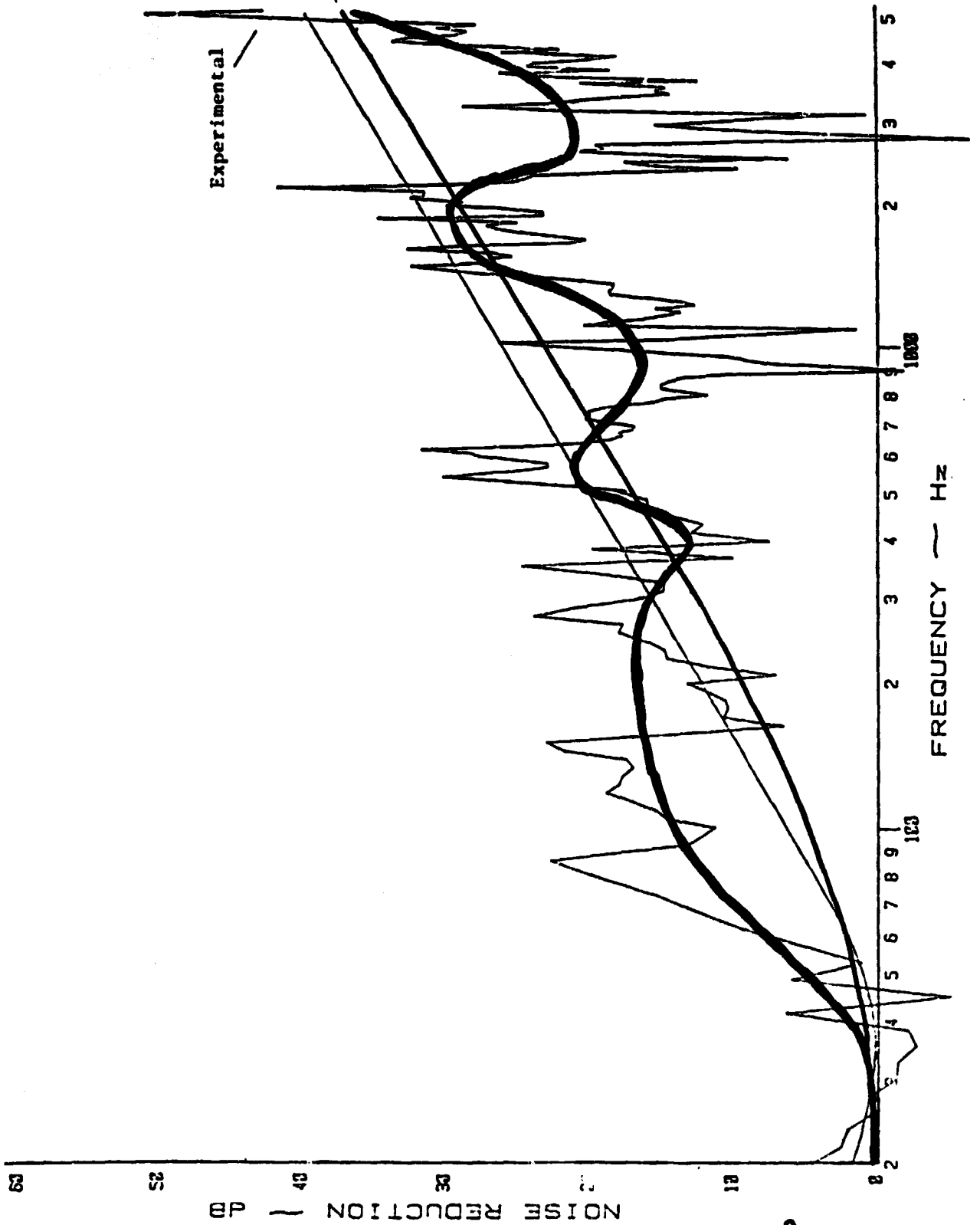


FIGURE 7 - $\theta = 40^\circ$

Experimental and Theoretical Noise Reduction Characteristics of a .025 Inch Thick Aluminum Panel Under 40° Angle of Sound Incidence.

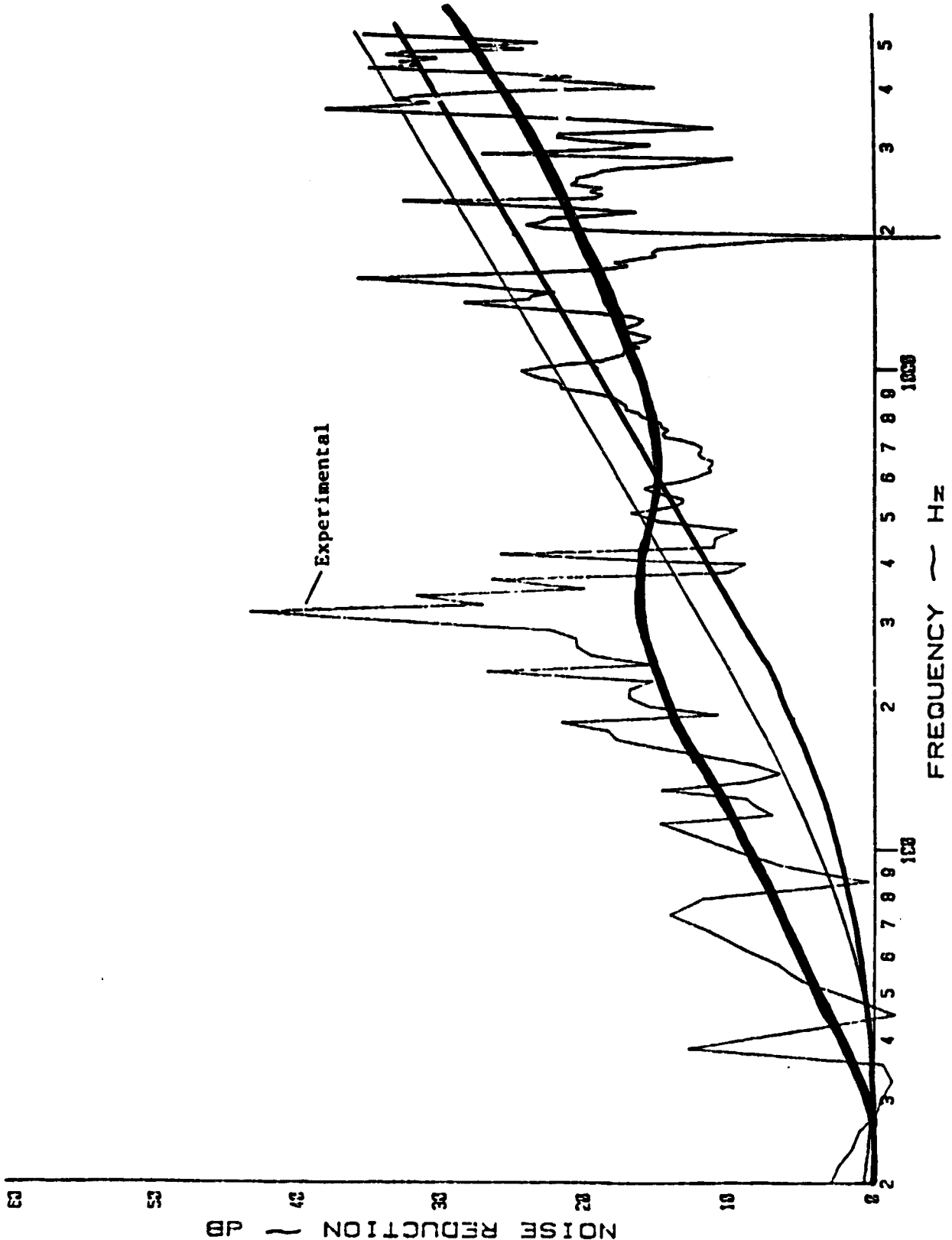


FIGURE 8 - $\theta = 60^\circ$

Experimental and Theoretical Noise Reduction Characteristics of a .025 Inch Thick Aluminum Panel Under 60° Angle of Sound Incidence.

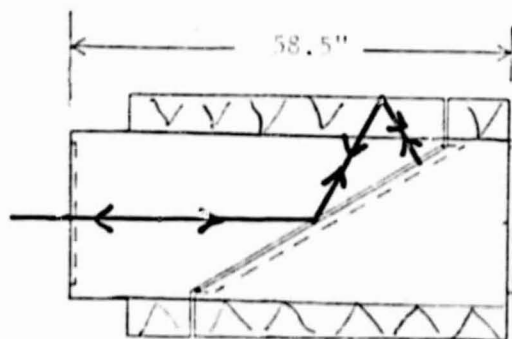
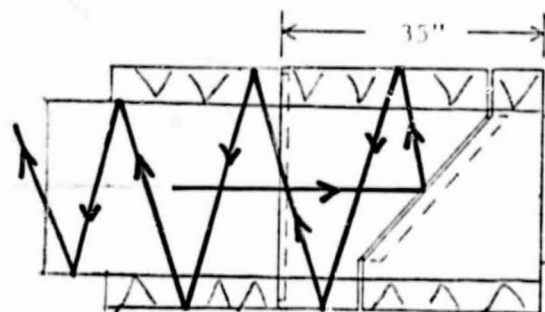
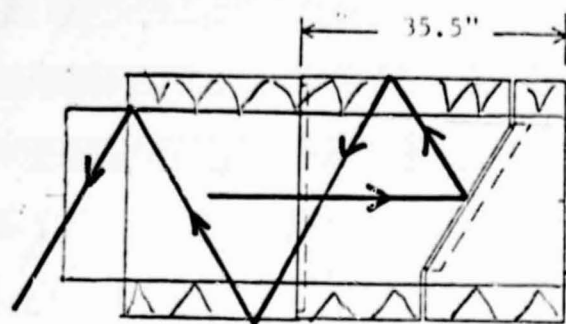
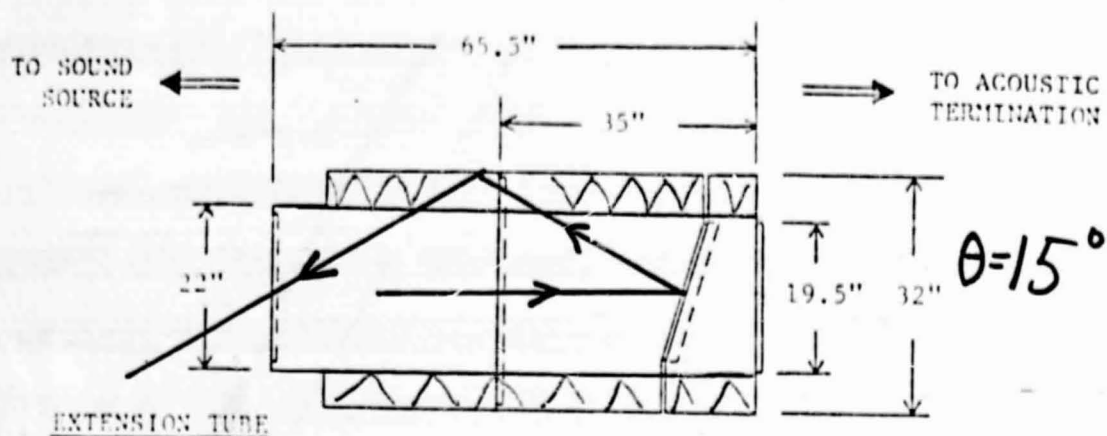


FIGURE 9